Spring 2018

Ecosystems, communities, and species: Understanding mammalian response to ancient carbon cycle perturbations

Abigail Carroll
University of New Hampshire, Durham

ECOSYSTEMS, COMMUNITIES, AND SPECIES: UNDERSTANDING MAMMALIAN RESPONSE TO ANCIENT CARBON CYCLE PERTURBATIONS

BY

ABIGAIL R. CARROLL
B.A., Smith College, 2007
M.S., University of New Hampshire, 2012

DISSERTATION

Submitted to the University of New Hampshire
in Partial Fulfillment of
the Requirements for the Degree of

Doctor of Philosophy
in
Earth and Environmental Sciences

May 2018

This dissertation has been examined and approved in partial fulfillment of the requirements for the degree of Doctor of Philosophy in Earth and Environmental Sciences by:

Dissertation Director, Dr. William C. Clyde
Professor of Earth Sciences

Dr. Rosemarie E. Came
Associate Professor of Earth Sciences

Dr. Joseph M. Licciardi
Professor of Earth Sciences

Dr. Rebecca J. Rowe
Associate Professor of Natural Resources

Dr. Henry C. Fricke
Professor of Geology, Colorado College

On 16 April 2018

Original approval signatures are on file with the University of New Hampshire Graduate School.

To Mom and Dad.

Thank you for inspiring me to care for and explore the natural world around me,

and for encouraging me to chase my dreams.

ACKNOWLEDGEMENTS

First and foremost, I thank my committee members for their time, patience, and thoughtful input throughout my journey to the doctoral degree: Dr. Rebecca Rowe, Dr. Joseph Licciardi, Dr. Rosemarie Came, and Dr. Henry Fricke. But I especially thank my advisor, Dr. William Clyde, for introducing me to the incredible Bighorn Basin of Wyoming and of course the mammal teeth (I'm never turning back now!), for continually supporting my academic goals and aspirations beyond my dissertation, and for being a truly great role model throughout my graduate experience.

I am indebted to the field assistants who have accompanied me into the field for the past several years: Tristan Amaral, Jean-Francois Benoit, David Conwell, Alexander Jacobsen, Sierra Jech, Marcelo Krause, Jeremy Riedel, Kaori Tsukui, and Gregory Welter. Without you, I would not have many mammal teeth to study! I must also thank so many friends and colleagues: Brooks Kohli for inspiring Chapter IV, and for his help with the Pairs program, Joel Johnson for his important insights and advice while serving on my pre-doctoral committee, and Jonathan Buzan and Matt Huber for insights into Eocene climate and climate modeling. I would also like to thank Hemmo Abels, Amy Chew, and Ross Secord for data access and resources, as well as Philip Gingerich for access to specimens at the University of Michigan's Museum of Paleontology.

This work would not have been possible without funding through a National Science Foundation Grant (EAR0958821) awarded to Dr. William Clyde. Field work was also supported through grants from the Geological Society of America, Paleontological Society, Sigma Xi, and the UNH EOS-ESRC-Earth Sciences Student Research Fund. I was able to present findings from this research at several conferences through the help of the UNH NRESS Student Support Fund and UNH Graduate School.

Finally, I thank my closest friends and family members, especially Sarah and Jen, you guys were life-savers. Rory, this last "push to the finish" would simply not have happened without you or your cheerleading. You are the best husband and father. And the greatest thank you of all goes to my parents— Thank you for sharing with me your love for nature, science, the outdoors, and most of all, for teaching me perseverance. Because of you, my little-girl dream of getting a Ph.D. "digging up" fossils came true!

TABLE OF CONTENTS

LIST OF TABLES

LIST OF FIGURES

ABSTRACT

ECOSYSTEMS, COMMUNITIES, AND SPECIES: UNDERSTANDING MAMMALIAN RESPONSE TO ANCIENT CARBON CYCLE PERTURBATIONS

by

Abigail R. Carroll

University of New Hampshire, May 2018

Abrupt perturbations of the global carbon cycle during the early Eocene are associated with rapid global warming events. Recent studies have observed mammal dwarfing during the most severe of these ancient global warming events (or "hyperthermals"), known as the Paleocene-Eocene Thermal Maximum (PETM, ~56 mya). Chapter I of this dissertation establishes a stratigraphic framework around two subsequent and smaller-magnitude warming events known as ETM2 and H2 (~53.7 mya and ~53.6 mya, respectively), which have recently been documented in the strata of the Bighorn Basin of Wyoming. Such a stratigraphic framework is crucial for placing fossil localities into stratigraphic context, which can then aid in the interpretation of mammalian response to these warming events. Chapter II shows that a decrease in mammal body size accompanies the ETM2 warming event. Body size decreases are evident in three of the four taxonomic groups analyzed in this study, but they are most clearly observed in early equids (horses). During ETM2, the most extensively-sampled lineage of equids decreased in size by ~14%, as opposed to ~30% during the larger PETM. Thus, decrease

in body size appears to be a common response for some early mammals during past global warming events, and the extent of dwarfing is related to the magnitude of the event.

Chapter III further investigates the observed early equid body size response to hyperthermal warming. The African Duiker (*Philantomba*) is used as a modern analog to investigate the relationship between body size and latitude, and to estimate early equid geographic range shift. Duikers were found to follow Bergmann's rule, with a statistically significant positive correlation between body size and latitude. If early equids shared the body size-latitude relationship to the same extent that Duikers do today, they would require only a 10° and 4° latitudinal range shift to explain their apparent body size decrease across PETM and ETM2 stratigraphic records, respectively.

Community structure changes are a typical response to environmental stressors. Chapter IV attempts to better understand this relationship in the context of extreme climate change. Fossil genera co-occurrence patterns are investigated through both the PETM and ETM2 hyperthermal events. The main body of both events is associated with an increase in the number of significant pairs of taxa, with segregated pairs found to be more common. Such patterns reflect dynamic changes within these early Eocene communities in response to warming climate, and can serve as models for better understanding the impacts of modern-day warming on mammals and ecosystems.

CHAPTER I

STRATIGRAPHIC FRAMEWORK FOR THE ETM2 AND H2 HYPERTHERMAL EVENTS, MCCULLOUGH PEAKS, BIGHORN BASIN, WY

Introduction

Climate change affects plants and animals in ways that are poorly understood. Much can be learned from the study of climate change in the geological past and its effect on contemporaneous biotas. Early Eocene global warming events, or "hyperthermals", are associated with large perturbations of the global carbon cycle, and thus serve as analogs of modern-day global warming. The largest of the hyperthermals was the Paleocene-Eocene Thermal Maximum (PETM), occurring approximately 56 mya and lasting some 180,000 years (Aziz et al. 2008; McInerney and Wing 2011). The PETM is recognized in the geological record by marine and terrestrial carbon isotope excursions (CIEs) of about −3‰ and −3 to −6‰ (McInerney and Wing 2011; Sluijs et al. 2006; Weijers et al. 2007), respectively, and an increase in global temperatures of 5–8 degrees Celsius within 10,000 years (McInerney and Wing 2011; Fricke et al. 1998; Fricke and Wing 2004).

Ecological consequences of the PETM's rapid shifts in carbon cycling and atmospheric temperatures have been recorded in both marine and terrestrial records, including profound biotic turnover. One of the most extensively studied terrestrial records of the PETM is located in the

Bighorn Basin of Wyoming. Here, the event is characterized by transient changes in vegetative composition, from warm temperate paleofloras to those that are indicative of dry tropical and subtropical climates (McInerney and Wing 2011). Terrestrial records of the PETM are also accompanied by significant mammalian turnover, including the abrupt introduction of several modern mammalian lineages (including perissodactyls, 'artiodactyls', and primates) and mammalian body size decrease in both immigrant and endemic taxa, observed through changes in the size of fossilized adult teeth (Gingerich 1989; Clyde and Gingerich 1998; Gingerich 2003; Secord et al. 2012; Rose et al. 2012). Since the discovery of the PETM in deep-sea cores and continental sections, subsequent smaller magnitude CIEs have also been discovered in marine records (Lourens et al. 2005; Stap et al. 2010). The second largest hyperthermal of the early Eocene, known as ETM2, occurred about 2 million years after the PETM (approximately 53.7 mya) and was associated with a deep sea CIE of >1.4‰ and ~3°C warming (Lourens et al. 2005; Stap et al. 2010) — about half the magnitude of the PETM (Stap et al. 2010). Another smaller amplitude hyperthermal, identified as "H2", appears in the marine record about 100,000 years after ETM2 (approximately 53.6 mya), with a CIE of ~0.8‰ and ~2°C warming (Stap et al. 2010).

More recently, geochemical evidence of ETM2 and H2 was uncovered in terrestrial sedimentary deposits within the Bighorn Basin (Fig.1-1), with CIEs of −3.8‰ and −2.8‰, respectively (Abels et al. 2012; Abels et al. 2016). With this discovery in mind, the purpose of this study is to:

1. Establish a new carbon-isotope and lithostratigraphic section within the Bighorn Basin in order to place additional fossils and fossil localities within stratigraphic context of the ETM2 and H2 CIEs.

2. Provide a higher resolution lithostratigraphic and carbon-isotope section at an established site, known as Gilmore Hill, first reported in Abels et al. (2012), in order to clarify the stratigraphic level of ETM2.
3. Develop a reliable stratigraphic correlation between the established (Abels et al. 2012) and newly described stratigraphic sections. A reliable stratigraphic correlation is crucial in order to describe the association between the ETM2 and H2 hyperthermal events and any biological or ecological changes observed in fossils of the same strata.

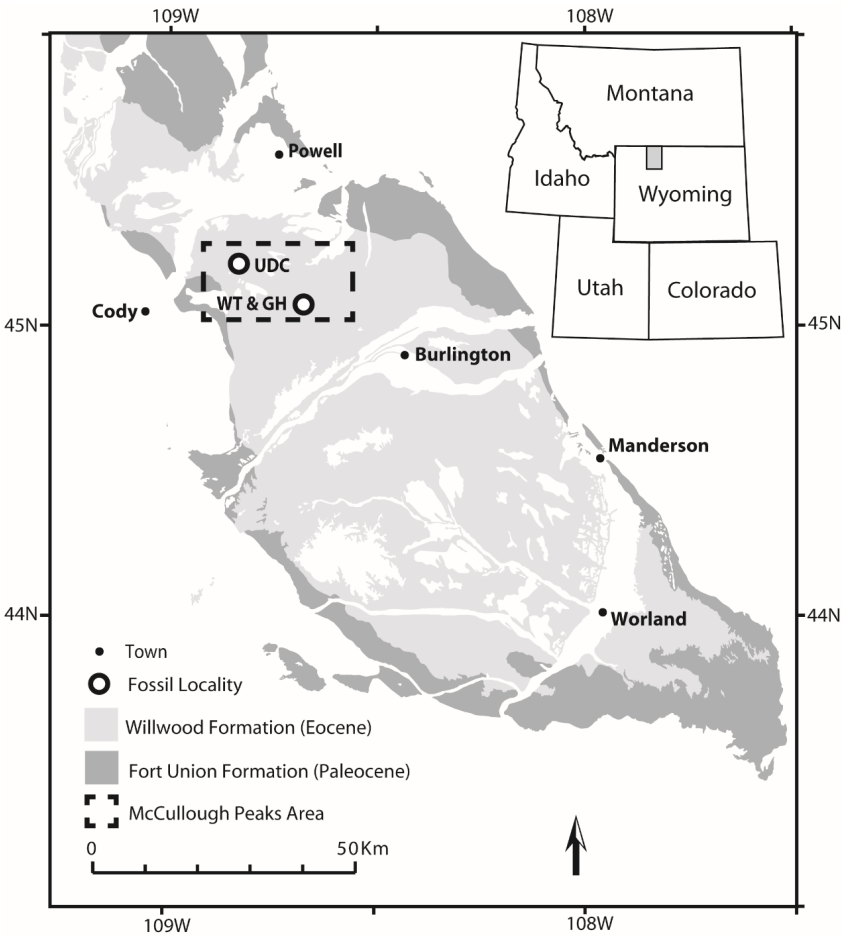

Figure 1-1. The Bighorn Basin is located in northwestern Wyoming, USA. Upper Deer Creek (UDC) and Gilmore Hill (GH) are established localities from prior study (Abels et al. 2012). White Temple (WT) is stratigraphic section newly described in this study. All sections are located within the McCullough Peaks region of the northern Bighorn Basin (outlined by dashed box, see close-up in fig. 1-2).

Background

Study Site

The Bighorn Basin is located in northwestern Wyoming, approximately 130 kilometers east of Yellowstone National Park (fig. 1-1). The basin formed during the Laramide orogeny and is bordered by the Beartooth Mountains to the northwest, Bighorn Mountains to the east, and Owl Creek Mountains to the south. It is composed of up to 4,500 meters of stratigraphically continuous (<100,000-year timescales; Abels et al. 2016) synorogenic continental sedimentary deposits that accumulated through the early Paleogene (Gingerich 2001; Bown et al. 1994; Kraus 2001). The stratigraphic sections discussed in this study are found within the Willwood Formation, which is an alluvial deposit of channel sandstones, siltstones, and pedogenically modified mudstones, suggesting a once well-drained fluvial system (Neasham and Vondra 1972; Bown and Kraus 1981, 1987).

Carbon Isotope Stratigraphy

Since the early 1990s, stable carbon isotope studies of pedogenic carbonates have been conducted in the paleosols of the basin in order to develop continental records of hyperthermal CIEs (Abels et al. 2012, 2016; Koch, Zachos, and Dettman 1995; Bowen et al. 2001, 2014). The carbon isotopic composition of pedogenic carbonate is useful for recording CIEs since soil CO_2, from which the carbonate precipitates, ultimately tracks atmospheric $\delta^{13}C$ (Koch, Zachos, and Dettman 1995). Today, soil CO_2 at depths greater than ~30 cm is dominantly a product of root respiration and within-soil organic matter decomposition since atmospheric CO_2 has an insignificant direct influence at this depth (Koch 1998; Koch et al. 2003). Combining a ~4.4‰ ^{13}C enrichment (relative to plant tissue) through diffusion of CO_2 to the atmosphere with an

enrichment of ~10.5‰ due to temperature-dependent carbonate precipitation fractionations, the $\delta^{13}C$ of soil carbonates today mirror the $\delta^{13}C$ of overlying flora with an offset of ~ −15‰ (Bowen et al. 2001; Koch 1998; Koch et al. 2003). Because pCO_2 may have changed over time, it should be noted that these ^{13}C enrichment values are present-day estimates and could be different in the past (Farquhar, O'Leary, and Berry 1982; Farquhar, Ehleringer, and Hubick 1989; Pearson and Palmer 2000). Carbonate nodules will form when high soil CO_2 production and organic decay leads to acidic solutions that leach the upper part of the soil. These fluids percolate down into the soil, and, in combination with an increase in the concentration of Ca^{2+} or pH, will promote calcite precipitation (Koch 1998).

Recent Stratigraphic Studies

Through the use of carbon isotope analyses of pedogenic carbonate, ETM2 and H2 have recently been identified in the McCullough Peaks region of the northern Bighorn Basin (fig. 1-2). Four stratigraphic sections have captured the ETM2 and H2 CIEs in this area - Gilmore Hill (GH), Upper Deer Creek (UDC), West Branch (WB), and Creek Star Hill (CSH). GH and UDC were first reported in Abels et al., 2012, and more recently WB and CSH by Abels et al., 2016. The correlation of these sites has been constrained through magnetostratigraphy and correlation of the CIEs (Abels et al. 2012, 2016). In all sections, the most negative CIE values fall within the mixed polarity zone between Chron C24r and Chron 24n.3n. All sites fall within the Wasatchian-5 stage of the North American Land Mammal Ages (NALMA) chronology. Additionally, precession- and eccentricity-scale patterns from the McCullough Peaks CIEs are very similar to marine CIE patterns, further confirming correlations between sections (Abels et al. 2016). An important note here is that the data from GH originally published by Abels et al.

(2012) interpreted the CIE captured by the paleosol carbonates as H2. However, since there was still uncertainty in the correlation, this study resampled the GH section from another nearby locality in order to better characterize it. This study focused on the correlation between the WT and GH to UDC, because many fossils that will be used to interpret evolutionary change in mammals were collected at all three of these locations.

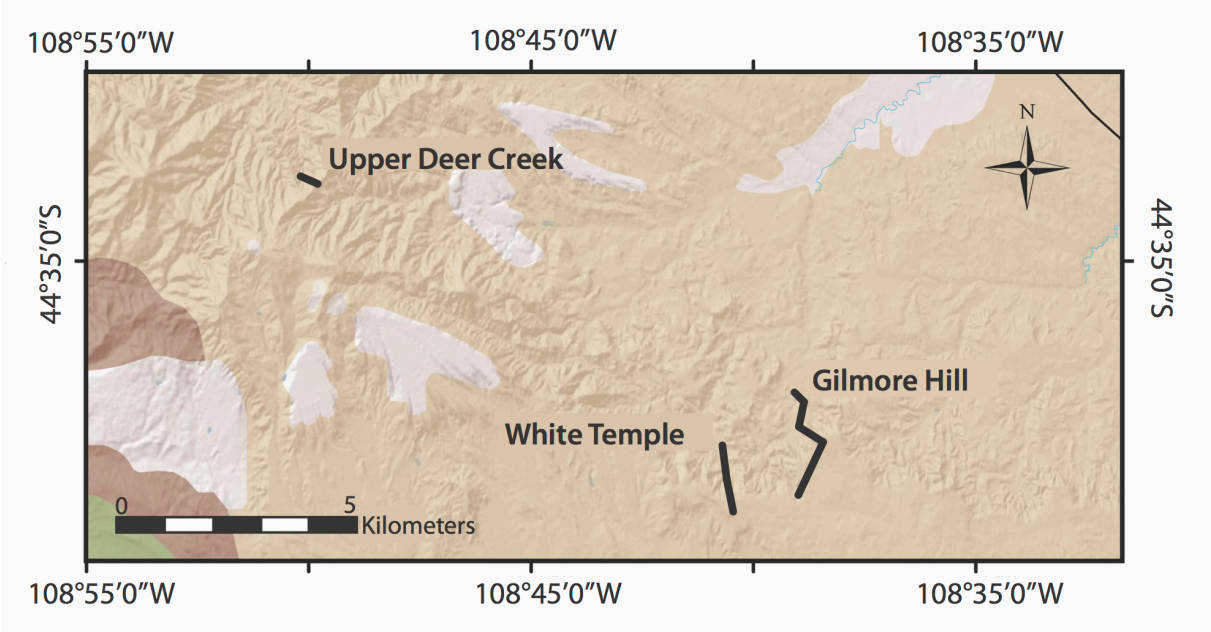

Figure 1-2. Geological map showing close-up view of the three stratigraphic sections within the McCullough Peaks that are the focus of this study. Light brown is early Eocene Willwood Formation, dark brown is Paleocene Fort Union Formation, green are Cretaceous units, and light tan is Quaternary.

Materials and Methods

Field Methods

All new and updated stratigraphic sections were measured using a Jacob's Staff and Abney level. The tops and bases of individual beds were identified in the section by digging through overlying weathered material to the underlying rock. Each bed was then described in terms of color, grain size, and other distinctive sedimentary features (e.g. mottling or burrowing).

Carbonate nodules were collected from the new and updated sections by trenching into underlying rock until *in situ* nodules were uncovered. Stacked transects of these trenches spanned a total of more than 100 meters. Nodules were sampled every ~10 to 50 cm within the trenches. Each sample of carbonate nodules was catalogued and noted in relation to the measured stratigraphic section.

Sampling for isotopic analysis

Carbonate nodules were ground flat using a 45-diamond-grit lap wheel in order to sample from the inside of the nodule. Prior to sampling, the ground surfaces of the carbonate nodules were inspected for signs of alteration (e.g., sparry calcite or hematite inclusions). Nodules that were visibly altered were excluded from sampling. Micritic carbonate was ground from the polished nodule surface using a Foredom k.2230 flex shaft rotary drill with diamond tip burrs (~1–2 mg of powder was collected from each nodule).

All paleosol carbonate samples were analyzed at the University of Arizona Environmental Isotope Laboratory with a Finnigan MAT 252 gas-source ratio mass spectrometer with attached Kiel III automatic sample preparation device. The carbonate nodule powders were reacted with dehydrated phosphoric acid at 70°C, and the final measurement was calibrated through repeated measurements of the NBS-18 and NBS-19 standards. Stable isotope ratio data were reported using "delta" (δ) notation, where $\delta = (R_{sample}/R_{standard} - 1) \times 1000$, reported in parts per thousand (‰). R stands for the ratio of the relative abundance of the heavy to light isotope. Based on the standards, the 1-sigma precision is ± 0.1‰ for $\delta^{18}O$ and ± 0.1‰ for $\delta^{13}C$.

Results & Discussion

Here, results are reported from a newly described stratigraphic section within Bighorn Basin referred to as White Temple (WT). The base of the WT section is located at N44.5297712°, W108.6757226°, and the top of the section is located at N44.5167142°, W108.6720318° (WGS 84 datum), 16 km southeast of UDC (fig. 1-2). The range of carbon isotope values in paleosol carbonate ($\delta^{13}C_{pc}$) at WT is between −14.3‰ to −8.6‰, and the average is −10.9‰. There are two distinct and well-defined excursions reaching −13.7‰ at 905.3 meters above the PETM (based on a 5-point moving average with a 95% CI of −14.0 to −13.3), and −11.3‰ (95% CI [−11.9, −10.7]) at 938.8 meters above the PETM (fig. 1-3; appendix A). These two carbon isotope excursions at WT can be confidently correlated to the ETM2 and H2 CIEs in the Deer Creek area of the McCullough Peaks (Abels et al. 2012; Abels et al. 2016). There is also a distinct purple marker bed that falls within the lower isotope excursion at WT, and it can be traced through the ETM2 CIE to the WBS, CSH, and UDC stratigraphic sections (fig. 1-4). This purple marker bed is defined by a purple mudstone overlaid by a white shelf-forming silty-sandstone, and was first identified as Purple 2 (P2) in the nearby Upper Deer Creek stratigraphic section (Abels et al., 2012). The smaller excursion that falls 33.5 meters above the larger excursion at WT is similar in magnitude to H2 at UDC, which falls 24.6 meters above ETM2 in that section.

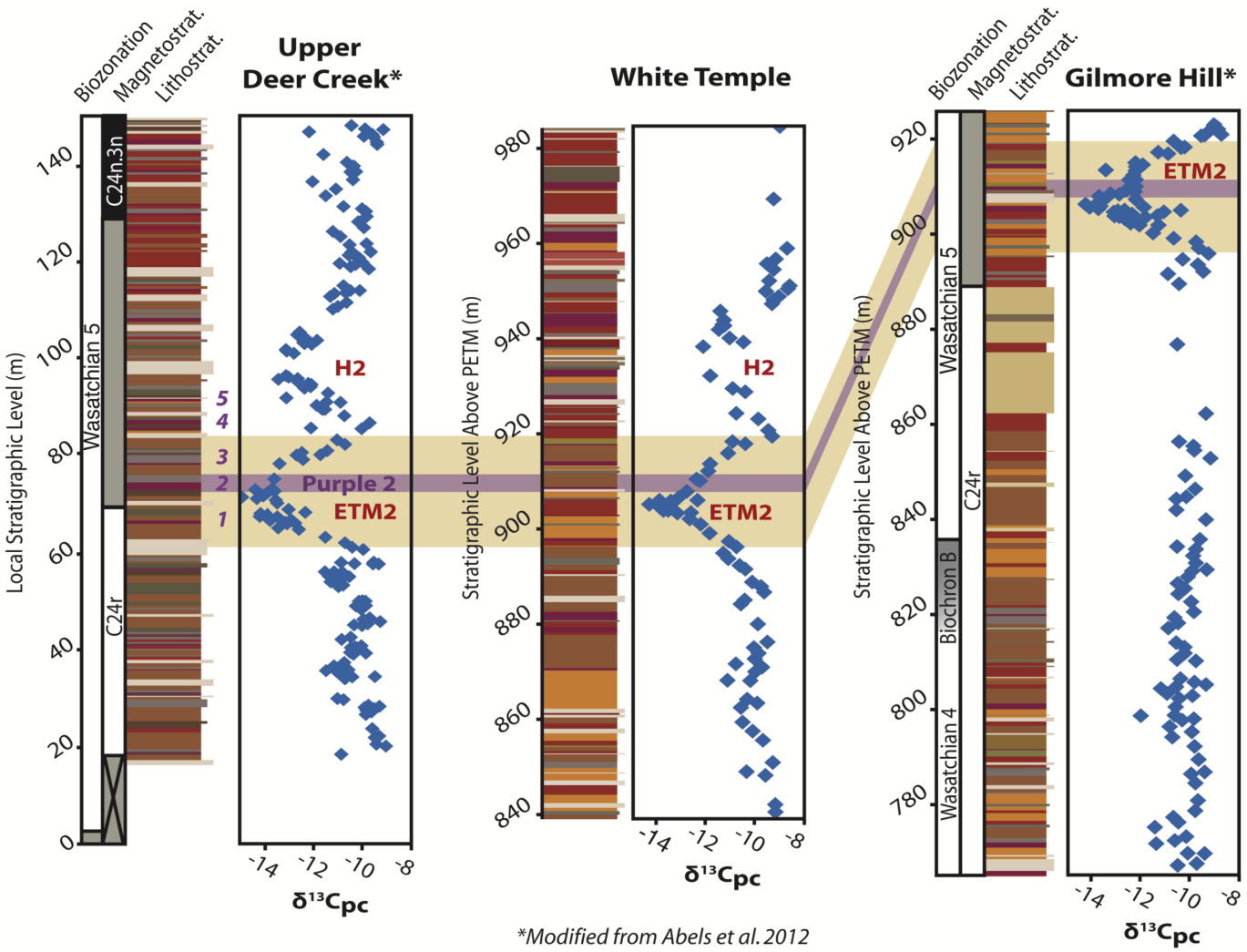

Figure 1-3. Lithostratigraphy, paleosol carbonate nodule isotope stratigraphy ($\delta^{13}C_{pc}$), biozonation, and magnetostratigraphy of the Gilmore Hill (GH), White Temple (WT), and Upper Deer Creek (UDC) sections. The tan shaded region highlights the body of ETM2 across all sections. The purple band represents the Purple 2 (P2) marker bed, which can be visually traced across all outcrop sections in the field, and is associated with the most negative values of the ETM2 CIE.

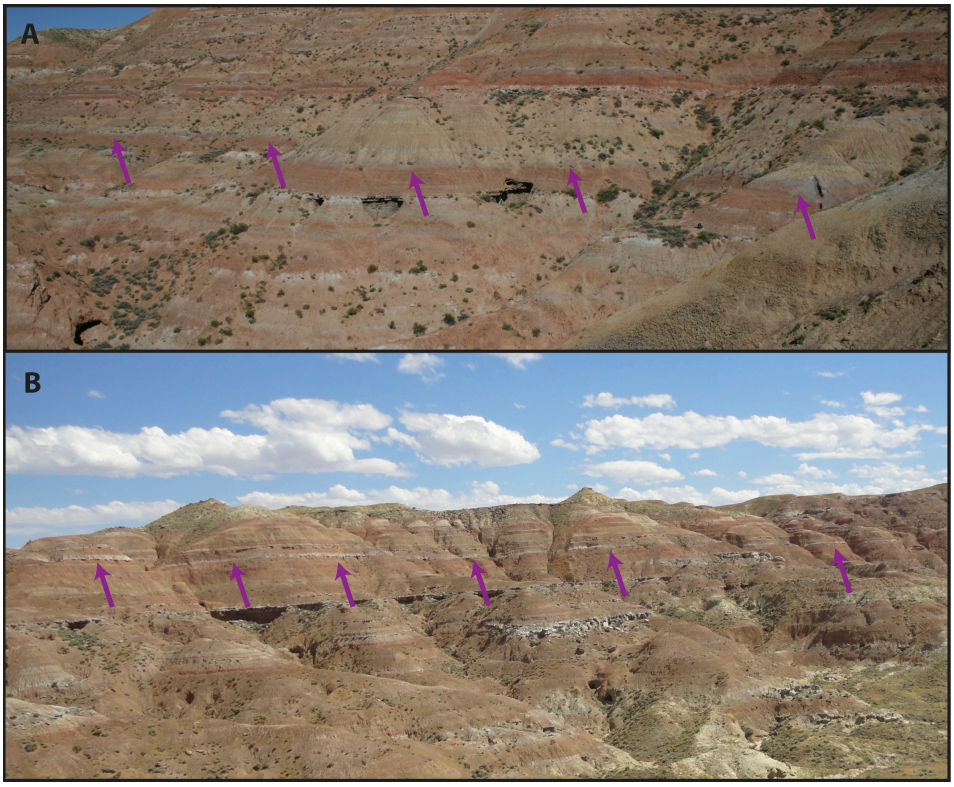

Figure 1-4. 'Purple 2' marker bed highlighted by purple arrows across two McCullough Peaks stratigraphic sections in this study: Upper Deer Creek (A), and White Temple (B).

An updated component of the Gilmore Hill (GH) stratigraphic section is located 1.5 km east of WT, the base at N44.521012°, W108.650241° and top of the updated part of the section at N44.519680°, W108.64923° (WGS 84 datum, fig. 1-2). Isotopic analyses of the newly sampled GH section carbonate nodules resulted in a minimum $\delta^{13}C$ of −13.5‰ (based on a 5-point moving average, 95% CI [−14.3, −12.7]) at the 906.1-meter level, and a maximum −9.0‰ (95% CI [−9.2, −8.7]) at the 921.1-meter level (appendix B). The previous GH minimum $\delta^{13}C$ was reported as −12.0‰, and maximum as −8.7‰ (fig. 1-5; Abels et al. 2012). The updated $\delta^{13}C$ minimum of −13.5‰ occurs within 2.7 meters of P2 and thus clearly represents the ETM2 CIE (and not the H2 CIE as originally proposed in Abels et al. 2012).

The results from the updated GH section now suggest that it is the ETM2 CIE that is preserved here, and not the H2 CIE as originally reported by Abels et al. (2012). This is confirmed by the larger magnitude peak in the newly sampled data, which is consistent with ETM2 rather than H2 as originally proposed. This new correlation is also confirmed by tracing of the P2 marker bed that lies within ETM2 at all other sections in the McCullough Peaks.

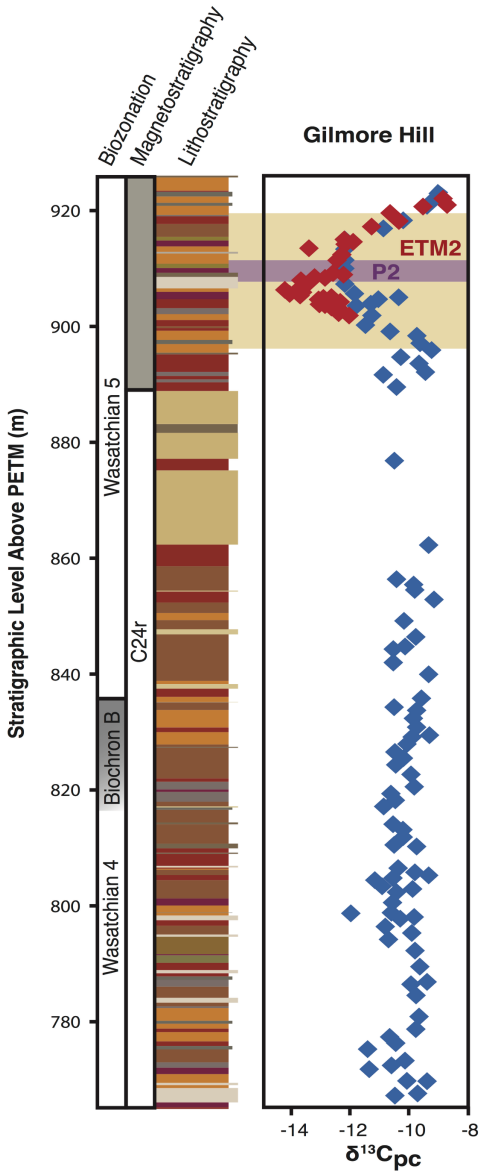

Figure 1-5. Newly sampled carbonate nodule $\delta^{13}C$ values at Gilmore Hill are represented by red diamonds (this study), while previously sampled Gilmore Hill nodules are represented by blue diamonds (Abels et al. 2012).

Conclusions

New carbon isotope data were gathered from pedogenic carbonate nodules collected from two new stratigraphic sections within the McCullough peaks region of the Bighorn Basin. These sections are referred to as White Temple (WT) and Gilmore Hill (GH). A carbon isotope stratigraphy from GH was previously reported in Abels et al. (2012), but was updated here to clarify the stratigraphic placement of ETM2. The new WT sections captured both ETM2 and H2. The lowest WT carbon isotope values reached −13.7‰ and −11.3‰, representing the ETM2 and H2 CIEs, respectively. The lowest carbon isotope values in the newly updated GH section reached −13.5‰, comparable to the ETM2 CIE values at the other McCullough Peaks sections, including nearby WT and UDC. Thus, the H2 CIE originally reported in the Abels et al. (2012) GH stratigraphic section is now interpreted as ETM2. Establishing new and updated stratigraphic sections is necessary to place additional fossils and fossil localities into stratigraphic context around ETM2 and H2.

CHAPTER II

REPETITIVE MAMMALIAN DWARFING DURING ANCIENT GREENHOUSE WARMING EVENTS

Introduction

The early Paleogene was marked by a series of extreme global warming events known as hyperthermals, characterized by global atmospheric carbon isotope excursions (CIEs). The largest hyperthermal, known as the Paleocene-Eocene Thermal Maximum (PETM), was also coincident with transient mammalian dwarfism[1] (Gingerich 1989, 2003; Clyde and Gingerich 1998; Aziz et al. 2008; McInerney and Wing 2011; Rose et al. 2012; Secord et al. 2012). To better understand whether body size change is a commonplace response to climate change and investigate the relationship between mammal body size, temperature, and atmospheric CO_2 levels, these variables should be analyzed across multiple hyperthermals. Until recently, hyperthermals other than the PETM have only been recorded in marine sediments. However, recent carbon isotopic analysis of paleosol carbonates from stratigraphic sections in the Bighorn Basin of Wyoming has uncovered continental records of two smaller magnitude early Eocene hyperthermals known as ETM2 and H2 (see Chapter I; Abels et al. 2012). Yet, their effects on terrestrial climates and ecosystems are not yet documented. Preliminary results indicated that

[1] Here, the term "dwarfing" is used to simply describe an observed size decrease, with no specific connotation of cause.

these hyperthermals were not associated with previously identified mammalian turnover events (Abels et al. 2012; see Chew, 2015 for suggestion of turnover within this interval in southern Bighorn Basin), and no detailed study has yet been carried out investigating within-lineage mammalian body size change as done for the PETM (D'Ambrosia et al. 2014a).

Using the newly documented terrestrial records of ETM2 and H2, this study addresses two important questions: 1) similar to the PETM, is mammalian body size change also found in association with ETM2 and H2; and if so, 2) is there a relationship between the magnitude of a hyperthermal and/or carbon cycle perturbation, and the degree of mammalian dwarfing? Understanding the similarities and differences between biotic responses to the PETM and these other smaller hyperthermals is important for determining what kinds of biological responses might be typical for rapid global warming events like we are experiencing today.

Background

Geologic Setting

Mammalian fossils used in this study were collected from across three stratigraphic sections within the northern Bighorn Basin of Wyoming that span known locations of the ETM2 and H2 CIEs, and are referred to as the Upper Deer Creek (UDC) section, the White Temple (WT) section, and the Gilmore Hill (GH) section (see Chapter I; figs. 1-1, 1-3). The fossils in this study are from the Willwood Formation, which is composed dominantly of channel sandstones and brightly-colored pedogenically-modified overbank mudstone deposits (paleosols), suggesting paleoenvironments of open-canopy forests and relatively dry floodplains (Bown and Kraus 1987; Secord et al. 2008). Aside from numerous fossil mammals, the

Willwood Formation also preserves fossil reptiles, birds, amphibians and plants (Gingerich 2001).

Mammal teeth

Stable isotopes of fossil mammal tooth enamel were analyzed to complement the paleosol carbonate analyses used to develop carbon isotope stratigraphic sections (see Chapter I), confirm the stratigraphic position of specimens within the CIEs, and investigate the paleoecology of these extinct taxa. Due to the precipitation of mammal tooth enamel during ontogenesis, certain teeth may serve as records of an organism's paleoecology, including isotopic information about ingested water and consumed vegetation. This is possible because tooth enamel is composed of "bioapatite," $Ca_5(PO_4, CO_3)_3(OH, CO_3)$, which precipitates in equilibrium with body water (Bryant and Froelich 1995; Kohn 1996; Podlesak et al. 2008). Further, in terms of preservation, enamel is more resistant to recrystallization and post-mortem diagenesis than is bone or dentine due to comparatively smaller amounts of collagen and a larger crystal size (Koch 1997; Kohn and Cerling 2002).

Carbon isotopes in tooth enamel of non-carnivores reflect the $\delta^{13}C$ of consumed vegetation, which tracks $\delta^{13}C_{atmosphere}$ through isotopic fractionation processes associated with photosynthesis (Farquhar et al. 1989; O'Leary 1988; Kohn and Cerling 2002). Oxygen isotopes in mammalian body water ultimately record the isotopic values of ingested meteoric water and, with use of established physical models for a range of mammal sizes, can be used to estimate $\delta^{18}O_{meteoric\ water}$, which is in turn linked to local atmospheric temperature (Longinelli 1984; Bryant and Froelich 1995; Kohn 1996; Podlesak et al. 2008; Kohn and Cerling 2002).

Using tooth size as a proxy for body size, evidence for mammalian dwarfing has been recorded in terrestrial records of the PETM (Gingerich 1989; Clyde and Gingerich, 1998; Secord et al. 2012). Teeth in adult mammals scale proportionally to body size. Out of all tooth positions, the first lower molar (M_1) tends to exhibit the strongest correlation between crown area and body weight across most taxonomic groups of mammals. However, the crown area of other molars has also been shown to be highly correlated to body size (Gingerich 1974; Legendre 1986; Damuth 1990; see Materials & Methods section for further discussion of body size calculations). A high-resolution study focusing on the earliest equid *Sifrhippus* demonstrated a decrease of at least 30% in body size during the first 130,000 years of the PETM, followed by a 76% rebound in body size during the recovery phase of the PETM (Secord et al. 2012). It is possible that the PETM records may begin on an unconformity within the central and southern Bighorn Basin, and, as a result, early PETM fossil records may not encapsulate the true extent of dwarfism. Assuming pre- and post-PETM environmental conditions were equal, pre- and post-PETM body size could also be assumed as equal. In this case, based on a comparison between mid-PETM and post-PETM body size cited in the high-resolution study of Secord et al (2012), the extent of early equid PETM dwarfing may have reached ~44%.

For the purpose of comparison, our ETM2 and H2 study focuses on body size change in the early equid lineage *Arenahippus pernix (*see Methods section for note on taxonomy). Fossils of early equids are common in lower Eocene deposits of the Bighorn Basin, making a comparison between the PETM and ETM2 hyperthermal events possible. This study further investigated three other commonly occurring mammalian lineages: *Diacodexis metsiacus*, an early rabbit-sized artiodactyl that had cursorial/saltatorial locomotive adaptations (Rose 2006); *Hyopsodus simplex*, a generalist herbivorous archaic ungulate with weasel-like body proportions

(Rose 2006); and *Cantius abditus*, an early frugivorous primate similar to modern lemurs (Rose 2006), although sample sizes for these three lineages were less favorable.

Materials and Methods

Field collection and taxonomic identification

Fossil specimens tend to accumulate in surface exposures along small hills and slopes in the McCullough Peaks region. All fossils discovered at WT and GH were recorded with GPS and collected during summer field seasons from 2009 through 2015. UDC fossils were recorded with differential GPS, and were collected during the summers of 2010 through 2012. All specimens were measured into the nearest established stratigraphic section, and cataloged in the University of Michigan Museum of Paleontology. These data were then transferred to an existing relational database that is used to organize paleontological information. Fossils are often found *in situ* as they erode out of the outcrop. A study focused within the PETM interval at Polecat Bench in the Bighorn Basin has shown that there is potential for some down-slope movement of fossils after erosion (Wood et al. 2008). The amount of down-slope movement is dependent on variables such as erodibility of the fossil source horizon's rock type, and the length in time that the source horizon has been exposed to such erosion. Other factors likely include topographic characteristics such as slope angle (Rick 1976). Such down-slope mixing would tend to increase the variance of observed body sizes within stratigraphic horizons and thus dampen any body size patterns that may be observed (Wood et al. 2008).

All specimens that were included in this study were identified as being from within one of the following four species based on the morphological characteristics available: *Arenahippus pernix* (Gingerich 1991), *Diacodexis metsiacus* (McKenna 1960), *Cantius abditus* (Gingerich

1981), and *Hyopsodus simplex* (Loomis 1905). These taxa have been thought to be part of anagenetic lineages that evolved through the early Eocene in the Bighorn Basin and thus are typically referred to as chronospecies (Gingerich 1977, 1981, 1989, 1991, 1994; Fricke et al 1998). Some disagreement exists over the best taxonomy to use for some of these taxa (e.g., Froehlich 1999, 2002), however, the morphological continuity of these lineages is well established based on the densely sampled stratigraphic and paleontological record available in the Bighorn Basin (Gingerich 1981, 1991, 1994; Rose 2006;).

Sampling for isotopic analysis

Stable isotope results from *Arenahippus* tooth enamel are used to complement the stable isotopic results from pedogenic carbonates. Isotopic analysis of mammal teeth is restricted to *Arenahippus* because they are the most commonly appearing fossils in mid- to late-Wasatchian field collections of the McCullough Peaks, while also being of a large enough size to yield a sufficient amount of material from each tooth due to the relatively high molar crowns and large tooth area. Isotopic results from tooth enamel are more limited than from carbonate nodules because well-preserved teeth that are conducive to sampling are relatively rare and the method is destructive so sampling was minimized.

Samples of *Arenahippus* tooth enamel were drilled from cheek teeth of the mandible, producing a sufficient sample size of three to four milligrams of enamel powder. The P_4, M_1, M_2, and M_3 tooth positions were all sampled based on previous research suggesting that there are no systematic isotopic changes across tooth rows (D'Ambrosia et al. 2014b). Teeth with clear signs of alteration, wear, or thin enamel were excluded from analysis. Tooth enamel was drilled with the Foredom k.2230 flex shaft rotary drill with diamond tip burrs. Enamel was removed in

vertical strips along the growth axis in order to average out an intra-tooth seasonal signal. Modeled after the methods of Koch (1997), enamel powder was treated with NaOCl followed by 1 M buffered acetic acid (with a pH of ~4.5), both for 24 hours. Before and after the acid treatment, tooth enamel was rinsed five times with deionized water and spun dry in a RevSpin centrifuge for 20 seconds between each rinse. The final step was to dry samples in a 60°C for several hours.

Body size

Tooth measurements were made on teeth of *Arenahippus*, *Diacodexis*, *Hyopsodus*, and *Cantius*. All teeth were collected from localities stratigraphically spanning ETM2 and H2 (see stratigraphic framework established in Chapter I). Using Fowler-Sylvac Ultra-Cal Mark III digital calipers, the length and width of every tooth crown was measured (in mm) three times, and the mean of these measurements was used. Tooth size was converted to body size utilizing a relevant linear regression that is based on the tooth size-body size relationship in all artiodactyls and perissodactyls (Legendre 1986), non-selenodont ungulates (Damuth 1990), and primates (Gingerich 1982; Legendre 1986). These groups were selected for body size conversions because they represent the closest taxonomic groups to the early mammals referred to in this study.

In order to compare all tooth positions on the same scale, non-M_1 tooth area measurements were normalized to their predicted M_1 size using tooth size regressions. The predicted M_1 tooth areas were developed from regressions based on all jaws available with an M_1 and associated M_2, M_1 and associated M_3, and M_1 and associated P_4 (appendix C). In certain cases, very few jaws from a particular taxon have both M_1s and associated M_3s or P_4s, etc. In

this case, a regression was not formulated and the other teeth were not used. For instance, a particular taxon may have many M_1s with associated M_2s, but very few M_1s with associated M_3s, so the M_3 size data were not used. When multiple teeth exist from a single individual (i.e., an observed M_1 and/or multiple predicted M_1s), only the observed M_1 is included in the analyzed data set (or the next "best" predicted tooth is used, based on regression strength). When a single individual with both teeth of the same position exists, an average of the tooth size is used.

Statistical analyses

Moving averages with 95% confidence intervals (CIs) were calculated for tooth size data within each lineage in order to identify stratigraphic patterns. The natural log of each observed and predicted M_1 was plotted against stratigraphic level. A 5-point running mean of tooth size was then applied across the stratigraphic intervals. If multiple teeth occurred at the same stratigraphic interval, an average of the teeth was taken prior to the application of the running mean. Upper and lower 95% CIs were then applied to the 5-pt moving average values.

A simple binning technique was used to calculate the average tooth size, and thus average body size, change across the CIEs. Teeth were determined to be within a CIE if they came from stratigraphic levels with paleosol carbonate $\delta^{13}C$ values of less than -11.5‰. This cutoff value was based on a natural gap in the $\delta^{13}C$ data that lies approximately half way between the lowest CIE $\delta^{13}C$ value (-14.3‰) and highest background $\delta^{13}C$ value (-8.6‰). As a result, the ETM2 CIE falls between 900 and 915 meters above the PETM, and H2 falls between 932 and 939 meters. It should be noted that only two paleosol carbonate values represent the H2 CIE given this criterion, and no tooth specimens from any taxa in our study fall within this limited stratigraphic range.

The natural autocorrelation of tooth size data throughout a lineage makes it difficult to apply standard statistical analyses, so a bootstrapping approach was used here instead. Tooth size data from each lineage were bootstrapped to determine if pre-CIE tooth sizes were significantly different from CIE tooth sizes and if CIE tooth sizes were significantly different from post-CIE tooth sizes. Tooth size data from each lineage were binned into pre-CIE, CIE, and post-CIE groups according to the criteria outlined above. The number of tooth size data points in each bin was determined for a given lineage ($N_{pre\text{-}CIE}$, N_{CIE}, and $N_{post\text{-}CIE}$). The original data set for each lineage was then resampled with replacement (bootstrapped) 1000 times, creating subsamples with the same $N_{Pre\text{-}CIE}$, N_{CIE} and $N_{Post\text{-}CIE}$ as the original sample. At each iteration, the difference was calculated between the means of the bootstrapped subsamples. The distribution of the differences between the means of the bootstrapped subsamples was then used to determine the significance of the observed difference between the means of the pre-CIE, CIE, and post-CIE tooth size subsamples. Observed differences falling in a 2.5% tail of the bootstrapped distribution were considered significant. No teeth for any of the studied taxa were found in the H2 CIE so this approach could not be used to study that hyperthermal.

Results

Arenahippus tooth enamel $\delta^{13}C$ from GH and WT exhibited the lowest values of −15.0‰ at 910.4 meters, within the ETM2 CIE, indicating these fossils are in fact associated with the hyperthermal events identified in the surrounding paleosol carbonate nodule records (fig. 2-1, appendix D). While $\delta^{18}O$ of the same *Arenahippus* tooth enamel appears to respond to ETM2 warming, there is a large amount of variability in the data (average ETM2 $\delta^{18}O \pm 2\sigma$ is 20.6±3.5‰), which is also the case during the PETM (24.1±3.5‰; fig. 2-1, appendix D; Secord

et al. 2012). This variability likely reflects the impact of aridity on leaf water $\delta^{18}O$, or the impact of multiple seasons of birth on $\delta^{18}O$ of molar tooth enamel (Levin et al. 2006; D'Ambrosia et al. 2014b).

When comparing ETM2 $\delta^{13}C$ paleosol carbonate ($\delta^{13}C_{pc}$) records to the observed and predicted M_1 tooth size patterns of *Arenahippus*, it is clear that tooth size exhibits a short-term decrease within the same stratigraphic bounds as ETM2 (fig. 2-2, appendix E). Just prior to the lower stratigraphic boundary of ETM2 (~899 meters) the natural log of *Arenahippus* average tooth area (±2σ) is 3.63±0.25 (equal to 37.71 mm^2) corresponding to an estimated body size of ~7.70 kg (table 2-1; Legendre 1986). *Arenahippus* then decreases in size by ~14% to an ln(tooth area) of 3.53±0.30 (34.12 mm^2) , or ~6.60 kg as the ETM2 CIE peaks around −14‰ $\delta^{13}C_{pc.}$. As the CIE recovers to background $\delta^{13}C_{pc}$, *Arenahippus* rebounds ~20% in size to 3.65±0.46 (38.47 mm^2), or ~7.93 kg. The pre-CIE to CIE decrease in *Arenahippus* body size is significant ($p = 0.016$) using a bootstrapping analysis (see "Statistical analyses" under the Materials and Methods section).

Though data are more limited for *Diacodexis*, *Hyopsodus* and *Cantius*, both *Diacodexis* and *Cantius* follow similar trends to *Arenahippus* in terms of a body size decrease occurring concordantly with the ETM2 CIE (fig. 2-3, appendix E). *Diacodexis* shows a statistically significant ($p = 0.010$) pattern very similar to *Arenahippus* between the pre- and mid-ETM2 records, beginning with an average ln(tooth area) of 2.63±0.14 (13.87 mm^2), approximating to a body size of 1.62 kg, and then decreasing by ~15% to an average ln(tooth area) of 2.53±0.31 (12.55 mm^2), approximating to a body size of 1.37 kg within ETM2 (table 2-1). Barring some anomalously small tooth sizes found at the 851–852 meter level in the *Cantius* dataset, these

primates show their smallest ln(tooth area) of 2.82±0.18, or 16.78 mm^2 within the peak $\delta^{13}C_{pc}$ values of the ETM2 CIE, however that change is not significant (p = 0.315).

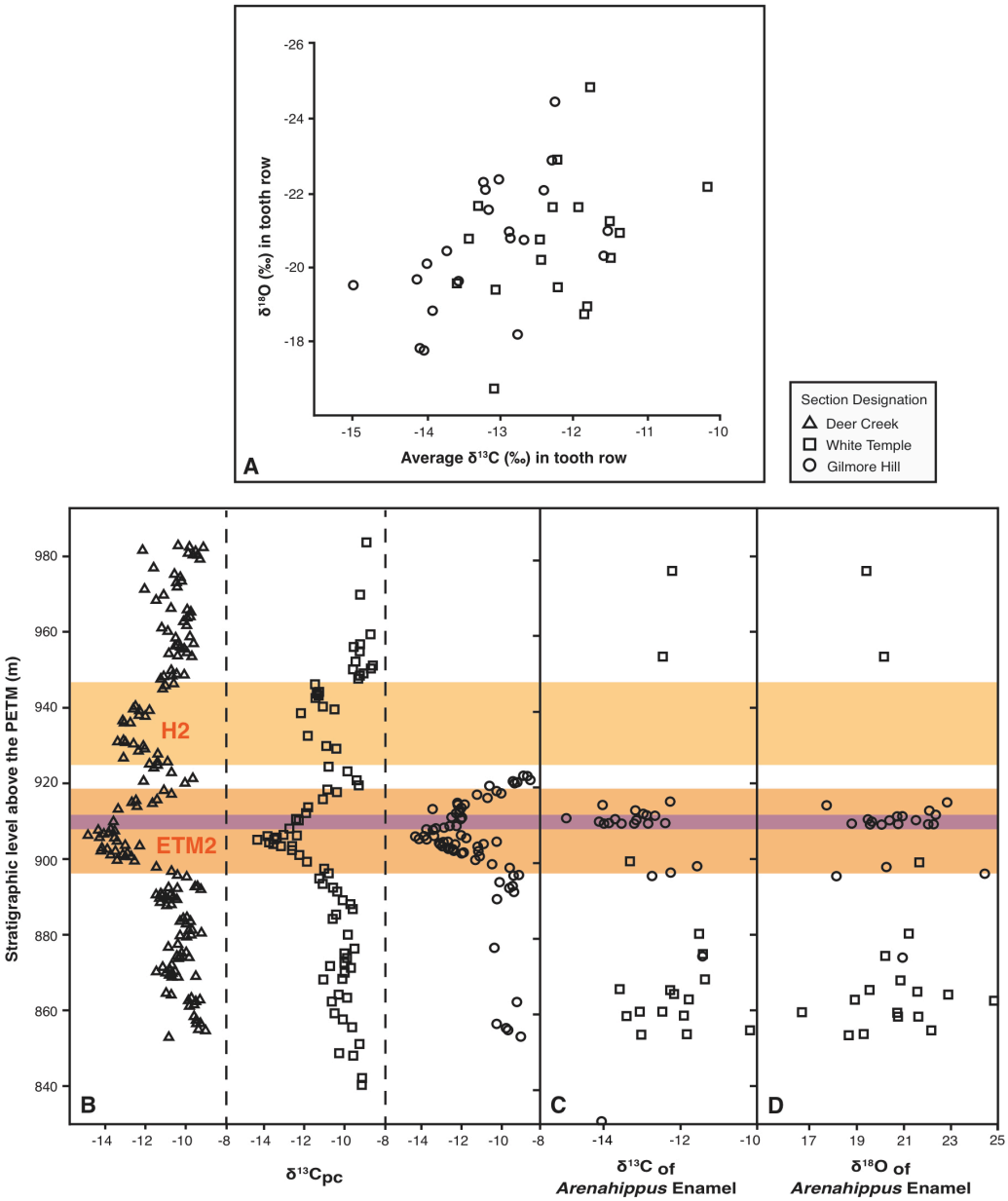

Figure 2-1. Carbon and oxygen isotope data from *Arenahippus*. Top scatter plot (A) represents $\delta^{13}C$ vs. $\delta^{18}O$ for tooth enamel samples from this study showing a weak but significant correlation ($p<0.05$). Bottom figure describes (B1) $\delta^{13}C$ from paleosol carbonate nodules from three sections highlighting the P2 marker bed (purple line), and ETM2 and H2 CIEs, plotted next to $\delta^{13}C$ and $\delta^{18}O$ of *Arenahippus* tooth enamel (B2, B3 respectively). Note that $\delta^{13}C$ in enamel show the CIE but $\delta^{18}O$ does not show a clear excursion, which could indicate offsetting fractionation effects or diagenetic oxygen exchange.

Hyopsodus exhibits no clear change in body size through ETM2. Pre-ETM2 specimens exhibit an ln(tooth area) of 2.21±0.18, or 9.12 mm^2. *Hyopsodus* then shifts to 2.22±0.25, or 9.21 mm^2 going into mid-ETM2 levels—a scant and statistically insignificant 0.01 natural log unit difference (p = 0.651; table 2-1). Sample sizes in the post-ETM2 bin were very small (n = 1 to 7) so the statistical power for those tests is very low. The resulting body size changes from ETM2 to post-ETM2 for all taxa were therefore insignificant. No teeth for any of the studied taxa were found in the H2 CIE so no analyses of body size change across H2 could be performed.

Table 2-1. Binned average tooth size and body size estimates across ETM2.

Taxon	Bin	*n*	Average Tooth Size [ln(l × w)]	95% Confidence Interval*	Body Size Estimate (kg)		Natural Log (ln) Unit Difference	P-value	% Body Size Change Between Bins
	Pre	21	3.63	0.25	7.70	*Pre to Mid*	−0.10	**0.016**	−14.3%
Arenahippus†	Mid	29	3.53	0.30	6.60				
	Post	7	3.65	0.46	7.93	*Mid to Post*	+0.12	0.032	+20.1%
	Pre	21	2.63	0.14	1.62	*Pre to Mid*	−0.10	**0.010**	−15.0%
Diacodexis†,‖	Mid	12	2.53	0.31	1.37				
	Post	4	2.71	0.57	1.83	*Mid to Post*	+0.18	N/A	+32.9%
	Pre	23	2.21	0.18	0.78	*Pre to Mid*	+0.01	0.651	+1.94%
Hyopsodus‡	Mid	14	2.22	0.25	0.79				
	Post	2	2.06	0.59	0.62	*Mid to Post*	−0.16	N/A	−7.36%
	Pre	22	2.85	0.25	2.51	*Pre to Mid*	−0.03	0.315	−4.26%
Cantius§,‖	Mid	9	2.82	0.18	2.41				
	Post	1	2.77	--	2.22	*Mid to Post*	−0.05	N/A	−7.79%

Bold p-values are significant, and are based off of bootstrapping analyses described in Materials & Methods section. P-values were not determined for n<5 (N/A). †Body size calculation based off of Legendre (1986) 'artiodactyl + perissodactyl' tooth area-body size regression; ‡ Body size calculation based off of Damuth (1990) 'non-selenodont ungulates' regression; § Body size calculation from Gingerich et al (1982) and Legendre (1986) 'primate' regressions; ‖ Post-ETM2 calculations for Diacodexis & Cantius are based on a single data point. *Equal to two standard deviations (2σ).

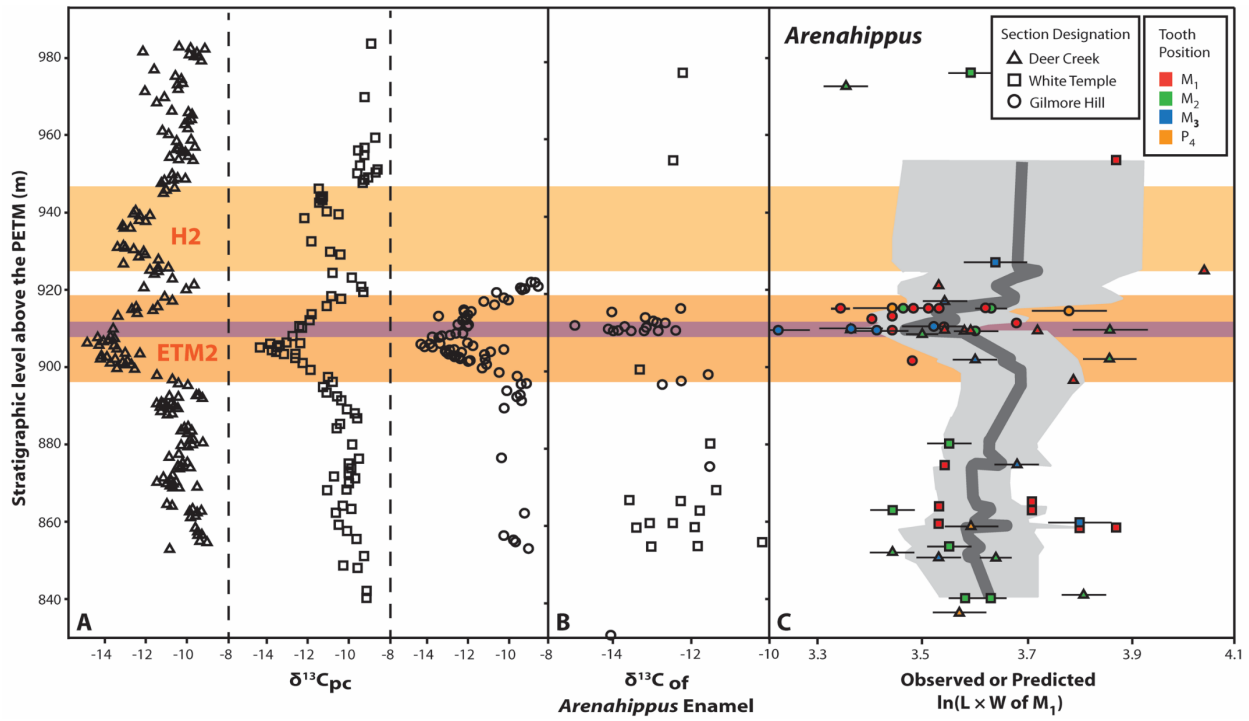

Figure 2-2. Comparison of $\delta^{13}C$ of pedogenic carbonate, $\delta^{13}C$ of *Arenahippus* tooth enamel and *Arenahippus* tooth size. Orange bands represent body of ETM2 and H2 CIEs. Purple band represents the P2 marker bed. Isotopic data from paleosol carbonate nodules are represented in part A. UDC was aligned with GH and WT using the Purple 2 bed (see Figure 1-3). *Arenahippus* tooth enamel carbon isotope values (B), in association with *Arenahippus* tooth sizes (C) were collected across all three McCullough Peaks stratigraphic sections. Tooth size represents the observed M_1 *ln*(tooth area) or the predicted M_1 value based on tooth size regressions. Dark grey line represents a 5-point moving average of all tooth size values, while the light grey shaded region represents the 95% CI for the mean. See figure legend for section and tooth position designations. Black horizontal bars on tooth sizes represent propagated analytical error (2σ).

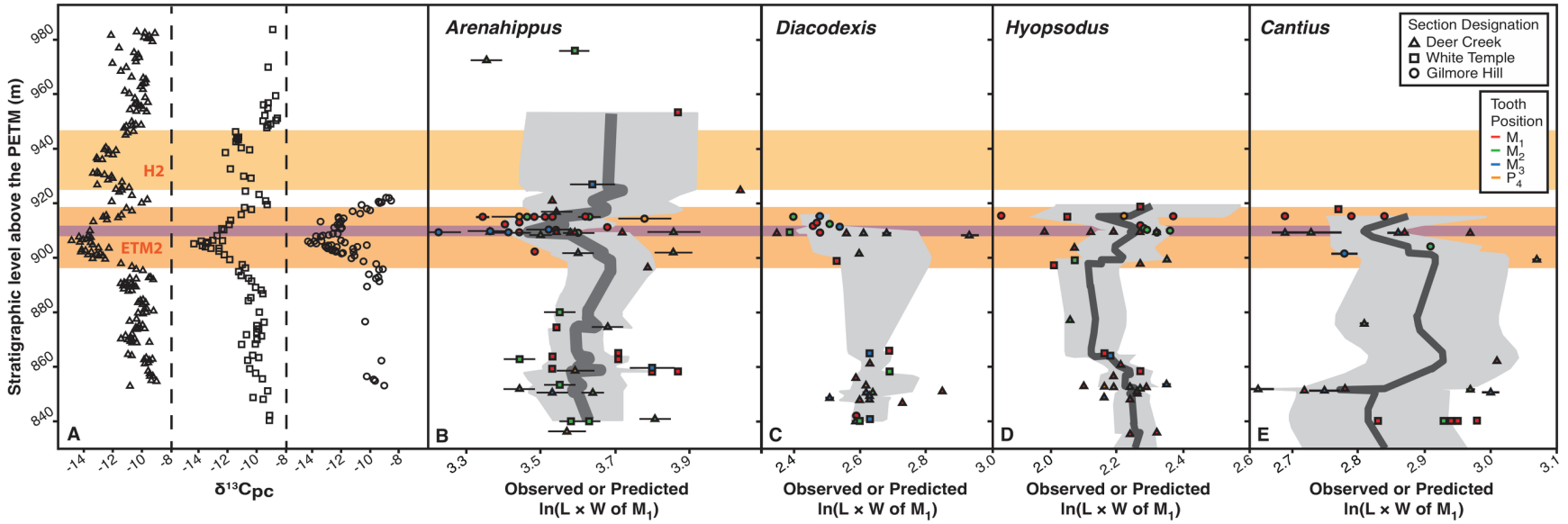

Figure 2-3. Isotopic data from paleosol carbonate nodules (A), *Arenahippus* tooth size (B), *Diacodexis* tooth size (C), *Hyopsodus* tooth size (D), and *Cantius* tooth size (E), across all three McCullough Peaks stratigraphic sections. Tooth size represents the observed M_1 *ln*(tooth area) or the predicted M_1 value based on tooth size regressions. Dark grey lines represent a 5-point moving average of the tooth size values, while the light grey shaded region represents the 95% CI for the mean. See figure legend for section and tooth position designations. Black horizontal bars represent propagated analytical error (2σ).

Discussion

Body size response to ETM2

Arenahippus and *Diacodexis* tooth size data demonstrate statistically significant reductions in mammalian body size during ETM2 greenhouse warming as was found during the Paleocene-Eocene Thermal Maximum (PETM). With only two early Eocene hyperthermals to compare so far, it is not yet possible to determine an empirical relationship between body size and CIE magnitude. However, it is clear that the smaller ETM2 CIE is associated with less extreme dwarfing, while the larger PETM CIE is associated with larger magnitude body size change, suggesting a monotonic relationship**.** The dwarfing pattern is shown most clearly by *Arenahippus pernix*, the best-sampled taxon in our study (n=57). *Arenahippus* decreases in size by ~14% going into the −3.8‰ ETM2 CIE, which is less than the ~30% decrease in body size going into the −5.9‰ PETM CIE (fig. 2-4; Abels et al. 2012; Secord et al. 2012). The precise percent body size change measured across these hyperthermals depends somewhat on how the baseline is chosen but no matter how that is done, the proportional body size change at the PETM is much greater than that at ETM2. Furthermore, given the complex scaling of CIEs detected from pedogenic carbonates compared to marine carbonate (Smith et al. 2007; Schubert and Jahren 2013; Abels et al. 2016), it may be argued that it is instead more appropriate to compare our body size data with marine surface water records of these CIEs as those come closest to atmospheric carbon isotope changes. Additionally, body size changes were driven by environmental changes that were a result of carbon cycle changes of which the carbon isotopes are a derivative, not a direct measure. Either way, our data still suggest a monotonic relationship with the CIE magnitude (fig. 2-4).

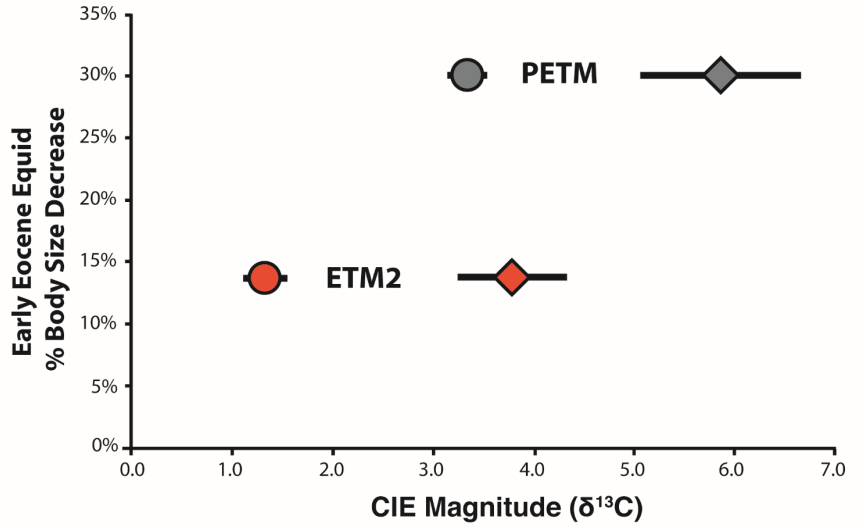

Figure 2-4. Body size changes at PETM and ETM2, compared to both marine (circle) and terrestrial (diamond) expressions of the CIEs. Early equids show a decrease in body size of ~30% at the PETM (Secord et al. 2012), while only decreasing in size by ~14% at ETM2. The PETM was a much larger magnitude event at ~3.4±0.1‰ (benthic foraminifera), and ~5.9±0.9‰ (terrestrial) above background $\delta^{13}C$ levels, while ETM2 was a smaller magnitude event at ~1.3±0.2‰ (benthic foraminifera), and ~3.8±0.6‰ (terrestrial) above background $\delta^{13}C$ levels (Abels et al. 2016).

While this study did observe a decrease in body size for *Arenahippus* and *Diacodexis* during ETM2, measurable teeth for all taxa were less abundant in post-ETM2 stratigraphic levels in these sections, making it difficult to derive meaningful post-CIE body size change estimates. Furthermore, *Diacodexis* and *Cantius* first appeared in the Bighorn Basin during the PETM and their fossils have not yet been reported at high enough resolution to record body size change within the PETM, making pre- to mid-CIE dwarfing comparisons difficult for these taxa. Despite the unavailability of pre- to mid-PETM tooth size data for *Diacodexis* and *Cantius*, it should be noted that their mid- to post-PETM body size decrease of 10 to 14% is much less than for *Sifrhippus* (an early equid closely related to *Arenahippus*) at the PETM (Secord et al. 2012). This suggests that their pre- to mid-ETM2 size decrease would have also been quite small (assuming their post-PETM background size was equivalent to their pre-PETM size). Thus, a smaller body size decrease for these two lineages in this study is not surprising. *Hyopsodus*'

body size did not change significantly going into ETM2, which contradicts the ~46% decrease in body size during the PETM (table 2-1; fig. 2-3; Secord et al. 2012), however this taxon is known from only two specimens before the PETM (Rose 1981) so body size estimates across that CIE are very poorly constrained.

Drivers of body size change

Body size change during periods of climate change is commonly seen throughout historical and geological records among mammals and other organisms (Sheridan and Bickford 2011). For instance, since the last glacial maximum, body size trends in woodrat (*Neotoma* sp.) populations have been shown to track known temperature fluctuations (smaller body sizes associated with warming; Smith et al. 1995). A similar trend was observed in historical records of pocket gophers (*Thomymus talpoides*; Hadly et al. 1998). Both studies concluded that body size responses reflected microevolutionary change. Studies of modern animal populations have also yielded similar body size results. Soay sheep (*Ovis aries*), red deer (*Cervus elaphus*), and California squirrels (*Spermophilus beecheyi*) have all exhibited phenotypic responses to climate change (Post et al. 1997; Blois et al. 2008; Ozgul et al. 2009). The sheep and deer show body size decrease in response to increasing temperatures (Post et al. 1997; Ozgul et al. 2009), whereas the squirrels show a decreased body size in response to decreased precipitation (Blois et al. 2008). Secord et al. (2012) suggested that temperature change might have been the strongest driver of body size change in equids during the PETM. Their results show a strong negative correlation between body size and oxygen isotope values (a proxy for atmospheric temperatures) of mammal teeth from various co-existing lineages (Secord et al. 2012). Both body size and

oxygen isotope datasets exhibited a slight lag behind the $\delta^{13}C$, suggesting temperature rather than pCO_2 (i.e., via plant nutritional quality) was the most direct driver of body size change.

Among the mechanisms proposed for body size change, the prevailing hypotheses often draw on modern observations of Bergmann's rule to argue that homeothermic mammals surviving at higher temperatures and/or lower latitudes generally exhibit a high surface-area-to-volume ratio in order to efficiently release body heat (Gardner et al. 2011; Sheridan and Bickford 2011). In this way, Bergmann's rule can also help explain why shifts to a smaller body size may be a common response to warming higher-latitude regions. Similar to modern day observations, a smaller body size across the early Eocene hyperthermal events may have resulted whether through immigration of smaller lower latitude members of the taxon's population, or as an anagenetic response of the lineage as a whole – or some combination of the two (Gingerich 2003, 2006; Burger 2012; Secord et al. 2012; Rankin et al. 2015).

Nutrient availability, along with, and as a consequence of, rising temperatures and drought, may also have a direct effect on body size. Assuming that a negative CIE equates to high pCO_2, decreased water and nutrient availability associated with increased pCO_2 and temperature levels could limit plant growth, and thus the body size of consumers (Sheridan and Bickford 2011). Nutrient availability in soils can be further affected by increasing temperatures, drought, and associated wildfires. This results in soil nitrogen losses, leading to even further reduced plant growth and net primary productivity (Vitousek et al. 1982; Sheridan and Bickford 2011). Ultimately, primary consumers may exhibit a reduction in body size.

Studies of modern lineages of plants, birds, and mammals indicate that reproductive biology, specifically short generation times, may amplify size declines in association with rising temperatures and drought. For instance, drought conditions have been known to lead to smaller

offspring (Franks and Weis 2008; Sheridan and Bickford 2011). Given the close relationship between body size and generation time in mammals, it is possible that as temperatures and/or droughts increase, smaller mammal body size will ensue, followed by shorter generation times, leading to a positive feedback cycle.

Lastly, it is possible that differing precipitation patterns between the two hyperthermal events may have controlled differences in body size change at the events, though the nature of the differing precipitation patterns is not clear. Hydrological records of the PETM suggest more variable and overall drier soils, which are likely linked to precipitation changes (Kraus et al. 2013, 2015). Less precipitation may have exacerbated the dwarfing response during the PETM —first in terms of type and quality of consumed vegetation, and second in terms of offspring size. In contrast, hydrological records of ETM2 suggest an increase in soil moisture during this event (Abels et al. 2016), perhaps mitigating the dwarfing response. In the same way that the fundamental carbon cycle causes of the PETM and ETM2 may be different (Kirtland Turner 2014; Abels et al. 2016), the mechanism for body size change at the two events may also be different. Irrespective of the exact mechanism, however, it is clear that body size dwarfing in some mammal lineages is closely linked with hyperthermals and may be a common response. This suggests dwarfing will be a likely natural response for some mammals to future global warming.

CHAPTER III

TESTING RANGE SHIFT AS AN EXPLANATION FOR HYPERTHERMAL MAMMAL BODY SIZE CHANGES

Introduction

Previous work has suggested that decreases in mammal body size may be a common response to rapid global warming events. For instance, fecal pellets collected from woodrat (*Neotoma cinerea*) paleomiddens spanning the last 25,000 years showed signs of a body size-temperature relationship, with body size decreasing during warming episodes (Smith et al. 1995). During the Paleocene-Eocene Thermal Maximum (PETM; ~56 mya), early equids decreased in body size by 30% (Secord et al. 2012) in response to ~5-8 degrees Celsius of warming in less than 130,000 years (Fricke et al. 1998; Fricke and Wing 2004; McInerney and Wing 2011; Secord et al., 2012). During a subsequent hyperthermal event known as ETM2 (~54 mya), the same lineage of equids decreased in size by ~14% in response to ~3 degrees Celsius of warming over ~40,000 years (Lourens et al. 2005; Stap et al. 2010; Abels et al. 2015; D'Ambrosia et al. 2017). These results suggest that the extent of mammal body size decrease may scale with the magnitude of a hyperthermal event (see Chapter II and D'Ambrosia et al. 2017). Here, I test whether a northward geographic range shift of smaller-sized early equids may account for the body size decrease associated with PETM and ETM2, rather than an *in situ* body size change.

Recent studies have found evidence for body size decrease in modern mammals as a potential response to modern day climate change. For example, moose (*Alces alces*) of Isle Royale National Park are developing smaller body sizes, as estimated by skull size, in response to increasing winter temperatures (Hoy et al. 2018). This study, which included four decades of data, also found a significant decrease in life span, suggesting that the phenotypic response of body size may not necessarily be adaptively successful. Adult body mass of moose in Sweden has been shown to correlate with latitude, with climate conditions appearing to be the major drivers behind such growth patterns (Sand et al. 1995). Norway's red deer (*Cervus elaphus*) populations show a similar relationship between body size and winter temperatures (Post et al. 1997). Deer born following warm winters were smaller than those born after cold winters, suggesting climatic conditions can influence *in utero* development. With shorter and less harsh winters, more smaller-sized and slow-growing Soay sheep (*Ovis aries*) are thriving on the island of Hilda of the St. Kilda archipelago. This has resulted in an increase in their population and changes to their community structure (Ozgul et al. 2009). Finally, California ground squirrels (*Spermophilus beecheyi*) have demonstrated a significant correlation between body size and precipitation since the last glacial maximum (~26.5 kyr to 19.0-20.0 kyr; Clark et al. 2009), with smaller sized individuals found in association with drier conditions (Blois et al. 2008). While these examples illustrate that body size decrease is often associated with warming temperatures, the particular mechanisms and time scales associated with such changes vary across taxa and locations.

Ecological drivers and processes influencing body size response to climate change

Despite the many examples of decreasing mammal body size during periods of global warming, the exact cause of this association remains unclear. There are many potential abiotic and biotic factors that could influence mammalian body size response to climate change. Because individual taxa survive and reproduce under unique limiting factors that define their niche, exact drivers can be difficult to isolate— especially in examples from the fossil record, considering sample size and stratigraphic resolution issues. Studies of modern mammals dwarfing in response to environmental change posit abiotic drivers such as temperature, precipitation, and seasonality, and biotic drivers such as primary productivity, and prey competition (James 1970; McNab 1970; Geist 1987; Millar and Hickling 1990; Thurber and Peterson 1991; Sheridan & Bickford 2011; Orcutt & Hopkins 2016). Gingerich (2003) suggested that decreased nutritional quality of forage due to increased CO_2 levels could play a major role in observed body size shifts (Fajer et al. 1989; but see Habeck and Lindroth 2013 for a discussion of body size decrease in response to impacts of ozone on vegetation quality).

Response to these abiotic and biotic drivers can be varied, including: (i) phenotypic plasticity, or how an organism responds to the environment through a non-permanent phenotypic change, (ii) anagenesis, permanent adaptive evolutionary change within a lineage, and/or (iii), geographic range shift, with a taxonomic group tracking shifting environmental changes, or a physical displacement of one population of organisms by another within the same ecocline (Koch 1986; Rankin et al. 2015; Burger 2012; Orcutt and Hopkins 2016). For example, a positive correlation between body size and latitude is observed in many mammals today (often referred to as "Bergmann's Rule"; Bergmann 1847), and is commonly thought to be based on a thermoregulatory response in endotherms across latitudinal temperature gradients. As latitudinal

temperature gradients shift and become less extreme due to climate change, it is possible that smaller individuals occupying lower latitudes may shift their ranges northward.

Here, I test whether the occupation of Bighorn Basin by dwarfed equids during the PETM and ETM2 hyperthermals may have been the result of a northward range shift rather than an *in situ* change in body size. The range shift interpretation requires that early horses were widespread and their body size distribution followed Bergmann's Rule. Early Paleogene fossil equid specimens have been found as far north as the northern Bighorn Basin in Wyoming, and as far south as the San Juan Basin of New Mexico, exhibiting a wide geographic range. This study uses the latitude-body size relationship of modern analogs to the early Eocene horses in order to elucidate the body size pattern found within the stratigraphic records of the Bighorn Basin. With this in mind, it must first be determined if, and which, modern analogs to early Eocene equids follow Bergmann's Rule. After establishing such a modern analog, the following questions can be investigated: (i) Could geographic range shift in the modern analog account for the observed magnitude of body size change in hyperthermal equids, and if so how much range shift would be necessary? And, (ii) can climatic factors explain the latitudinal body size gradient of the modern analog, and can this be applied to our understanding of hyperthermal body size change?

Bergmann's rule and range shift in the fossil record

In documenting the latitudinal body size gradient, Bergmann (1847) proposed that body size was correlated with the latitudinal temperature gradient because thermoregulatory pressures for endotherms scale with body size. Larger endothermic organisms have a low surface area-to-volume ratio and are thus able to better retain heat which is advantageous in cooler higher latitudes. In contrast, because smaller organisms have a larger surface area-to-volume ratio they

lose heat more readily and thus have a difficulty staying warm and are better adapted to warmer lower latitude regions. Bergmann's rule, the increase in body size with increasing latitude, has been recorded in many modern birds and mammals both through comparison among species and within lineages (Ashton et al. 2000; Meiri and Dayan 2003; Blackburn and Hawkins 2004). However, recent studies question Bergmann's proposed mechanism either suggesting the relationship between body size and temperature is much more complex (Lovegrove and Mowoe 2013; Orcutt and Hopkins 2013), or postulating alternative hypotheses for the relationship between body size and latitude including ecological character release and dispersal (McNab 1971; Geist 1987, Meiri et al. 2004; Riemer et al. 2018). Non-climate hypotheses have gained traction as Bergmann's rule has been documented in vertebrates that are not endothermic (see Millien et al. 2006).

The fossil record provides numerous examples of taxa that shift their geographic ranges during periods of climatic change. For example, many Pleistocene (2.588 Mya to 11.7 kya) flora and fauna shifted their ranges in response to global environmental changes like glaciations and climate change-induced vegetation changes, especially since the early Holocene (11.7 kya to present; see review by Brown et al. 1996; Lyons 2003, 2005). Via fossil evidence, the most common range shifts involved the displacement of southern populations by northern populations, or with lower elevation taxa displaced by montane taxa, such as with the yellow-cheeked vole (*Microtus xanthognathus*), northern bog lemming (*Synaptomys borealis*), arctic shrew (*Sorex arcticus*), and the collared lemming (*Dicrostonyx*; Graham 1986). While less common, some taxa extended their ranges northward towards the end of the Late Pleistocene, including jaguars (*Felis onca*), woodrats (*Neotoma*), and ground squirrels (*Spermophilus*; Graham 1986).

The early Paleogene (beginning 66 Mya) also represented a time of major faunal turnover within the terrestrial record, with many new lineages of mammals appearing for the first time in the North American fossil record, including 'artiodactyla', peryssodactyla, and primates (see reviews by Gingerich et al. 2003, 2006). It is hypothesized that many of these taxa immigrated to North America via high-latitude land bridges when Earth's temperatures were warmer than average and biogeographic ranges could be widened (Gingerich et al. 2003, 2006). Evidence of northward range shifts in early Eocene mammals has been observed in at least two different North American taxa. *Meniscotherium,* a dog-sized condylarth, commonly found in PETM and post-PETM strata of Colorado, and New Mexico is purported to be an early Eocene immigrant taxon (Gingerich 1982a, 1989; Williamson & Lucas 1992; Dirks et al. 2009). However, in contrast to most other immigrant taxa of this period, its lack of fossil evidence from post-PETM northern Bighorn Basin records implies that *Meniscotherium* may have only appeared during the PETM as a result of a brief northward range shift (Gingerich & Smith 2006). Fossil evidence spanning the late Paleocene in Colorado to early Eocene in Wyoming, also suggests that *Ectocion parvus*, an early phenacodontid, shifted its biogeographic range Northward during the PETM (Gingerich 2003; Burger, 2012). These examples suggest that a similar biogeographic range shift in early equids could explain the observed body size decrease in Bighorn Basin records, especially during ETM2, when equids were clearly already established within North America.

Materials and Methods

Early equids and Modern analogs

In order to test whether range shift can be a viable explanation for the early equid body size changes observed during Paleogene hyperthermals, this study identifies a modern analog to early equids that exhibit Bergmann's Rule. The geographic range expanse of the modern analog is then used to calculate a modern relationship between latitude and body size.

The early equids referred to in this study include *Sifrhippus grangeri*, *Sifrhippus sandrae* and *Arenahippus pernix.* These early equids were similar to modern horses in that they had long limbs with some cursorial adaptations (Radinsky, 1969; Rose, 2006), but unlike modern horses in that they exhibit a brachydont dental morphology, suggesting a diet of fruits, seeds, and leaves (Gingerich, 1981; Rensberger et al., 1984; Janis, 1990; MacFadden, 1992, 2000), and are generally considerably smaller. Paleoenvironmental analyses suggest they dwelled in open-canopy forests (Secord et al., 2008).

Salounias & Semprebon (2002) suggested that the Yellow-backed Duiker (*Cephalophus silvicultor*) was the closest living analog to the early Eocene equids based on dental microwear characteristics. However, an adult *C. silvicultor* is estimated to weigh in between 45 and 50 kg, suggesting it was much larger than *S. granger*, *S. sandrae*, or *A. pernix*, which were estimated to weigh in between 3.9 and 7.9 kg throughout the early Eocene (Secord et al., 2012; D'Ambrosia et al., 2017; see Chapter II). With both body size and life history in mind, these earliest Eocene equids were perhaps most similar to the Blue Duiker and Maxwell's Duiker (*Philantomba monticola* and *Philantomba maxwellii*, respectively), and to a similar African antelope taxon, the dik-dik (*Madoqua* spp.). *P. monticola* are estimated to weigh between 3.5 and 9 kg (Kingdon 2015), *P. maxwellii* weigh between 8 and 10 kg (Rails 1973), and *Madoqua* weigh between 3

and 6 kg (Kingdon 2015). Because the original formulation of Bergmann's rule was meant to explain genus-level trends (Bergmann, 1847; Watt et al., 2010; Orcutt & Hopkins, 2016), this study will test Bergmann's rule in duikers (*Philantomba* sp.) and dik-diks (*Madoqua* sp.) at the generic level.

Data collection

Duiker and Dik-dik specimens were previously collected during dozens of zoological expeditions to Africa beginning in the late 1890s through early 1990s, and are currently housed at the American Museum of Natural History (New York City), the National Museum of Natural History (Washington, D.C.), and the Field Museum of Natural History (Chicago). After access to these specimens was granted, I collected geographic data and tooth measurements (used to estimate body size), in order to better understand duiker and dik-dik body size relationships with latitude (Appendices E and G). The length and width of every first lower molar (m/1) crown was measured using Fowler-Sylvac Ultra-Call Mark III digital calipers. This measurement was taken three times and the average value was recorded. Measurements of the m/1s are collected because allometric scaling of m/1s has shown that they are the best tooth position for estimating adult mammal body size (Gingerich et al. 1982), and they are useful in making direct comparisons to the fossil data which were also used to estimate body size using m/1s. Care was taken to exclude deciduous teeth of juveniles. Locality information was collected with each specimen, and from this location, geographic coordinates (latitude, longitude) were estimated (Fig. 1; Appendices E, F). Locality information represents the center of each individual specimen's home range, which is estimated between 2.5 and 4 hectares for *Philantomba* (Estes 1991), and 4 to 6 hectares and 8.5 to 13.7 hectares for *Madoqua* (Kingswood and Kumamato 1996), with larger ranges

coinciding with the dry season. There were 172 specimens of *Philantomba* measured, representing a latitudinal range of 9.0°N to 15.5°S. There were 125 specimens of *Madoqua* measured, representing a latitudinal range of 11.4°N to 11.2°S.

To test whether each genus follows Bergmann's Rule, a bivariate linear regression analysis of the natural log (ln) of m/1 tooth area on latitude was performed. Because these genera span latitudes north and south of the equator, "absolute latitude" was calculated and used in this analysis so that all specimens could be compared at once. Specimens collected north of the equator and collected south of the equator were also analyzed separately.

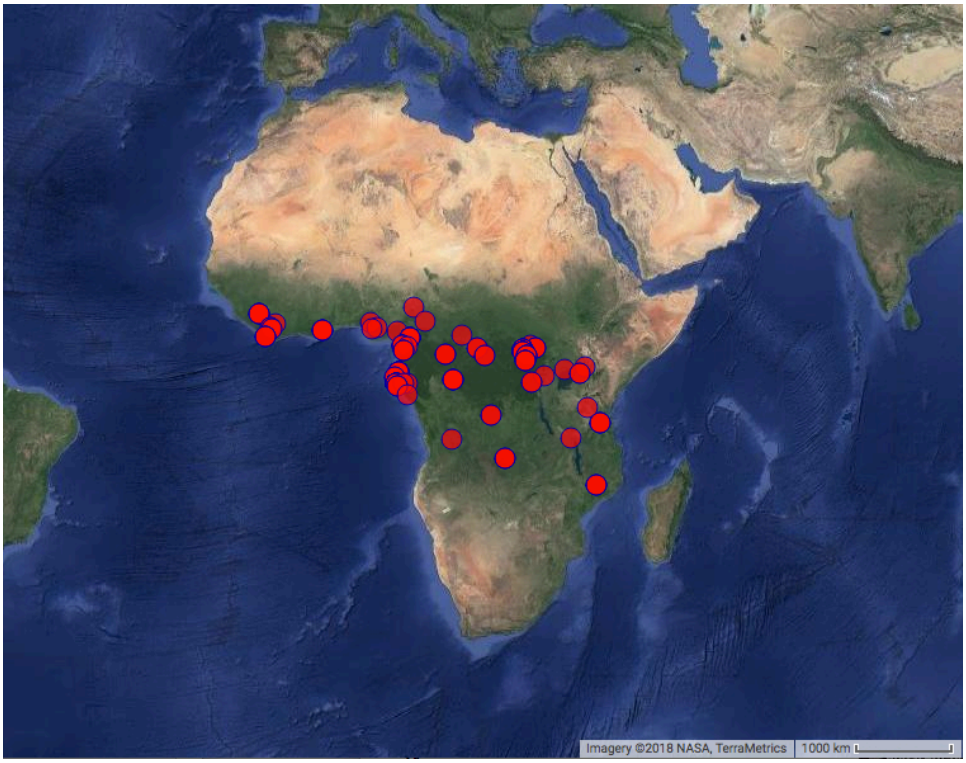

Figure 3-1. Locations of *Philantomba* specimens (red dots) across the African continent that were measured for this study (superimposed on Google Earth imagery). 172 specimens were measured representing a latitudinal range of 9.0°N to 15.5°S. Many specimens shared localities.

For each locality, the following climate data were extracted from the WorldClim database (~1 km resolution, www.worldclim.org): mean monthly temperature (in which the coldest month mean temperature and warmest month mean temperature were used), mean annual temperature, mean annual precipitation, and temperature seasonality (representing temperature variation over a year, based on the standard deviation of monthly mean temperatures; Appendix F). For a complete description of methods used to collect and interpolate the WorldClim dataset see Hijmans et al., 2005.

Results

Testing for Bergmann's Rule

To test whether *Philantomba* specimens follow Bergmann's Rule (i.e., exhibit a positive correlation between body size and latitude), a bivariate linear regression analysis of the natural log (ln) of *Philantomba* m/1 tooth area on latitude yielded a statistically significant positive correlation ($r^2 = 0.1811$, $n = 172$, $p < 0.0001$; see Table 3-1, Fig. 3-2). A bivariate comparison between latitude and *Philantomba* tooth size for specimens south of the equator (spanning 0.0917°S to 15.4460°S) yielded a statistically significant correlation ($r^2 = 0.1671$, $n = 61$, $p < 0.005$; see Table 3-1, Fig. 3-3). Finally, a bivariate comparison between latitude and *Philantomba* tooth size for specimens north of the equator (spanning 0.1000°N to 8.9952°N) yielded an even stronger statistically significant correlation ($r^2 = 0.3015$, $n = 111$, $p < 0.0001$; see Table 3-1, Fig. 3-3).

The bivariate linear regression analysis of *Madoqua* ln(m/1 tooth area) on latitude yielded a statistically significant *negative* correlation ($r^2 = 0.4636$, $n = 125$, $p < 0.0001$; see Table 3-1, Fig. 3-4). This evidence clearly demonstrates that *Madoqua* do not follow Bergmann's rule. In

fact, they show the opposite body size-latitude relationship. This further demonstrates that many ecological and physiological variables may influence body size. While this result is interesting in and of itself and will be the subject of a future investigation, an attempt to understand this observation is beyond the scope of the current study as it is not useful in that the range shift hypothesis assumes equids followed Bergmann's rule. Furthermore, the fact that not all modern analogs to early Eocene equids follow Bergmann's rule suggests that the equids may not have followed it either. However, this does not mean that Bergmann's rule and range shift are not possible explanations for the hyperthermal body size decrease, and the hypothesis should still be tested. Thus, because the PETM and ETM2 range shift hypotheses assume that early equids followed Bergmann's rule, *Madoqua* will not be considered for further analysis.

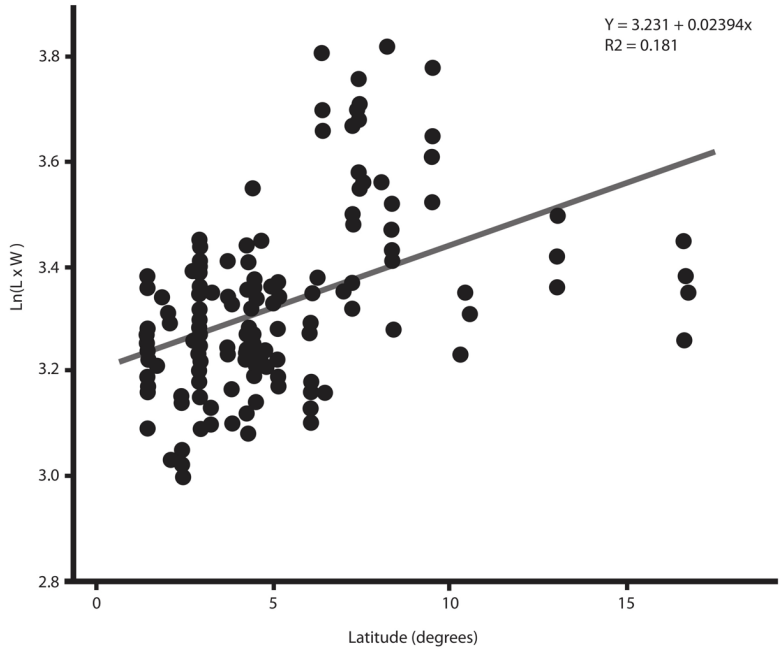

Figure 3-2. *Philantomba* tooth size across all latitudes (in the form of absolute latitude). Note the positive correlation between tooth size and latitude.

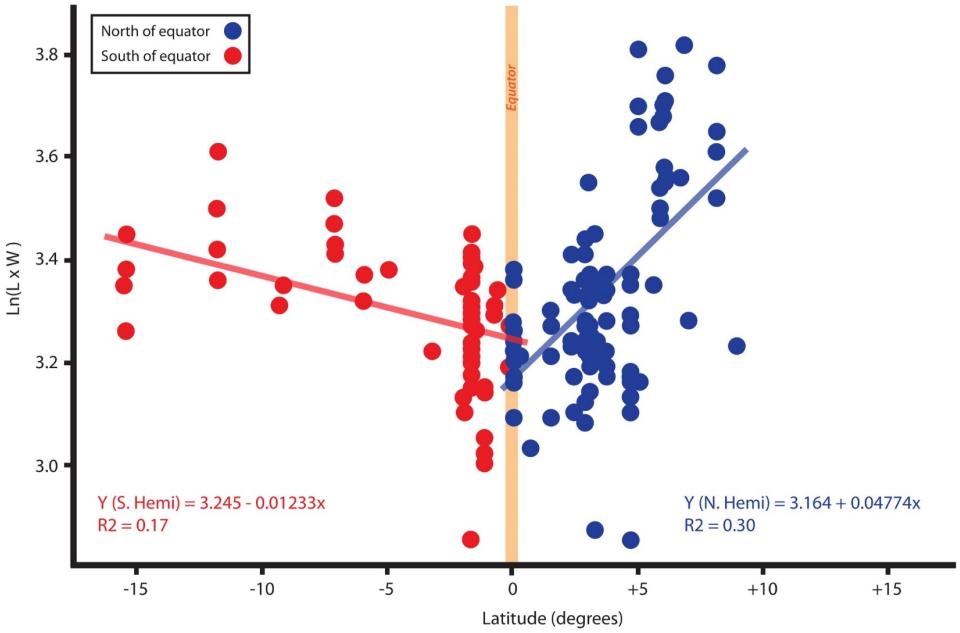

Figure 3-3. *Philantomba* tooth size across northern hemisphere latitudes (blue), and southern hemisphere latitudes (red). Note the negative correlation between tooth size and latitude in both hemispheres.

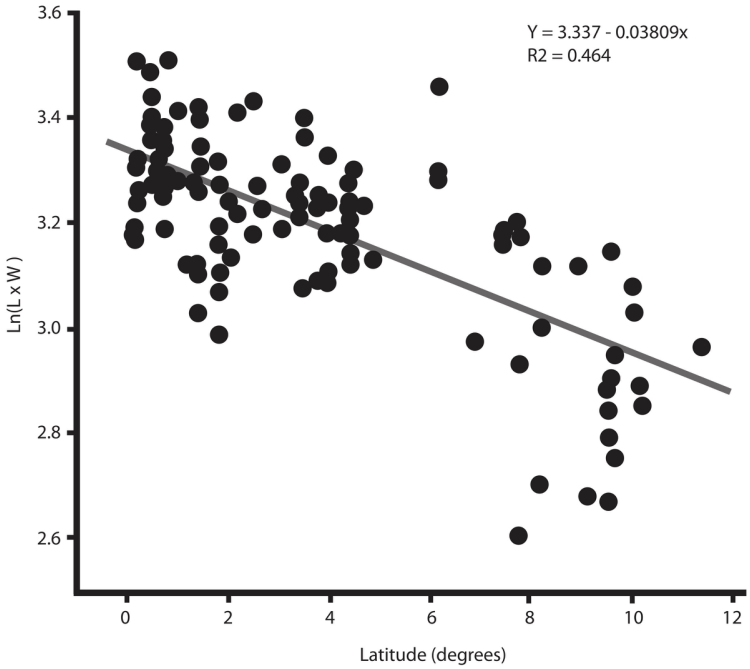

Figure 3-4. *Madoqua* tooth size across all latitudes (in the form of absolute latitude). Note the negative relationship between tooth size and latitude.

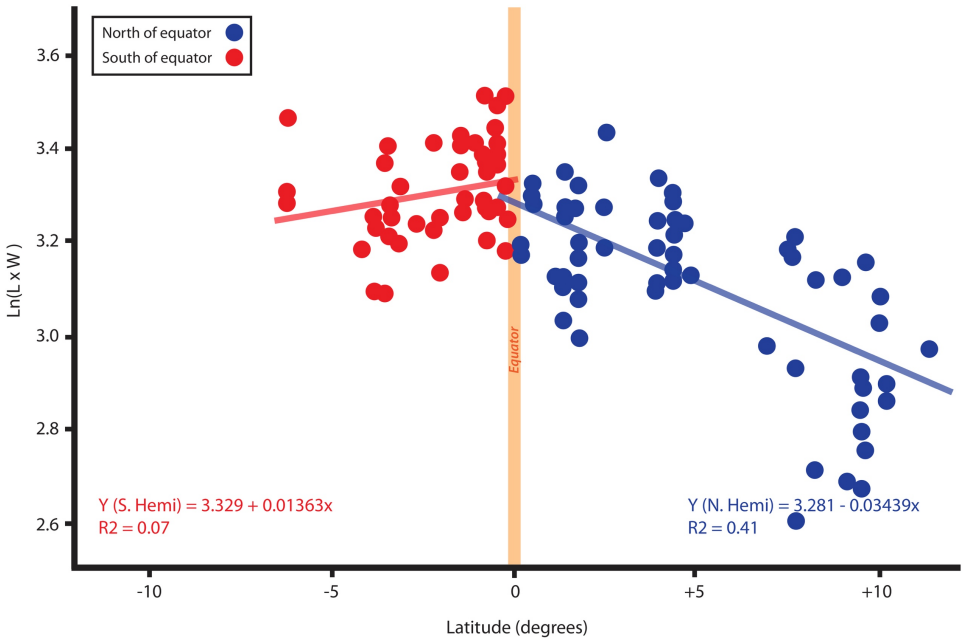

Figure 3-5. *Madoqua* tooth size across northern hemisphere latitudes (blue), and southern hemisphere latitudes (red). Note the negative relationship between tooth size and latitude.

Tooth size, latitude, and the environment

General linear regression analyses were performed to better understand the relationship between *Philantomba* tooth size with latitude, cold month average temperature, warm month average temperature, rainfall, annual mean temperature, and seasonality (see Table 3-2). When considering any latitude formulation (North, South, or the absolute value of latitude), latitude explains between 17% and 30% of the variation in tooth size, with high statistical significance ($p < 0.001$; Figs. 3-2 & 3-3). Longitude does equally well at describing tooth size variation, especially North of the equator ($r^2 = 0.12$ to 0.45; Fig. 3-6A), again with high statistical significance ($p < 0.001$). Mean annual temperature is a statistically significant predictor of tooth size south of the equator ($r^2 = 0.20$, $p < 0.001$; Fig. 3-6B), while cold and warm month mean temperatures south of the equator also describe tooth size variation with high statistical significance ($r^2 = 0.26$, $p < 0.0001$ and $r^2 = 0.18$, $p < 0.001$, respectively; Figs. 3-6C & 3-6D).

Rainfall describes some variation North of the equator ($r^2 = 0.11$, $p < 0.001$; Fig. 3-6E), but less so south of the equator ($r^2 = 0.06$, $p > 0.05$; Fig. 3-6E). In summary, the most important tooth size predictors north of the equator are longitude and latitude. South of the equator, the most important tooth size predictors are cold month mean temperature and mean annual temperature. Each of these variables accounts for ≥20% variation of tooth size ($p < 0.001$). These r-squared values are on the lower end of r-squared values from a similar study on North American mammals by Koch 1986 (ranging from 0.18 to 0.77), aside from the longitudinal effect on tooth size, which is much stronger in this study in north-of-equator specimens.

Estimating the contribution of individual predictor variables to the overall trends in tooth size is difficult because most of the variables are inherently correlated to each other. Strong correlations were found via a multivariate Pearson product-moment correlation matrix between latitude and all obvious temperature variables (in order of strongest correlation to least: cold month mean temperature, mean annual temperature, seasonality, and warm month mean temperature; $r = 0.71$, 0.59, -0.57, and 0.54, respectively; Appendix H). In contrast, precipitation and tooth size are most strongly correlated with longitude ($r = -0.49$ and $r = -0.43$, respectively). In addition, annual temperature was highly correlated with the warmest and coldest month mean temperatures ($r > 0.95$), and warmest month mean temperatures were highly correlated with coldest month mean temperatures ($r = 0.89$).

Table 3-1. Summary of *Philantomba* and *Madoqua* geographic range data. Linear regression statistics are included, which summarize the ln(tooth size) relationship with latitude. Note that *Philantomba* exhibits a positive relationship with latitude, while *Madoqua* exhibits a negative relationship with latitude.

	Sample size	Latitudinal Range		Slope	r^2
Philantomba spp. - Absolute Latitude	172	15.5°S	9.0°N	0.024	0.18
Philantomba spp. - North of Equator	111	0.1°N	9.0°N	0.048	0.30
Philantomba spp. - South of Equator	61	0.1°S	15.5°S	-0.012	0.17
Madoqua spp. - Absolute Latitude	126	11.2°S	11.4°N	-0.038	0.46
Madoqua spp. - North of Equator	68	0.2°N	11.4°N	-0.034	0.04
Madoqua spp. - South of Equator	58	0.2°S	11.2°S	0.014	0.07

Table 3-2. Generalized linear regressions between *Philantomba* M/1 tooth area and environmental variables. For each variable on tooth size, a slope of the regression and coefficient of determination (r^2) is given. Temperature slopes are in °C and rainfall slopes are in millimeters. The probability that the slope is equal to zero is indicated by the following symbols: *** ≤ 0.0001, ** ≤0.001, * ≤0.05. No symbol means ≥ 0.05.

	Latitude		Longitude		Cold Month		Warm Month		Rainfall		Mean Temperature		Seasonality	
Philantomba from...	slope	r^2	slope	r^2	slope	r^2	slope	r^2	slope	r^2	slope	r^2	slope	r^2
North of Equator	0.0477	0.30 ***	0.0106	0.45 ***	0.0040	0.06 *	0.0034	0.07 **	0.0001	0.11 **	0.0033	0.05 *	0.00006	0.004
South of Equator	0.0123	0.17 **	0.004	0.12 **	0.0019	0.26 ***	0.0019	0.18 **	0.0001	0.06	0.0019	0.20 **	0.0001	0.17 *
Absolute Latitude	0.0239	0.18 ***	0.0063	0.19 ***	0.0004	0.0003	0.00009	0.0001	0.00009	0.07 ***	0.0002	0.0007	0.0004	0.009

Stepwise multiple linear regression was used to determine which variables, and in which combinations, might best describe the observed variations in *Philantomba* tooth size. When considering both absolute and northern latitudes, all variables are included in best fit models describing tooth size variation (see Table 3-3), with annual precipitation being the most important variable. The second most important variable for tooth size across absolute latitude is cold month mean temperature, and the second most important term for northern latitudes is warm month mean temperature. In latitudes south of the equator, the best fit model only includes cold month temperature to best describe tooth size variation.

Table 3-3. Stepwise multiple linear regression results for tooth size measurements at all latitudes (absolute latitude), northern hemisphere latitudes, and southern hemisphere latitudes.

Dataset	Steps		β	r^2
Absolute latitudes	1	Annual precipitation	0.56	0.07
	2	Cold month mean temperature	-4.24	0.09
	3	Warm month mean temperature	6.65	0.11
	4	Seasonality	-2.45	0.23
	5	Annual mean temperature	-2.68	0.29
Northern hemisphere latitudes	1	Annual precipitation	0.53	0.11
	2	Warm month mean temperature	9.72	0.15
	3	Annual mean temperature	-1.71	0.22
	4	Seasonality	-4.38	0.35
	5	Cold month mean temperature	-7.95	0.50
Southern hemisphere latitudes	1	Cold month mean temperature	-0.24	0.26

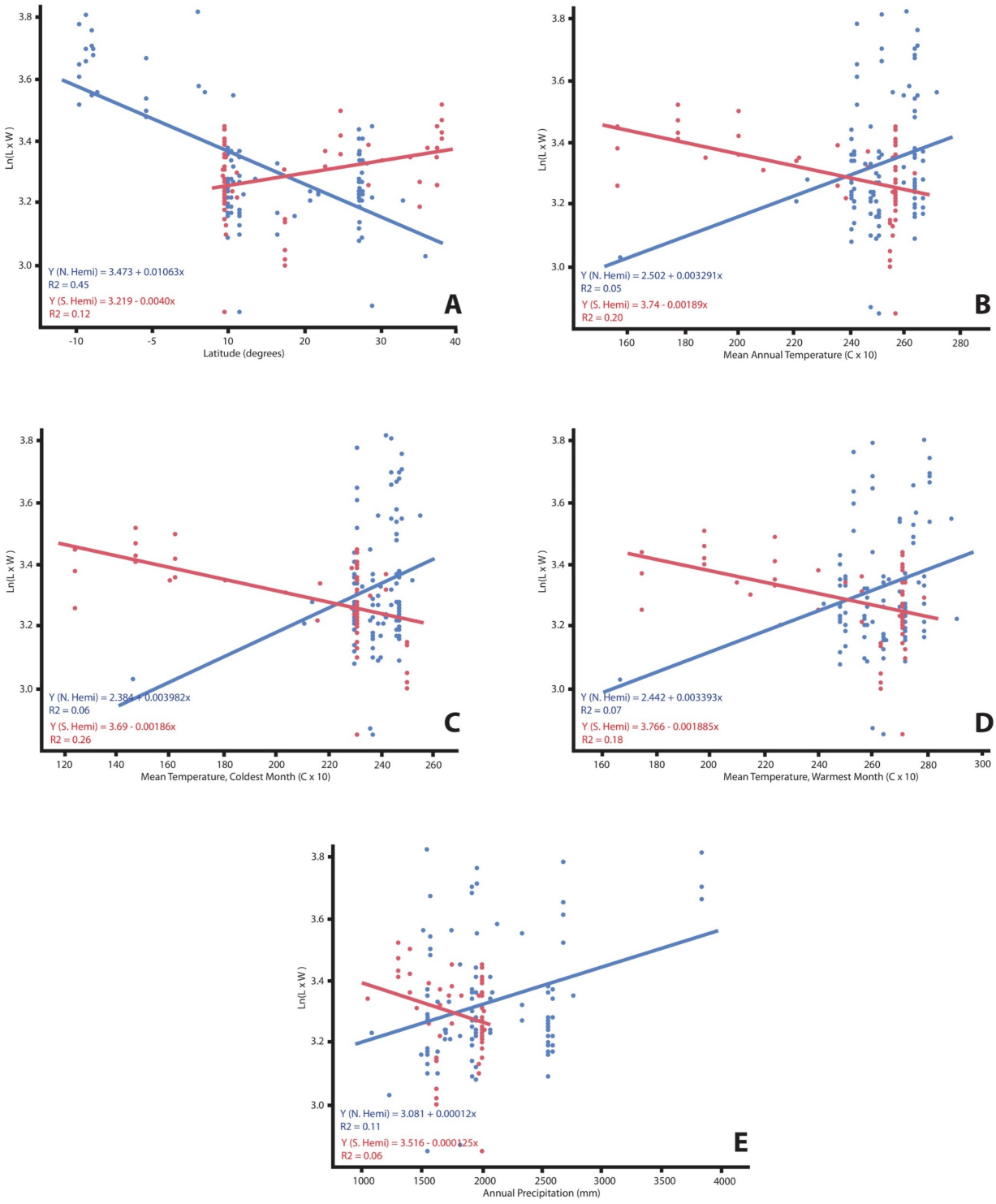

Figure 3-6. *Philantomba* tooth size (ln(area)) versus (A) longitude, (B) mean annual temperature, (C) mean temperature of the coldest month, (D) mean temperature of the warmest month, and (E) annual precipitation. Specimens from northern hemisphere latitudes are blue, and southern hemisphere latitudes are red.

Discussion

Philantomba and Bergmann's Rule

The statistically significant negative correlation between *Philantomba* tooth size and latitude suggests that *Philantomba* does indeed follow Bergmann's rule. *Philantomba*'s biological similarities to the early equids and the fact that it exhibits Bergmann's Rule make it a fitting taxon to test whether the body size changes observed during the early Paleogene hyperthermals could be due to a climate driven range shift. For *Philantomba*, a tooth size range of ln(tooth area) of 2.85 (17.29 mm^2) to a ln(tooth area) of 3.82 (45.60 mm^2) is found over a geographic range spanning a distance of 9.00° north of the equator to 15.45° south of the equator, with lowest tooth size values found at lower latitudes close to the equator and highest tooth size values found at higher latitudes. This translates to a tooth size increase of 0.024 natural log units per degree latitude when considering the absolute value of the latitude range. These observations conform to similar observations between body size and latitude in several modern North American mammal taxa (Koch, 1986; see Table 3-4 for comparison).

Hyperthermal range shifts

If the latitude-tooth size relationship of early equids was similar to that of duikers (the best-known analog), then the difference between their pre- and mid-PETM tooth size values suggests a total latitudinal range of approximately 9.6 degrees. Similarly, the ETM2 tooth size values suggest a geographic range of 4 degrees latitude (Table 3-4). When considering the latitude-tooth size relationships of other extant North American mammals (Koch 1986), these estimate ranges from 7 to 30 degrees latitude and 3 to 13 degrees latitude for the PETM and ETM2, respectively (Table 3-4).

Table 3-4. Summary of *Philantomba* geographic range data compared to North American mammal geographic range data (previously reported in Koch, 1986). This summary includes latitudinal range values, linear regression slopes and correlations (r^2) between tooth size and latitude, the percent of increase in ln(tooth area) across geographic latitude ranges, and the natural log-unit difference associated with this percent increase. Early equid equivalent ranges are calculated from the average ln(tooth area) of equids prior to, and within, the associated hyperthermal event.

								Early equid equivalent geographic range (degrees latitude)	
	n	**Latitudinal Range**		**Slope**	**r^2**	**% increase in tooth size**	**ln difference**	**ETM2**	**PETM**
Philantomba spp.	172	15.5°S	9.0°N	0.0239	0.18	33.6	0.29	4.2	9.6
Odocoileus virginianus	85	10.0°N	47.7°N	0.0140	0.77	53.9	0.43	7.1	16.4
Mephitis mephitis	68	25.6°N	48.3°N	0.0076	0.18	13.4	0.13	13.2	30.3
Scalopus aquaticus	118	29.7°N	45.3°N	0.0327	0.31	45.6	0.37	3.1	7.0
Sciurus carolinensis	166	25.2°N	48.4°N	0.0080	0.24	15.2	0.15	12.5	28.8
Dedelphis virginiana	81	14.9°N	44.3°N	0.0108	0.47	24.7	0.22	9.3	21.3

The PETM would require a northward geographic range shift equivalent to a population moving from the San Juan Basin in New Mexico to the Bighorn Basin, and for ETM2 would require a similar northward range shift from the Piceance Basin in Colorado to the Bighorn Basin. As it happens, both basins preserve early equids similar to those from the Bighorn Basin, so we know that their ranges generally extended that far (van Houten 1945; Gingerich 1991). Therefore, hypothetically, if early equids from the most southern extents of their geographic range shifted into the most northern extents of their geographic range during either of the early Eocene hyperthermals, the entirety of the tooth size decrease observed in the stratigraphic record can be explained.

Though latitudinal temperature gradients of the early Eocene hyperthermals are still debated, both range shift predictions assume that the Earth had the similar temperature gradients as today (Sluijs et al. 2006; Head et al. 2009; Ho and Laepple 2016; Frieling et al. 2017), even during the hyperthermal events. Thus, the range estimates here are probably minima, as a shallower temperature gradient would require greater shifts in geographic range.

Many organisms are already shifting their geographic ranges in response to modern day climate change at rates higher than previously reported (Hicking et al., 2006; Chen et al., 2011). In fact, the median rate of range shift in terrestrial organisms is estimated to be 16.9 kilometers per decade, with mammals exhibiting an even higher range shift range of 19.0 kilometers per decade (Chen et al., 2011). Assuming range shift rates were similar during the PETM and ETM2, a range shift for mammals from the central San Juan Basin to the central Bighorn Basin (~840 kilometers) would take early equids approximately 440 years to complete. A range shift between the central Piceance and Bighorn Basins (~465 kilometers) would take only roughly 240 years to complete. Both range shift completion times are significantly shorter than most

estimates for the onset of the PETM and ETM2 hyperthermals (McInerney and Wing 2011; Stap et al. 2010; Secord et al. 2012; Abels et al. 2012, 2015). Therefore, a range shift response during hyperthermals is not only plausible in terms of the magnitude of the decrease in body size that is observed in the fossil record, but also in terms of the rate of change that is observed.

Body size and the environment

When comparing *Philantomba* tooth size to biotic variables (considering specimens from both north and south of the equator), linear regression models suggest that annual rainfall is the most important predictor of tooth size, followed by cold month mean temperature. This is similar to mammal taxa from North America, in which similar stepwise regression analyses suggest precipitation is the second most important variable, after cold month mean temperature (Koch, 1986). Such North American mammal fauna include opossums (*Didelphis virginiana*), eastern moles (*Scalopus aquaticus*), and eastern grey squirrels (*Sciurus virginianus;* Koch, 1986).

Different environmental variables may act as more important drivers of *Philantomba* body size in northern versus southern populations. *Philantomba* north of the equator exhibit a slightly stronger and more statistically significant correlation between body size and latitude than do *Philantomba* south of the equator. It turns out that the most important variable predicting tooth size for north-of-equator specimens is precipitation, while for south-of-equator specimens the only variable to significantly predict tooth size is cold month mean temperature (Table 3-3 in results). Climatological patterns in Africa make sense of this in that there is a very steep precipitation gradient moving northward from the equator, as latitudes approach warm semi-arid and warm desert climates such as the Sahara, due to the northern extent of the intertropical

convergence zone (ITCZ) reaching 10° latitude (Sultan and Janicot 2000; Suzuki 2011; Köppen Climate Classification System; Figure 3-7). A shallower gradient of humid conditions spreads across a larger geographical distance south of the equator, as latitudes cross tropical savanna and humid subtropical climates (Köppen Climate Classification System). As a result of the ITCZ, a rain belt moves northward into sub-Saharan Africa by August, and moves southward to sub-central Africa by March. Equatorial Africa remains in the rain belt through the entire year, making it the wettest portion of the continent (Sultan and Janicot 2000; Suzuki 2011). These climate patterns support precipitation as the limiting factor for north-of-equator *Philantomba* populations, and a limiting factor other than precipitation in south-of-equator populations. Recent studies have pointed to interactions between temperature and precipitation, even when temperature and precipitation alone are not limiting factors (Smith 2012). Future work looking into *Philantomba* body size drivers should consider interactions that include combinations of such variables, such as the mean temperature of the wettest and driest quarters, and precipitation rates of the coldest and warmest quarters, etc.

Interestingly, these interpretations may also explain why equid body size change was different during the PETM versus ETM2. Hydrological conditions have been found to be quite different during the PETM compared to ETM2. The PETM saw drier soils suggesting less precipitation (Kraus et al., 2013, 2015), and is associated with more extreme equid dwarfism (Secord et al., 2012). On the other hand, ETM2 soils suggest a wetter climate, and also saw less extreme equid dwarfing (Kraus et al., 2013, 2015; D'Ambrosia et al., 2017). Similar to duikers, there was likely more than one climate variable driving Bergmann's rule in the early equids. Therefore, the differing climatic conditions during the two hyperthermals likely had unique influences on the equid body size at those times.

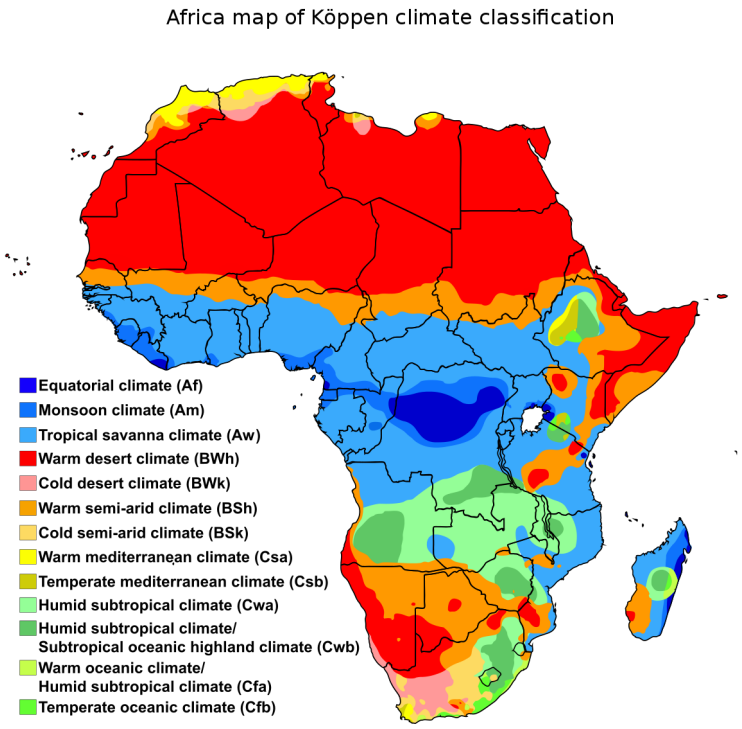

Figure 3-7. Climate zones of Africa based on the Koppen climate classification system (image modified by Ali Zifan, Wikimedia Commons). Note the equatorial region, which remains in a rain belt throughout the year, making it the wettest region of the continent. Also note the steep gradient from equatorial Africa to the arid Saharan Desert climate.

Conclusions

Maxwell's duiker and the Blue duiker of Africa (*Philantomba maxwellii* and *Philantomba monticola*, respectively) are a fitting analog for early Eocene equids, especially in terms of body size and life history. Tooth size data from modern duiker collections suggest they follow Bergmann's rule with duiker body size positively correlated with latitude. This modern analog therefore provides the unique opportunity to inform on whether clinal body size change could be the cause of mammalian dwarfing during early Eocene hyperthermals. If early equids did indeed follow Bergmann's rule to the same extent that duikers do today, they would require a 10° and 4° latitudinal range shift to explain their body size decrease across PETM and ETM2

stratigraphic records, respectively. Based on modern range shift rates, these values are plausible within the approximate 10,000-year time frame it took for PETM and ETM2 to reach their most extreme temperatures. Future work could further test this hypothesis by comparing San Juan Basin and Piceance Basin equid specimen size to Bighorn Basin specimen size in sediments dated to precisely the same time as the PETM and ETM2. One would expect to observe approximately the same difference in body size between basins that is observed across the PETM and ETM2 strata (30% and 14%, respectively).

Drivers of the duiker body size-latitude relationship include precipitation and cold month mean temperatures, and thus could also be major drivers of early equid range shifts. The finding that there are differing climatic controls on body size across a single taxon reinforces the idea that Bergmann's rule may often be controlled by more complex environmental factors aside from just temperature and latitude.

CHAPTER IV

TAXA CO-OCCURRENCE ACROSS THE PETM AND ETM2 HYPERTHERMALS: AN ANALYSIS OF COMMUNITY STRUCTURE IN BIGHORN BASIN FOSSIL ASSEMBLAGES

Introduction

In this chapter, I investigate whether pairwise patterns in taxa co-occurrences were impacted by early Eocene hyperthermals (see Chapters I and II for an in-depth discussion of these events). Understanding which taxa form non-random pairs elucidates processes such as environmental filtering, dispersal, and species interactions. Knowing how these processes changed in the face of ancient rapid climate change may lead to a better understanding of how mammal communities may be impacted by modern-day climate change.

Wyoming's Bighorn Basin lends itself to high-resolution studies of the evolution of many taxonomic groups through the early Paleogene. This is largely due to the thick and stratigraphically-continuous sedimentary deposits which preserve abundant fossil assemblages across thousands of fossils localities. Many studies have focused on effects of climatic and other environmental changes on the evolution of mammals and the biological diversity within and among taxa. For instance, early studies tied mammal diversity change, including turnover, richness, and evenness, to general changes in temperature regimes throughout the early Paleocene and Eocene, and noted major changes in faunal composition and diversity at the

boundary between the Paleocene and Eocene Epochs (Rose 1981, Gingerich 1989), with many taxa appearing in the fossil record for the first time at the beginning of the Eocene, including 'Artiodactyla', Perissodactyla, and Primates. Gingerich (1989) also found that characteristic Paleocene faunas disappeared from the fossil record at the end of the Paleocene, such as the crocodile-like reptile *Champsosaurus* and the early primate-like mammal *Plesiadapis*. Gunnell et al. (1995) observed the taxonomic composition and frequencies of mammal genera across the Paleogene among five major trophic categories: carnivores, herbivores, insectivores, omnivores, and frugivores. They found that the trophic structure and composition of Bighorn Basin mammal taxa changed through the early Paleogene in response to fluctuations between closed, humid forests and open, drier woodlands.

With the discovery of the Paleocene-Eocene Thermal Maximum (PETM) and Eocene Thermal Maximum 2 (ETM2) hyperthermal events (see Chapters I and II for in-depth discussions), more recent studies have focused on impacts of these major climate change events on the structure of mammal communities. Clyde and Gingerich (1998) studied the impacts of the PETM on mammal community diversity, body size structure, and trophic structure. They found an abrupt increase in species richness and evenness at the Paleocene-Eocene boundary (= PETM), with generally larger immigrant species becoming permanent members of Eocene mammal communities (i.e., 20% of the taxa and 50% of the individuals). In addition to this discovery, a short-term, but significant, decrease in body size was observed in many mammal lineages found in association with the PETM, suggesting some relationship between body size and increased global temperatures (Clyde and Gingerich 1998; Secord et al. 2012; D'Ambrosia et al. 2017; see Chapter II). Chew (2009) used species diversity metrics and appearance rates to assess that faunal turnover events (known as "biohorizons") were associated with climatic

variations, including a cooling episode after the PETM and prior to the Early Eocene Climatic Optimum (a longer-term warming event). Further research found an association between faunal change and what may be the ETM2 and H2 warming events (Chew and Oheim 2013; Chew 2015), though direct characterization of these events through local stratigraphic carbon-isotope records was not available to confirm the relationship at the time of that study.

Recently, paleontological and modern studies of plant and animal communities have employed a new null model approach for assessing community assembly which identifies pairwise species associations (Ulrich 2008; Gotelli & Ulrich 2010; Blois et al. 2014; Smith et al. 2015; Lyons et al. 2016; Kohli et al. *in press*). Non-random species pairs can be either segregated (taxa found together less often than random) or aggregated (taxa found together more often than random). Segregated pairs may occur due to negative species interactions, differing habitat preferences, and/or dispersal limitation, while aggregated pairs may occur in response to positive species interactions, similar habitat preferences and shared dispersal traits (Gotelli and Ulrich 2010; Lyons et al. 2016).

Here I present an exploratory analysis of non-random co-occurrence patterns across the PETM and ETM2 hyperthermal events. First, I assess whether there are significant pairs of taxa across the PETM and/or ETM2 events, and whether there is a consistent directional change in the type or number of associations across these events. Second, I assess how these pairwise associations may reflect the processes of environmental filtering, dispersal, or species interactions, and thus inform on the mechanisms structuring community dynamics under climate change.

Methods and Materials

Pairs analysis

Data were analyzed using the FORTRAN programs Pairs (version 1.0) developed by Ulrich (2008). Pairs evaluates matrix-wide patterns of co-occurrence by applying a Bayesian approach to detect non-random associations between taxa. Data are organized into matrices in which the rows are taxa and the columns are sites (or in the case of this study, fossil localities). The numerical entries in the matrix cells represent either presence (1) or absence (0) of a taxon at a particular locality. Pairs then calculates a "C-score" for each possible taxon-pair, which indicates the nature of the taxon association (aggregated vs. segregated), and when converted to a "Z-score" a measure of the association strength. P values for each taxon pair are calculated by randomly reshuffling the matrix 1,000 times, but preserving the column and row totals during each iteration. This is referred to as the fixed-fixed method, and is preferable for fossil assemblages when species richness may vary across localities due to taphonomic or field collection biases (Gotelli et al. 2000; Blois et al. 2014; Lyons et al. 2016). Further, the Pairs program compares a Bayes distribution of co-occurrence scores to the actual distribution of scores in order to identify those well above the null expectation, in order to reduce the false detection error rate.

Mammal fossil data

For the PETM analysis, mammal fossil occurrences were drawn from the Paleobiology Database (www.paleobiodb.org) using the group name 'mammalia' and the following parameters: time intervals = Thanetian and Ypresian, longitude minimum = -111.8, longitude maximum = -104.7, latitude minimum = 43.3, latitude maximum = 45.0. This dataset consists of 142

species occurrences across 97 localities, representing 124 meters of stratigraphy. The PETM data were divided into three bins based on stratigraphic level above, below, and within the hyperthermal event. The pre-PETM bin is composed of the last 45 meters of the Clarkforkian-3 (Cf-3) North American Land Mammal Age (NALMA) zone and represent the very end of the Paleocene. The mid-PETM bin is composed of 37 meters of strata encapsulating the Wasatchian-*m* (Wa-*m*) and Wa-0 NALMA zones, which are also defined by the body of the PETM carbon isotope excursion. The transition from Cf-3 to Wa-*m* represents the boundary between the Paleocene and Eocene periods. The post-PETM bin is composed of first 62 meters of Wa-1, and represents the period in time just after the end of the PETM. Matrix dimensions for Pairs analysis were as follows: pre-PETM was organized into 27 species × 20 sites, mid-PETM was organized into 65 species × 60 sites, and post-PETM was organized into 50 species × 27 sites.

ETM2 fossil data were borrowed from Chew (2015), which examined mammal faunal change in the context of ETM2 and H2. These data consist of 120 species occurrences across 104 localities, representing 36 meters of stratigraphy. Similar to the PETM data, ETM2 data were divided into three bins based on stratigraphic level above, below, and within a faunal event known as B-1 (and what is proposed to represent ETM2; Chew 2015). The pre-ETM2, mid-ETM2, and post-ETM2 bins are all composed of 12 meters of strata. Matrix dimensions for Pairs analysis were as follows: pre-ETM2 was organized into 32 species × 26 sites, mid-ETM2 was organized into 47 species × 43 sites, and post-ETM2 was organized into 41 species × 35 sites.

Results

Data analyses across all three PETM stratigraphic bins yielded a total of 16 significant taxon pairs out of 3,656 analyzed. Segregated pairs were more common than aggregated pairs. The mid-PETM bin had the highest number of significant pairs (N=12, 8 segregated and 4 aggregated), while the pre- and post-PETM bins yielded 1 and 3 significant pairs, respectively (Table 4-1). Both bins yielded only segregated pairs. The strongest Z-scores were found among the segregated taxa ($z > 2.79$; Table 4-2, Appendix I).

Data analyses across all three ETM2 stratigraphic bins yielded a total of 10 significant taxon pairs out of 2,397 analyzed. Similar to the PETM, there were more segregated than aggregated pairs. The mid-ETM2 bin had the highest number of significant pairs (N=6, 4 segregated and 2 aggregated), while the post-ETM2 bin yielded 2 segregated and 2 aggregated pairs (Table 4-1). The pre-ETM2 bin had no significant pairs. The strongest Z-scores were again found among the segregated taxa ($z > 2.84$; Table 4-2. Appendix I).

Table 4-1. Summary of statistics for the Pairs analyses through the PETM and ETM2 hyperthermal events.

Bin	Number of taxon occurrences	Number of localities	Total number of pairs	Number of segregated pairs	Number of aggregated pairs
Pre-PETM	27	20	1	1	0
Mid-PETM	65	60	12	8	4
Post-PETM	50	27	3	3	0
Pre-ETM2	32	26	0	--	--
Mid-ETM2	47	43	6	4	2
Post-ETM2	41	35	4	2	2

Discussion

Similar patterns in taxon pair associations were observed across both PETM and ETM2 hyperthermals. In both events, the most significant pairs occurred within the body of the hyperthermal events (i.e., the mid- bins), with 12 significant pairs associated with the PETM and 6 significant pairs associated with ETM2. Within the PETM dataset, the only aggregated pairs were those found within the body of the hyperthermal (without any of the same species present in a pre-PETM significant pair). Some taxa appear in multiple segregations. These results are perhaps not surprising, considering other studies of these early Eocene hyperthermals find the greatest changes in community assembly associated with the height of these hyperthermal events, including increased mammalian turnover rates and species richness (Gingerich and Clyde 1998; Gingerich 2006; Chew 2015). Many new taxa are found to immigrate into the Bighorn Basin during the PETM, and this is also a suggested pattern during ETM2 (Chew and Oheim 2013; Chew 2015).

Before interpreting these results in terms of changes in community assembly, it is important to first explore any potential analytical artifacts or taphonomic biases that may influence the results. For instance, future investigations into hyperthermal co-occurrence patterns should consider the impacts of various binning schemes. Stratigraphic thickness was used to set the hyperthermal bins rather than length of time. Thickness of strata may be an inappropriate choice in systems with variable sedimentation rates. For the Bighorn Basin record, this is not a concern because sediment accumulation rates have been shown to be reasonably uniform over these hyperthermal intervals (Clyde et al., 2007). In addition, future investigations into hyperthermal co-occurrence patterns should consider whether the binning scheme and subsequent number of species and localities in a bin impact the detection of certain species pairs.

Table 4-2. Taxon pairs involved in significant segregations or aggregations across the early Eocene hyperthermal events.

Bin	Segregated Pairs	Aggregated Pairs
Pre-PETM	*Phenacodus, Probathyopsis*	--
Mid-PETM	*Arfia, Coryphodon* *Tuscahomys, Palaeanodon* *Chriacus, Neoliotomus* *Copecion, Thryptacodon* *Copecion, Haplomylus* *Sifrhippus, Haplomylus* *Ectocion, Neoliotomus* *Copecion, Neoliotomus*	*Herpetotherium, Leptacodon* *Hyopsodus, Chriacus* *Niptomomys, Ectypodus* *Viverravus, Niptomomys*
Post-PETM	*Coryphodon, Didymictis* *Coryphodon, Labidolemur* *Didymictis, Dipsalidictis*	--
Pre-ETM2	--	--
Mid-ETM2	*Copecion, Uintacyon* *Homogalax, Uintacyon* *Diacodexis, Uintacyon* *Eohippus, Uintacyon*	*Didymictis, Prolimnocyon* *Oxyaena, Didelphodus*
Post-ETM2	*Esthonyx, Absarokius* *Eohippus, Palaeosinopa*	*Eohippus, Diacodexis* *Xenicohippus, Prolimnocyon*

Sampling methods may also have an adverse impact on interpretations of co-occurrence patterns. For instance, some field collection techniques may result in size biases in terms of fossils found. Surficial fossil prospecting will likely lead to larger-sized specimens being found more often, while screen-washing techniques or quarrying may lead to samples more heavily skewed toward smaller specimens. Surficial prospecting is by far the most common collecting technique in the Bighorn Basin, and often the exclusive collection technique in northern Bighorn Basin localities (Rose et al. 2012). In a similar regard, modes of fossil preservation may also influence the type and size of fossils collected. Ways to solve for this issue include using

isotaphonomic approaches which restrict the analysis to fossil assemblages that were sampled from similar sedimentary facies and collected using similar techniques (Clyde and Gingerich 1998).

Assuming that the co-occurrence results yield accurate reflections of true community dynamics, the observed patterns can be used to understand biotic assemblages during hyperthermals. Interestingly, many carnivorous taxa are found both as aggregated and segregated pairs. For instance, the carnivorous miacid *Didymictus* forms a segregated pair with another specialized carnivore *Dipsalidictis* within the PETM, but is found aggregated with another carnivore, *Prolimnocyon,* during ETM2. Also, during ETM2, the martin-like *Oxyaena* is found in an aggregated pair with *Didelphodus*, a ground dwelling-carnivore. The aggregations of various carnivores suggest that while they may share similar geographic range, they may still co-exist by occupying separate habitat guilds or niches, or by consuming separate types of prey. For example, the aggregated carnivores of ETM2 (*Didymictus* and *Prolimnocyon*, *Oxyaena* and *Didelphodus*) differed in body size from one another, supporting the idea of differing guild occupation. These patterns of co-occurrence may also reflect changing prey dynamics (also in response to the rapid climate change). Many large mammals are found in segregated pairs with small mammals within the body of both hyperthermals. For instance, *Uintacyon* was a large, arboreal omnivore that is rarely found with smaller-bodied ground-dwelling herbivores and omnivores like *Diacodexis*, *Copecion*, *Homogalax*, and *Eohippus* within ETM2. One explanation for this pattern may have to do with competition over resources within the same habitat. Another explanation may have to do with the nature of the ETM2 warming event, and perhaps these smaller-bodied mammals dispersed out of local sites when climatic conditions rapidly changed. While beyond the scope of the exploratory nature of this study, future work in

analyzing individual taxon pairs should incorporate explicit ecological and biological characteristics of the taxa (guild, body size, locomotor mode, etc.) in order to more rigorously assess the potential biological or environmental causes for species associations in the fossil record (for an example, see Blois et al. 2014 and Kohli et al. *in press*).

In a recent study considering species co-occurrence patterns over the last 300 million years, fossil assemblages prior to the Holocene period were dominated by aggregated pairs, with no significant change in proportions of aggregated vs. segregated found across the PETM or during any other major extinction or climate change event (Lyons et al. 2016). The results from this study of the Bighorn Basin assemblages find that segregated pairs dominate the PETM and ETM2 non-random taxon associations. Thus, the tempo-spatial scale analyzed (and binned) must clearly play an important role in the analyses and resulting interpretations. Indeed, Gingerich (2006) pointed out that large-scale studies of mammal diversity across the entire Cenozoic have failed to capture any significant changes in biodiversity across the Paleocene-Eocene boundary (Prothero 1999, Alroy et al. 2000) even though more detailed analyses show that it is characterized by a profound biotic reorganization (Clyde and Gingerich 1998; Gingerich 2006).

Conclusions

While much research has been conducted on mammal community dynamics through the fossil record of the Bighorn Basin, little work has focused on patterns of taxonomic co-occurrence through time. Recent studies of modern and fossil taxa have implemented high-resolution pairwise co-occurrence analyses on datasets across both space and time. Such analyses have the potential to infer the types of species interactions, habitat preferences, and

dispersal dynamics associated with non-randomly aggregated and segregated taxon pairs. This study explored early Eocene fossil mammal data from the Bighorn Basin with this new statistical approach, analyzing co-occurrence patterns through two early Eocene hyperthermal events (PETM and ETM2). Preliminary results show an increase in significant taxon pairs during the height of both hyperthermal events, with segregated pairs more common. This result suggests the overall changes in community dynamics associated with these climate change events, such as turnover and species richness, also may have had important implications on interactions between individual taxa. However, other sampling and taphonomic factors cannot yet be ruled out so the exact biotic and environmental controls on these interactions will be the focus of a future study.

LIST OF REFERENCES

Abels, H. A., V. Lauretano, A. van Yperen, T. Hopman, J. C. Zachos, L. J. Lourens, P. D. Gingerich, and G. J. Bowen. 2016. "Carbon Isotope Excursions in Paleosol Carbonate Marking Five Early Eocene Hyperthermals in the Bighorn Basin, Wyoming." *Climate of the Past Discussions* 11 (3): 1857–85.

Abels, H. A., W. C. Clyde, P. D. Gingerich, F. J. Hilgen, H. C. Fricke, G. J. Bowen, and L. J. Lourens. 2012. "Terrestrial Carbon Isotope Excursions and Biotic Change during Palaeogene Hyperthermals." *Nature Geoscience* 5 (5): 326–29.

Abeni, F., F. Petrera, M. Capelletti, A. Dal Prà, L. Bontempo, A. Tonon, and F. Camin. 2015. "Hydrogen and Oxygen Stable Isotope Fractionation in Body Fluid Compartments of Dairy Cattle According to Season, Farm, Breed, and Reproductive Stage." *PLOS ONE* 10 (5).

Ashton, K. G., M. C. Tracy, and A. de Queiroz, 2000. "Is Bergmann's Rule Valid for Mammals?," *The American Naturalist* 156 (4): 390-415.

Aziz, H. A., F. J. Hilgen, G. M. van Luijk, A. Sluijs, M. J. Kraus, J. M. Pares, and P. D. Gingerich. 2008. "Astronomical Climate Control on Paleosol Stacking Patterns in the Upper Paleocene–lower Eocene Willwood Formation, Bighorn Basin, Wyoming." *Geology* 36 (7): 531–534.

Bergmann, C. 1847. Ueber die Verhältnisse der Wärmeökonomie der Thiere zu ihrer Grösse. *Gottinger Studien* 3: 595–708.

Blois, J. L., R. S. Feranec, and E. A. Hadly. 2008. "Environmental Influences on Spatial and Temporal Patterns of Body-Size Variation in California Ground Squirrels (Spermophilus Beecheyi)." *Journal of Biogeography* 35 (4): 602–13.

Bowen, G. J., B. J. Maibauer, M. J. Kraus, U. Röhl, T. Westerhold, A. Steimke, P. D. Gingerich, S. L. Wing, and W. C. Clyde. 2014. "Two Massive, Rapid Releases of Carbon during the Onset of the Palaeocene–Eocene Thermal Maximum." *Nature Geoscience* 8 (1): 44–47.

Bowen, G. J., P. L. Koch, P. D. Gingerich, R. D. Norris, S. Bains, and R. M. Corfield. 2001. "Refined Isotope Stratigraphy across the Continental Paleocene Eocene Boundary on Polecat Bench in the Northern Bighorn Basin." University of Michigan Papers on Paleontology 33: 73–88.

Bown, T. M., Kraus, M. J., 1981. Vertebrate fossil-bearing paleosol units (Willwood Formation, lower Eocene, northwest Wyoming, USA: Implications for taphonomy, biostratigraphy, and assemblage analysis. *Palaeogeogr. Palaeoclimatol. Palaeoecol*. 34, 31–56.

Bown, T. M., and Mary J. Kraus. 1987. "Integration of Channel and Floodplain Suites, I. Developmental Sequence and Lateral Relations of Alluvial Paleosols." *Journal of Sedimentary Research* 57 (4).

Brown, J. H., G. C. Stevens, and D. M. Kaufman. 1996. "THE GEOGRAPHIC RANGE: Size, Shape, Boundaries, and Internal Structure." *Annual Review of Ecology and Systematics* 27 (1): 597–623.

Burger, B. J. 2012. "Northward Range Extension of a Diminutive-Sized Mammal (*Ectocion Parvus*) and the Implication of Body Size Change during the Paleocene–Eocene Thermal Maximum." *Palaeogeography, Palaeoclimatology, Palaeoecology* 363–364: 144–50.

Chen, I.-C., J. K. Hill, R. Ohlemuller, D. B. Roy, and C. D. Thomas. 2011. "Rapid Range Shifts of Species Associated with High Levels of Climate Warming." *Science* 333 (6045): 1024–26.

Chew, A. E. 2015. "Mammal Faunal Change in the Zone of the Paleogene Hyperthermals ETM2 and H2." *Clim. Past. Discuss*. 11: 1223–37.

Chew, A. E., and Oheim, K. B. 2013. "Diversity and Climate Change in the Middle-Late Wasatchian (Early Eocene) Willwood Formation, Central Bighorn Basin, Wyoming." *Palaeogeography, Palaeoclimatology, Palaeoecology* 369: 67–78.

Clark, P. U., A. S. Dyke, J. D. Shakun, A. E. Carlson, J. Clark, B. Wohlfarth, J. X. Mitrovica, S. W. Hostetler, and A. M. McCabe. 2009. "The last glacial maximum." *Science* 325 (5941): 710-714.

Clyde, W. C, and Gingerich, P.D. 1998. "Mammalian Community Response to the Latest Paleocene Thermal Maximum: An Isotaphonomic Study in the Northern Bighorn Basin, Wyoming." *Geology* 26 (11): 1011.

D'Ambrosia, A. R., Clyde, W. C., Fricke, H. C., and Chew, A. E. 2014. "Stable Isotope Patterns Found in Early Eocene Equid Tooth Rows of North America: Implications for Reproductive Behavior and Paleoclimate." *Palaeogeography, Palaeoclimatology, Palaeoecology* 414: 310–19.

D'Ambrosia, A. R., Clyde, W. C., Fricke, H. C., Snell, K.E., and Gingerich, P.D. 2014. "Repetitive Mammalian Dwarfism Associated with Early Eocene Carbon Cycle Perturbations." In *Rendiconti Online Della Società Geologica Italiana*, 31: 52–53. Ferrara, Italy.

D'Ambrosia, A. R., Clyde, W. C., Fricke, H. C., Gingerich, P.D., and Abels, H.A. 2017. "Repetitive Mammalian Dwarfing during Ancient Greenhouse Warming Events." *Science Advances* 3 (3): e1601430.

Damuth, J. 1990. "Problems in Estimating Body Masses of Archaic Ungulates Using Dental Measurements." In *Body Size in Mammalian Paleobiology: Estimation and Biological Implications*, 229–53. Cambridge: Cambridge University Press.

Dirks, W., Anemone, R. L., Holroyd, P. A., Reid, D. J., and Walton, P.. 2009. "Phylogeny, Life History and the Timing of Molar Crown Formation in Two Archaic Ungulates, *Meniscotherium* and *Phenacodus* (Mammalia,'Condylarthra')." In *Comparative Dental Morphology*, 13:3–8. Karger Publishers.

Estes, R. 1991. *The Behavior Guide to African Mammals*. Berkeley and Los Angeles, California: University of California Press.

Fajer, E. D., M. D. Bowers, and F. A. Bazzaz. 1989. "The effects of enriched carbon dioxide atmospheres on plant—insect herbivore interactions." *Science* 243: 1198-1200.

Farquhar, G. D., J. R. Ehleringer, and K. T. Hubick. 1989. "Carbon Isotope Discrimination and Photosynthesis" *Annual Review of Plant Biology* 40: 503–37.

Farquhar, G. D., M. H. O'Leary, and Joe A. Berry. 1982. "On the Relationship between Carbon Isotope Discrimination and the Intercellular Carbon Dioxide Concentration in Leaves." *Functional Plant Biology* 9 (2): 121–137.

Franks, S. J., and A. E. Weis. 2008. "A Change in Climate Causes Rapid Evolution of Multiple Life-History Traits and Their Interactions in an Annual Plant." *Journal of Evolutionary Biology* 21 (5): 1321–34.

Fricke, H. C., and S. L. Wing. 2004. "Oxygen Isotope and Paleobotanical Estimates of Temperature and Δ18O–latitude Gradients over North America during the Early Eocene." *American Journal of Science* 304 (7): 612–635.

Fricke, H. C., W. C. Clyde, J. R. O'Neil, and P. D. Gingerich. 1998. "Evidence for Rapid Climate Change in North America during the Latest Paleocene Thermal Maximum: Oxygen Isotope Compositions of Biogenic Phosphate from the Bighorn Basin (Wyoming)." *Earth and Planetary Science Letters* 160 (1–2): 193–208.

Frieling, J., H. Gebhardt, M. Huber, O. A. Adekeye, S. O. Akande, G.-J. Reichart, J. J. Middelburg, S. Schouten, and A. Sluijs. 2017. "Extreme Warmth and Heat-Stressed Plankton in the Tropics during the Paleocene-Eocene Thermal Maximum." *Science Advances* 3 (3): e1600891.

Gardner, J. L., A. Peters, M. R. Kearney, L. Joseph, and R. Heinsohn. 2011. “Declining Body Size: A Third Universal Response to Warming?” *Trends in Ecology & Evolution* 26 (6): 285–91.

Geist, V. 1987. Bergmann’s rule is invalid. *Canadian Journal of Zoology* 65:1035–11038.

Gingerich, P. 2006. “Environment and Evolution through the Paleocene–Eocene Thermal Maximum.” *Trends in Ecology & Evolution* 21 (5): 246–53.

Gingerich, P. D. 2003. “Mammalian Responses to Climate Change at the Paleocene-Eocene Boundary: Polecat Bench Record in the Northern Bighorn Basin, Wyoming.” Special Papers-Geological Society of America, 463–478.

Gingerich, P. D., B. H. Smith, and K. Rosenberg. 1982. “Allometric Scaling in the Dentition of Primates and Prediction of Body Weight from Tooth Size in Fossils.” *American Journal of Physical Anthropology* 58 (1): 81–100.

Gingerich, P. D. 1974. “Size Variability of the Teeth in Living Mammals and the Diagnosis of Closely Related Sympatric Fossil Species.” *Journal of Paleontology*, 895–903.

Gingerich, P. D. 1989. “New Earliest Wasatchian Mammalian Fauna from the Eocene of Northwestern Wyoming: Composition and Diversity in a Rarely Sampled High-Floodplain Assemblage.” *Univ. Mich. Pap. Paleontol*. 28: 37–71.

Gingerich, P. D., and E. L. Simons. 1977. “Systematics, Phylogeny, and Evolution of Early Eocene Adapidae (Mammalia, Primates) in North America.” Contributions from the Museum of Paleontology, University of Michigan 24: 245–79.

Gingerich, P. D., and R. A. Haskin. 1981. “Dentition of Early Eocene *Pelycodus jarrovii* (Mammalia, Primates) and the Generic Attribution of Species Formerly Referred to *Pelycodus*.” Contributions from the Museum of Paleontology, University of Michigan 25: 327–37.

Gingerich, P. D., B. H. Smith, and K. Rosenberg. 1982. “Allometric Scaling in the Dentition of Primates and Prediction of Body Weight from Tooth Size in Fossils.” *American Journal of Physical Anthropology* 58: 81–100.

Gotelli, N. J., and W. Ulrich. 2010. "The empirical Bayes approach as a tool to identify non-random species associations." *Oecologia* 162 (2): 463-477.

Graham, R. W. 1986. "Response of mammalian communities to environmental changes during the late Quaternary." *Community Ecology*: 300-313.

Gunnell, G. F., M. E. Morgan, M. C. Maas, and P. D. Gingerich. 1995. "Comparative paleoecology of Paleogene and Neogene mammalian faunas: trophic structure and

composition." *Palaeogeography, Palaeoclimatology, Palaeoecology* 115, (1-4): 265-286.

Habeck, C. W., and R. L. Lindroth. 2013. "Influence of Global Atmospheric Change on the Feeding Behavior and Growth Performance of a Mammalian Herbivore, Microtus ochrogaster." *PloS one* 8: e72717.

Hadly, E. A., M. H. Kohn, J. A. Leonard, and R. K. Wayne. 1998. "A Genetic Record of Population Isolation in Pocket Gophers during Holocene Climatic Change." *Proceedings of the National Academy of Sciences* 95 (12): 6893–6896.

Head, Jason J., Jonathan I. Bloch, Alexander K. Hastings, Jason R. Bourque, Edwin A. Cadena, Fabiany A. Herrera, P. David Polly, and Carlos A. Jaramillo. 2009. "Giant Boid Snake from the Palaeocene Neotropics Reveals Hotter Past Equatorial Temperatures." *Nature* 457 (7230): 715–17.

Hickling, R., D. B. Roy, J. K. Hill, R. Fox, and Chris D. Thomas. 2006. "The Distributions of a Wide Range of Taxonomic Groups Are Expanding Polewards." *Global Change Biology* 12 (3): 450–55.

Ho, S. L., and T. Laepple. 2016. "Flat Meridional Temperature Gradient in the Early Eocene in the Subsurface Rather than Surface Ocean." *Nature Geoscience* 9 (8): 606–10.

Hoy, S. R., R. O. Peterson, and J. A. Vucetich. 2018. "Climate Warming Is Associated with Smaller Body Size and Shorter Lifespans in Moose near Their Southern Range Limit." *Global Change Biology*.

James, F. C. 1970. "Geographic Size Variation in Birds and Its Relationship to Climate." *Ecology* 51 (3): 365–90.

Janis, C.M., 1990. The correlation between diet and dental wear in herbivorous mammals, and its relationship to the determination of diets in extinct species. In: Boucot, A.J. (Ed.), *Evolutionary paleobiology of behavior and coevolution*. Elsevier, Amsterdam, pp. 241–259.

Kirtland Turner, S., P. F. Sexton, C. D. Charles, and R. D. Norris. 2014. "Persistence of Carbon Release Events through the Peak of Early Eocene Global Warmth." *Nature Geoscience* 7 (10): 748–51.

Koch, P. L, J. C Zachos, and D. L Dettman. 1995. "Stable Isotope Stratigraphy and Paleoclimatology of the Paleogene Bighorn Basin (Wyoming, USA)." *Palaeogeography, Palaeoclimatology, Palaeoecology* 115 (1–4): 61–89.

Koch, P.L. 1986. "Clinal Geographic Variation in Mammals: Implications for the Study of Chronoclines." *Paleobiology* 12 (3): 269–81.

Koch, P. L. 1998. “Isotopic Reconstruction of Past Continental Environments.” *Annual Review of Earth and Planetary Sciences* 26 (1): 573–613.

Koch, P. L., N. Tuross, and M. L. Fogel. 1997. “The Effects of Sample Treatment and Diagenesis on the Isotopic Integrity of Carbonate in Biogenic Hydroxylapatite.” *Journal of Archaeological Science* 24 (5): 417–29.

Koch, P. L., W. C. Clyde, R. P. Hepple, M. L. Fogel, S. L. Wing, and J. C. Zachos. 2003. “Carbon and Oxygen Isotope Records from Paleosols Spanning the Paleocene-Eocene Boundary, Bighorn Basin, Wyoming.” Special Papers, Geological Society of America 369: 49–64.

Kohli, B. A., R. C. Terry, R. J. Rowe, in press. “A trait-based framework for discerning drivers of species co-occurrence across heterogeneous landscapes.” *Ecography*.

Kohn, M. J, and T. E Cerling. 2002. “Stable Isotope Compositions of Biological Apatite.” *Reviews in Mineralogy and Geochemistry* 48 (1): 455-488

Kohn, M. J. 1996. “Predicting Animal Δ18O: Accounting for Diet and Physiological Adaptation.” *Geochimica et Cosmochimica Acta* 60: 4811–29.

Kraus, M. J., D. T. Woody, J. J. Smith, and V. Dukic. 2015. “Alluvial Response to the Paleocene–Eocene Thermal Maximum Climatic Event, Polecat Bench, Wyoming (U.S.A.).” *Palaeogeography, Palaeoclimatology, Palaeoecology* 435: 177–92.

Kraus, M. J., F. A. McInerney, S. L. Wing, R. Secord, A. Baczynski, and J. I. Bloch. 2013. “Paleohydrologic Response to Continental Warming during the Paleocene–Eocene Thermal Maximum, Bighorn Basin, Wyoming.” *Palaeogeography, Palaeoclimatology, Palaeoecology* 370: 196–208.

Legendre, S. 1986. “Analysis of Mammalian Communities from the Late Eocene and Oligocene of Southern France.” *Palaeovertebrata* 16: 191–212.

Levin, N. E., T. E. Cerling, B. H. Passey, J. M. Harris, and J. R. Ehleringer. 2006. “A Stable Isotope Aridity Index for Terrestrial Environments.” *Proceedings of the National Academy of Sciences* 103 (30): 11201–11205.

Longinelli, A. 1984. “Oxygen Isotopes in Mammal Bone Phosphate: A New Tool for Paleohydrological and Paleoclimatological Research?” *Geochimica et Cosmochimica Acta* 48 (2): 385–390.

Loomis, F. B. 1905. “Hyopsodidae of the Wasatch and Wind River Basins.” *American Journal of Science* 114: 416–24.

Lourens, L. J., A. Sluijs, D. Kroon, J. C. Zachos, E.Thomas, U. Rohl, J. Bowles, and I. Raffi. 2005. “Astronomical Pacing of Late Palaeocene to Early Eocene Global Warming Events.” *Nature* 435 (7045): 1083–87.

Lovegrove, B. G., and M. O. Mowoe. 2013. “The Evolution of Mammal Body Sizes: Responses to Cenozoic Climate Change in North American Mammals.” *Journal of Evolutionary Biology* 26 (6): 1317–29.

Lyons, S. K., K. L. Amatangelo, A. K. Behrensmeyer, A. Bercovici, J. L. Blois, M. Davis, W. A. DiMichele et al. 2016. "Holocene shifts in the assembly of plant and animal communities implicate human impacts." *Nature* 529: 80.

McInerney, F. A., and S. L. Wing. 2011. “The Paleocene-Eocene Thermal Maximum: A Perturbation of Carbon Cycle, Climate, and Biosphere with Implications for the Future.” *Annual Review of Earth and Planetary* Sciences 39 (1): 489–516.

McKenna, M. C. 1960. “Fossil Mammalia from the Early Wasatchian Four Mile Fauna, Eocene of Northwest Colorado.” *University of California Publications in Geological Sciences* 37: 1–130.

McNab, B. K. 1971. “On the Ecological Significance of Bergmann’s Rule.” *Ecology* 52 (5): 845–54.

Meiri, S., and T. Dayan. 2003. “On the Validity of Bergmann’s Rule: On the Validity of Bergmann’s Rule.” *Journal of Biogeography* 30 (3): 331–51.

Millar, J. S., and G. J. Hickling. 1990. “Fasting Endurance and the Evolution of Mammalian Body Size.” *Functional Ecology* 4 (1): 5.

Millien, V., K. Lyons, L. Olson, F. A. Smith, A. B. Wilson, and Yoram Yom-Tov. 2006. "Ecotypic variation in the context of global climate change: revisiting the rules." *Ecology Letters* 9 (7): 853-869.

Neasham, J. W., Vondra, C. F., 1972. Stratigraphy and petrology of the lower Eocene Willwood Formation, Bighorn Basin, Wyoming. *Geol. Soc. Am. Bull.* 83, 2167–2180.

O’Leary, M. H. 1988. “Carbon Isotopes in Photosynthesis.” *BioScience* 38 (5): 328–36.

Orcutt, J. D., and S. S. B. Hopkins. 2016. “Latitudinal Body-Mass Trends in Oligo-Miocene Mammals.” *Paleobiology* 42 (04): 643–58.

Ozgul, A., S. Tuljapurkar, T. G. Benton, J. M. Pemberton, T. H. Clutton-Brock, and T. Coulson. 2009. “The Dynamics of Phenotypic Change and the Shrinking Sheep of St. Kilda.” *Science* 325 (5939): 464–67.

Pearson, P. N., and M. R. Palmer. 2000. “Atmospheric Carbon Dioxide Concentrations over the Past 60 Million Years.” Nature 406: 695–99.

Podlesak, D. W., A.-M. Torregrossa, J. R. Ehleringer, M. D. Dearing, B. H. Passey, and T.E. Cerling. 2008. “Turnover of Oxygen and Hydrogen Isotopes in the Body Water, CO2, Hair, and Enamel of a Small Mammal.” *Geochimica et Cosmochimica Acta* 72 (1): 19–35.

Post, E., N.-C. Stenseth, R. Langvatn, and J.-M. Fromentin. 1997. “Global Climate Change and Phenotypic Variation among Red Deer Cohorts.” *Proceedings of the Royal Society of London B: Biological Sciences* 264 (1386): 1317–1324.

Radinsky, L.R., 1969. The early evolution of the Perissodactyla. *Evolution* 23, 308–326.

Rankin, B. D., J. W. Fox, C. R. Barrón-Ortiz, A. E. Chew, P. A. Holroyd, J. A. Ludtke, X. Yang, and J. M. Theodor. 2015. “The Extended Price Equation Quantifies Species Selection on Mammalian Body Size across the Palaeocene/Eocene Thermal Maximum.” *Proceedings of the Royal Society B: Biological Sciences* 282 (1812): 20151097.

Rensberger, J.M., Forsten, A., Fortelius, M., 1984. Functional evolution of the cheek toothpattern and chewing direction in Tertiary horses. *Paleobiology* 10, 439–452.

Rick, J. W. 1976. “Downslope Movement and Archaeological Intrasite Spatial Analysis.” *American Antiquity* 41 (2): 133.

Rose, K. D. 1981. “The Clarkforkian Land-Mammal Age and Mammalian Faunal Composition across the Paleocene-Eocene Boundary.” University of Michigan Papers on Paleontology 26 (1–197).

Rose, K. D. 2006. *The Beginning of the Age of Mammals*. Baltimore, MD: JHU Press.

Rose, K. D., A. E. Chew, R. H. Dunn, M. J. Kraus, H. C. Fricke, and S. P. Zack. "Earliest Eocene mammalian fauna from the Paleocene-Eocene thermal maximum at sand creek divide, southern Bighorn Basin, Wyoming." (2012).

Rose, K. D., L. T. Holbrook, R. S. Rana, K. Kumar, K. E. Jones, H. E. Ahrens, P. Missiaen, A. Sahni, and T. Smith. 2014. “Early Eocene Fossils Suggest That the Mammalian Order Perissodactyla Originated in India.” *Nature Communications* 5: 5570.

Sand, H., G. Cederlund, and K. Danell. 1995. "Geographical and latitudinal variation in growth patterns and adult body size of Swedish moose (*Alces alces*)." *Oecologia* 102 (4): 433-442.

Schubert, B. A., and A. H. Jahren. 2013. “Reconciliation of Marine and Terrestrial Carbon Isotope Excursions Based on Changing Atmospheric CO2 Levels.” *Nature Communications* 4: 1653.

Secord, R., J. I. Bloch, S. G. B. Chester, D. M. Boyer, A. R. Wood, S. L. Wing, M. J. Kraus, F. A. McInerney, and J. Krigbaum. 2012. “Evolution of the Earliest Horses Driven by Climate Change in the Paleocene-Eocene Thermal Maximum.” *Science* 335 (6071): 959–62.

Secord, R., S. L. Wing, and A. E. Chew. 2008. “Stable Isotopes in Early Eocene Mammals as Indicators of Forest Canopy Structure and Resource Partitioning.” *Paleobiology* 34 (2): 282–300.

Sheridan, J. A., and D. Bickford. 2011. “Shrinking Body Size as an Ecological Response to Climate Change.” *Nature Climate Change* 1 (8): 401–6.

Sluijs, A., S. Schouten, M. Pagani, M. Woltering, H. Brinkhuis, J. S. Sinninghe Damsté, G. R. Dickens, et al. 2006. “Subtropical Arctic Ocean Temperatures during the Palaeocene/Eocene Thermal Maximum.” *Nature* 441 (7093): 610–13.

Smith, A. B. (2013), Interactive effects of climate factors on range shifts. *Global Ecology and Biogeography*, 22: 334-343.

Smith, F. A, S. L Wing, and K. H Freeman. 2007. “Magnitude of the Carbon Isotope Excursion at the Paleocene-Eocene Thermal Maximum: The Role of Plant Community Change.” *Earth and Planetary Science Letters* 262 (1–2): 50–65.

Smith, F. A., Tomé, C. P., Elliott Smith, E. A., Lyons, S. K., Newsome, S. D., & Stafford, T. W., 2015. Unraveling the consequences of the terminal Pleistocene megafauna extinction on mammal community assembly. *Ecography* 39 (2), 223-239.

Smith, F. A., J. L. Betancourt, and J. H. Brown. 1995. “Evolution of Body-Size in the Woodrat over the Past 25,000 Years of Climate Change.” *Science* 270.

Snell, K. E., B. L. Thrasher, J. M. Eiler, P. L. Koch, L. C. Sloan, and N. J. Tabor. 2013. “Hot Summers in the Bighorn Basin during the Early Paleogene.” *Geology* 41 (1): 55–58.

Solounias, N., and G.Semprebon. 2002. “Advances in the Reconstruction of Ungulate Ecomorphology with Application to Early Fossil Equids.” American Museum Novitates 3366: 1–49.

Stap, L., L. J. Lourens, E. Thomas, A. Sluijs, S. Bohaty, and J. C Zachos. 2010. “High-Resolution Deep-Sea Carbon and Oxygen Isotope Records of Eocene Thermal Maximum 2 and H2.” *Geology* 38 (7): 607.

Sultan, B., and S. Janicot. 2000. "Abrupt shift of the ITCZ over West Africa and intra-seasonal variability." *Geophysical Research Letters* 27(20): 3353-3356.

Suzuki, T. 2011. "Seasonal variation of the ITCZ and its characteristics over central Africa." *Theoretical and Applied Climatology* 103 (1-2): 39-60.

Thurber, J. M., and R. O. Peterson. 1991. “Changes in Body Size Associated with Range Expansion in the Coyote (*Canis Latrans*).” *Journal of Mammalogy* 72 (4): 750–55.

Ulrich, W. "Pairs—a FORTRAN program for studying pair-wise species associations in ecological matrices." URL < www.keib.umk.pl/pairs> (2008).

Van Houten, F.B. 1945. “Review of Latest Paleocene and Early Eocene Mammalian Faunas.” *Journal of Paleontology* 19 (5): 421–61.

Vitousek, P. M., J. R. Gosz, C. C. Grier, J. M. Melillo, and W. A. Reiners. 1982. “A Comparative Analysis of Potential Nitrification and Nitrate Mobility in Forest Ecosystems” *Ecological Monographs* 52: 155–177.

Watt, C., S. Mitchell, and V. Salewski. 2010. Bergmann’s rule; a concept cluster? *Oikos* 119: 89–100.

Weijers, J. W. H., S. Schouten, A. Sluijs, H. Brinkhuis, and J. S. Sinninghe Damsté. 2007. “Warm Arctic Continents during the Palaeocene–Eocene Thermal Maximum.” *Earth and Planetary Science Letters* 261 (1–2): 230–38.

Williamson, T. E., Lucas, S. G. 1992. Meniscotherium (Mammalia, ‘Condylarthra’) from the Paleocene Eocene of Western North America. *Bull New Mex Mus Nat Hist Sci* 1: 1–75.

Wood, A. R., M. J. Kraus, and P. D. Gingerich. 2008. “Downslope Fossil Contamination: Mammal-Bearing Fluvial Conglomerates and the Paleocene-Eocene Faunal Transition (Willwood Formation, Bighorn Basin, Wyoming).” *Palaios* 23 (6): 380–90.

Zachos, J., M. Pagani, L. Sloan, E. Thomas, and K. Billups. 2001. “Trends, Rhythms, and Aberrations in Global Climate 65 Ma to Present.” *Science* 292 (5517): 686–93.

APPENDICES

Appendix A. White Temple (WT) carbonate nodule $\delta^{13}C$ section. Section designations: WT11 refers to the portion of the stratigraphic section measured and nodules collected in 2011, while WT12 represents the portion of the stratigraphic section measured and nodules collected in 2012. $\delta^{13}C$ carbonate values sometimes represent averages of multiple nodules from a particular level. Number of sampled nodules per level is indicated by *n*.

Section	Level above PETM (m)	*n*	$\delta^{13}C$ (average)	Section	Level above PETM (m)	*n*	$\delta^{13}C$ (average)
WT11	840.70	1	-9.15	WT11	905.04	1	-13.44
WT11	842.40	1	-9.17	WT11	905.10	1	-13.49
WT11	848.35	1	-9.56	WT11	905.34	1	-14.31
WT11	849.00	1	-10.30	WT11	905.88	1	-13.35
WT11	851.30	1	-9.29	WT11	906.24	1	-13.83
WT11	855.80	1	-9.63	WT11	906.55	1	-12.37
WT11	857.85	2	-10.07	WT11	906.66	1	-13.02
WT11	859.55	3	-10.48	WT11	908.20	2	-12.72
WT11	862.65	1	-10.61	WT11	910.45	1	-12.25
WT11	863.65	1	-9.88	WT11	910.95	1	-12.37
WT11	864.35	1	-10.28	WT11	912.35	1	-11.88
WT11	868.55	1	-11.04	WT11	914.00	1	-11.81
WT11	868.65	1	-10.12	WT11	915.95	1	-11.11
WT11	870.25	1	-9.99	WT11	917.95	1	-10.39
WT11	871.45	1	-9.67	WT11	918.65	1	-10.89
WT11	871.95	1	-10.73	WT11	919.70	1	-9.32
WT11	872.95	1	-9.99	WT11	920.95	1	-9.44
WT11	874.05	1	-9.86	WT11	923.50	1	-9.86
WT11	875.25	1	-10.01	WT11	924.80	2	-10.77
WT11	876.55	1	-9.50	WT11	929.35	1	-10.40
WT11	880.25	1	-9.83	WT11	930.25	1	-10.90
WT11	884.35	1	-10.58	WT12	932.85	1	-11.83
WT11	885.25	1	-10.41	WT12	938.80	1	-12.16
WT11	887.05	1	-9.65	WT12	939.85	1	-10.50
WT11	888.05	1	-9.72	WT12	940.55	1	-11.07
WT11	889.30	1	-10.07	WT12	942.95	1	-11.45
WT11	891.70	3	-10.38	WT12	943.55	1	-11.30
WT11	892.55	1	-10.57	WT12	944.00	1	-11.42
WT11	893.65	1	-11.06	WT12	944.35	1	-11.29
WT11	895.15	1	-11.24	WT12	946.25	1	-11.46
WT11	896.45	1	-10.77	WT12	948.00	1	-9.33
WT11	897.65	1	-11.03	WT12	948.70	1	-9.27
WT11	899.45	1	-11.87	WT12	949.40	1	-9.08
WT11	901.25	1	-12.24	WT12	950.50	1	-9.59
WT11	902.60	2	-12.60	WT12	950.90	1	-8.71
WT11	903.60	1	-12.58	WT12	951.30	1	-8.63
WT11	903.72	1	-13.15	WT12	952.35	1	-9.46
WT11	903.96	1	-13.51	WT12	955.25	1	-9.27
WT11	904.20	1	-13.59	WT12	956.30	1	-9.54
WT11	904.44	1	-13.58	WT12	957.15	1	-9.23
WT11	904.62	1	-13.74	WT12	959.60	1	-8.73
WT11	904.80	1	-13.32				

Appendix B. Updated Gilmore Hill (GH) carbonate nodule $\delta^{13}C$ section. Section designations: GH09 refers to "old" GH section reported in Abels et al. (2012), and GH13 refers to the most recently collected nodules. $\delta^{13}C$ carbonate values often represent averages of multiple nodules from a particular level. Number of sampled nodules per level is indicated by *n*.

Section	Level above PETM (m)	*n*	$\delta^{13}C$ (average)	Section	Level above PETM (m)	*n*	$\delta^{13}C$ (average)
GH09	831.10	1	-9.59	GH13	904.62	2	-12.82
GH09	833.10	1	-9.75	GH09	904.70	1	-10.22
GH09	834.30	1	-9.53	GH13	904.71	1	-12.55
GH09	835.10	1	-10.39	GH13	905.03	2	-13.62
GH09	836.05	1	-9.42	GH13	905.22	2	-13.61
GH09	840.30	1	-9.23	GH13	905.42	2	-14.02
GH09	842.75	2	-10.36	GH09	905.60	1	-11.71
GH09	844.50	2	-10.38	GH13	905.64	2	-13.61
GH09	845.55	2	-10.00	GH13	905.90	2	-14.11
GH09	846.80	1	-9.66	GH13	906.05	2	-14.19
GH09	849.25	2	-10.03	GH13	906.39	2	-13.76
GH09	853.15	1	-9.06	GH09	906.50	1	-11.96
GH09	854.95	2	-9.68	GH09	906.50	1	-11.96
GH09	855.35	2	-9.77	GH13	907.74	4	-13.30
GH09	856.50	2	-10.23	GH13	907.92	2	-13.62
GH09	862.30	1	-9.23	GH13	908.07	2	-13.35
GH09	876.60	2	-10.34	GH13	908.28	2	-13.18
GH09	889.55	1	-10.22	GH13	908.38	2	-12.78
GH09	891.40	2	-9.40	GH13	908.90	2	-12.21
GH09	892.50	1	-9.64	GH13	909.11	3	-12.51
GH09	893.00	1	-9.48	GH09	910.75	1	-11.99
GH09	894.00	2	-10.07	GH09	911.00	1	-11.92
GH09	895.80	1	-9.40	GH13	911.27	3	-12.42
GH09	895.90	1	-9.15	GH13	911.37	2	-12.36
GH09	897.80	1	-9.58	GH13	912.23	2	-12.21
GH09	898.80	1	-10.45	GH09	912.30	1	-12.02
GH09	899.95	1	-11.25	GH09	912.50	1	-12.03
GH09	901.05	1	-11.06	GH13	912.77	4	-12.06
GH13	901.71	2	-11.95	GH13	913.44	2	-13.35
GH13	901.81	2	-11.84	GH09	913.75	1	-11.94
GH09	902.05	1	-11.12	GH13	914.33	2	-12.13
GH09	902.05	1	-11.12	GH13	914.46	1	-11.81
GH13	902.21	2	-12.30	GH13	914.97	3	-12.15
GH13	902.48	2	-12.35	GH09	916.40	1	-10.67
GH13	902.78	5	-12.39	GH13	917.16	5	-11.22
GH13	903.02	2	-12.57	GH09	917.60	1	-10.01
GH13	903.12	2	-12.33	GH13	918.12	2	-10.25
GH13	903.23	2	-12.46	GH13	919.48	2	-10.58
GH13	903.43	2	-12.76	GH09	920.25	1	-9.34
GH09	903.50	1	-11.15	GH13	920.53	2	-9.42

GH13	903.82	1	-12.91	GH09	920.70	1	-9.24
GH13	904.03	1	-12.23	GH13	921.06	2	-8.61
GH09	904.10	1	-10.87	GH13	922.04	2	-8.73
GH13	904.29	2	-13.02	GH09	922.30	1	-8.95
GH13	904.47	2	-12.94	GH09	922.35	1	-8.93

Appendix C. Carbon and oxygen isotope data collected from *Arenahippus* tooth specimens. Teeth from same jaw (or "tooth row") were averaged together (these teeth share the same field number).

UMMP Specimen #	Field #	Lab Sample #	Left/ Right	Tooth Position	Meter Level (above PETM)	Section	$\delta^{13}C$	Average $\delta^{13}C$ (tooth row)	$\delta^{13}C$ Standard Deviation (tooth row)	Average $\delta^{18}O$ (tooth row)	$\delta^{18}O$ Standard Deviation (tooth row)
116408	GHF10014	AD083A	R	M/2	830.00	GH	-13.55	-14.07	0.72	17.77	1.30
116408	GHF10014	AD083B	R	M//3	830.00	GH	-14.58				
117206	MP12030	AD087A	L	P/4	874.05	GH	-11.52	-11.52		20.97	
117214	MP12035	AD088A	L	M/1 or 2	895.50	GH	-12.75	-12.75		18.16	
117253	MP12063	AD069a	R	M/1	896.13	GH	-12.31	-12.24	0.10	24.46	0.93
117253	MP12063	AD069b	R	M/2	896.13	GH	-12.26				
117253	MP12063	AD069c	L	M/1	896.13	GH	-12.29				
117253	MP12063	AD069d	L	M/2	896.13	GH	-12.10				
117197	MP12026	AD070a	R	P/4	898.00	GH	-11.58	-11.58		20.29	
117240	MP12056	AD071a	R	M/2	909.13	GH	-14.63	-13.98	0.60	20.07	1.70
117240	MP12056	AD071b	R	M/3	909.13	GH	-13.49				
117240	MP12056	AD071c	L	M/2	909.13	GH	-14.34				
117240	MP12056	AD071d	L	M/3	909.13	GH	-13.45				
117040	MP11058	AD025B	L	M/2	909.20	GH	-13.56	-13.56		19.60	
117106	MP11086	AD063a	L	P/4	909.20	GH	-11.20	-12.40	1.03	22.06	1.27
117106	MP11086	AD063b	L	M/1	909.20	GH	-13.00				
117106	MP11086	AD063c	L	M/2	909.20	GH	-12.98				
117172	MP12017	AD072a	R	M3	909.20	GH	-13.90	-13.90		18.81	
117176	MP12018	AD079a	R	M3	909.20	GH	-13.21	-13.21		22.28	
117259	MP12066	AD080a	L	M/?	909.20	GH	-12.49	-12.85	0.50	20.77	0.65
117259	MP12066	AD080b	R	M/?	909.20	GH	-13.21				
117184	MP12024	AD073a	L	M/3	909.70	GH	-14.12	-14.12		19.66	
117162	MP12015	AD085A	R	M/?	910.10	GH	-12.01	-13.15	1.61	21.53	2.91
117162	MP12015	AD085B	L	M/3	910.10	GH	-14.28				
117256	MP12065	AD074a	L	M/3	910.20	GH	-13.10	-13.71	0.86	20.41	2.49
117256	MP12065	AD074b	L	M/?	910.20	GH	-14.32				
117228	MP12046	AD075a	L	P/4	910.40	GH	-14.98	-14.98		19.50	
117169	MP12016	AD076a	L	M/2?	911.20	GH	-12.67	-12.67		20.72	
117166	MP12016	AD084A	R	P/4	911.20	GH	-12.87	-12.87		20.95	
117182	MP12023	AD077a	L	M/1 or 2	911.70	GH	-13.01	-13.01		22.37	
117132	MP11096	AD078a	R	P/4	912.70	GH	-12.46	-13.19	0.65	22.09	1.75
117132	MP11096	AD078b	R	M/1	912.70	GH	-13.71				

117132	MP11096	AD078c	R	M/2	912.70	GH	-13.41				
117155	MP12009	AD086A	L	P/4	914.20	GH	-14.03	-14.03		17.74	
117271	MP12076	AD081a	L	P/4	915.00	GH	-12.28	-12.28		22.88	
116992	MP11017	AD090A	R	M/1 or 2	853.55	WT	-13.03	-13.04	0.01	19.35	0.82
116992	MP11017	AD090B	R	M/2 or 3	853.55	WT	-13.04				
116993	MP11017	AD097A	L	M/2?	853.55	WT	-11.85	-11.85		18.69	
116995	MP11018	AD098A	R	M/2?	854.60	WT	-10.18	-10.18		22.15	
116981	MP11007	AD089A	R	P/3	858.45	WT	-12.83	-13.41	0.41	20.77	1.48
116981	MP11007	AD089B	R	M/1	858.45	WT	-13.70				
116981	MP11007	AD089C	R	M/2	858.45	WT	-13.43				
116981	MP11007	AD089D	R	M/3	858.45	WT	-13.70				
117112	MP11088	AD094A	L	M/2?	858.45	WT	-12.28	-11.92	0.52	21.61	2.95
117112	MP11088	AD094B	L	M/?	858.45	WT	-11.55				
117086	MP11077	AD103A	L	P/4	859.45	WT	-12.80	-12.46	0.48	20.72	1.40
117086	MP11077	AD103B	L	M/1	859.45	WT	-12.13				
117086	MP11077	AD093A	L	M/3	859.45	WT	-13.07	-13.07		16.66	
117038	MP11056	AD095A	L	M/1	862.80	WT	-11.77	-11.77		24.85	
117039	MP11057	AD101A	L	M/1	862.80	WT	-11.81	-11.81		18.90	
117097	MP11080	AD064a	L	P/4	864.15	WT	-12.34	-12.22	0.17	22.89	0.91
117097	MP11080	AD064b	L	M/1	864.15	WT	-12.10				
117074	MP11073	AD102A	L	P/4	865.15	WT	-12.28	-12.28		21.59	
117029	MP11047	AD091A	R	M/1	865.30	WT	-13.48	-13.58	0.14	19.53	1.41
117029	MP11047	AD091B	R	M/2	865.30	WT	-13.68				
117027	MP11045	AD100A	L	M/1 or 2	867.80	WT	-11.37	-11.37		20.90	
117014	MP11033	AD099A	L	P/4	874.65	WT	-11.29	-11.49	0.28	20.23	0.48
117014	MP11033	AD099B	L	M/1	874.65	WT	-11.69				
117035	MP11053	AD092A	L	P/4	880.25	WT	-11.37	-11.51	0.19	21.21	0.28
117035	MP11053	AD092B	L	M/1	880.25	WT	-11.64				
117363	MP13046	AD096A	L	P/4	899.15	WT	-12.06	-13.28	1.17	21.65	2.45
117363	MP13046	AD096B	L	M/2	899.15	WT	-14.59				
117363	MP13046	AD096C	L	M/3	899.15	WT	-12.76				
117363	MP13046	AD096D	R	M/2	899.15	WT	-14.47				
117363	MP13046	AD096E	R	M/3	899.15	WT	-12.54				
117274	MP12078	AD065a	R	P/4	953.15	WT	-12.20	-12.44	0.70	20.15	1.30
117274	MP12078	AD065b	R	M/1	953.15	WT	-12.25				
117274	MP12078	AD065c	R	M/2	953.15	WT	-13.46				
117274	MP12078	AD065d	R	M/3	953.15	WT	-11.87				
117276	MP12079	AD066a	L	M/2	976.00	WT	-12.28	-12.21	0.10	19.42	0.24
117276	MP12079	AD066b	L	M/3	976.00	WT	-12.13				

Appendix D. Stratigraphic levels and tooth size observations associated with each specimen in this study.

Genus	Species	UMMP Specimen #	Field #	Section	Meter Level (above PETM)	Tooth Position	Left/ Right	Average Length (mm)	Average Width (mm)	Observed/ Predicted Ln(Tooth Area)
Arenahippus	*pernix*		GH1603	GH	902.00	M/1	L	7.00	4.65	3.48
Arenahippus	*pernix*	117240	MP12056	GH	909.13	M/2	AVG	8.11	5.60	3.60
Arenahippus	*pernix*	117040	MP11058	GH	909.20	M/3	L	9.16	4.30	3.22
Arenahippus	*pernix*	117106	MP11086	GH	909.20	M/1	L	6.48	4.67	3.44
Arenahippus	*pernix*	117176	MP12018	GH	909.20	M/3	R	9.62	4.90	3.41
Arenahippus	*pernix*	117187	MP12024	GH	909.70	M/3	R	9.33	4.76	3.36
Arenahippus	*pernix*	117180	MP12021	GH	910.10	M/1	L	7.14	4.83	3.54
Arenahippus	*pernix*	117256	MP12065	GH	910.20	M/3	L	9.79	5.37	3.52
Arenahippus	*pernix*	117152	MP12007	GH	911.10	M/1	R	7.51	5.28	3.68
Arenahippus	*pernix*	117129	MP11095	GH	912.20	M/1	R	6.60	4.56	3.40
Arenahippus	*pernix*	117132	MP11096	GH	912.70	M/1	R	7.34	5.16	3.44
Arenahippus	*pernix*	117155	MP12009	GH	914.20	P/4	L	7.32	4.75	3.78
Arenahippus	*pernix*	93294	19880058	GH	915.00	M/2	R	7.82	5.10	3.46
Arenahippus	*pernix*	93298	19880062	GH	915.00	M/1	L	6.55	4.32	3.34
Arenahippus	*pernix*	93300	19880064	GH	915.00	M/1	L	7.40	5.05	3.62
Arenahippus	*pernix*	93301	19880065	GH	915.00	M/1	R	7.27	4.68	3.53
Arenahippus	*pernix*	93322	19880086	GH	915.00	M/1	R	7.14	4.70	3.51
Arenahippus	*pernix*	93326	19880090	GH	915.00	P/4	L	5.76	3.87	3.44
Arenahippus	*pernix*	93328	19880092	GH	915.00	M/1	L	6.94	4.68	3.48
Arenahippus	*pernix*	113252	20050307	GH	915.00	M/2	L	8.06	5.88	3.63
Arenahippus	*pernix*	116744	20110090	UDC	836.29	P/4	R	6.05	4.34	3.57
Arenahippus	*pernix*	116801	20110147	UDC	840.93	M/2	L	9.00	6.40	3.81
Arenahippus	*pernix*	116849	20110192	UDC	850.61	M/3	L	10.30	5.17	3.53
Arenahippus	*pernix*	116856	20110199	UDC	850.78	M/2	R	8.42	5.69	3.64
Arenahippus	*pernix*	116769	20110115	UDC	852.17	M/2	L	7.79	5.00	3.44
Arenahippus	*pernix*	116517	20100067	UDC	858.74	P/4	R	6.21	4.36	3.59
Arenahippus	*pernix*	117559	20120065	UDC	874.91	M/3	R	11.11	5.50	3.68
Arenahippus	*pernix*	116676	20110049	UDC	896.78	M/1	L	8.24	5.37	3.79
Arenahippus	*pernix*	116611	20100155	UDC	901.91	M/3	R	10.40	5.44	3.60
Arenahippus	*pernix*	116558	20100105	UDC	902.10	M/2	R	9.08	6.67	3.86

Arenahippus	*pernix*	116486	20100041	UDC	908.51	M/2	R	7.73	5.38	3.50
Arenahippus	*pernix*	94782	19881539	UDC	909.50	M/1	L	6.65	4.34	3.36
Arenahippus	*pernix*	94728	19881485	UDC	909.50	M/1	AVG	7.23	5.00	3.59
Arenahippus	*pernix*	94774	19881531	UDC	909.50	M/1	L	7.03	4.88	3.54
Arenahippus	*pernix*	94776	19881533	UDC	909.50	M/1	R	7.40	4.84	3.58
Arenahippus	*pernix*	94777	19881534	UDC	909.50	M/1	L	7.76	5.30	3.72
Arenahippus	*pernix*	116628	20110002	UDC	909.50	M/2	R	8.35	5.67	3.86
Arenahippus	*pernix*	116483	20100039	UDC	917.23	M/3	R	10.27	5.23	3.54
Arenahippus	*pernix*	116480	20100036	UDC	921.13	M/1	R	7.20	4.76	3.53
Arenahippus	*pernix*	116507	20100059	UDC	925.03	M/1	L	8.84	6.42	4.04
Arenahippus	*pernix*	116466	20100026	UDC	972.85	M/2	L	7.42	4.79	3.35
Arenahippus	*pernix*	93777	19880539	WT	840.00	M/2	L	8.18	5.53	3.58
Arenahippus	*pernix*	93783	19880545	WT	840.00	M/2	L	8.43	5.66	3.63
Arenahippus	*pernix*	116992	MP11017	WT	853.25	M/2	L	7.84	5.51	3.55
Arenahippus	*pernix*	116981	MP11007	WT	858.15	M/1	R	7.67	5.33	3.87
Arenahippus	*pernix*	117112	MP11088	WT	858.15	M/1	L	8.13	5.48	3.80
Arenahippus	*pernix*	117086	MP11077	WT	859.15	M/1	L	6.83	5.00	3.53
Arenahippus	*pernix*	117123	MP11091	WT	859.65	M/3	L	12.23	5.63	3.80
Arenahippus	*pernix*	117038	MP11056	WT	862.50	M/2	L	7.52	5.15	3.44
Arenahippus	*pernix*	117039	MP11057	WT	862.50	M/1	L	6.94	5.01	3.71
Arenahippus	*pernix*	117097	MP11080	WT	863.85	M/1	L	7.31	5.15	3.53
Arenahippus	*pernix*	117029	MP11047	WT	865.00	M/1	R	8.71	6.14	3.71
Arenahippus	*pernix*	117014	MP11033	WT	874.35	M/1	R	7.28	4.70	3.54
Arenahippus	*pernix*	117035	MP11053	WT	879.95	M/2	L	8.07	5.40	3.55
Arenahippus	*pernix*	117012	MP11031	WT	926.63	M/3	L	10.56	5.57	3.64
Arenahippus	*pernix*	117274	MP12078	WT	953.15	M/1	R	8.14	5.82	3.87
Arenahippus	*pernix*	117276	MP12079	WT	976.00	M/2	L	8.13	5.51	3.59
Cantius	*abditus*	117238	MP12054	GH	901.43	M/3	R	5.62	3.27	2.78
Cantius	*abditus*	117320	MP13013	GH	904.00	M/2	L	4.72	4.39	2.91
Cantius	*abditus*	93297	19880061	GH	915.00	M/1	L	4.27	3.44	2.69
Cantius	*abditus*	92223	19880087	GH	915.00	M/1	R	4.25	3.83	2.79
Cantius	*abditus*	113251	20050306	GH	915.00	M/1	R	4.45	3.85	2.84
Cantius	*abditus*	116735	20110084	UDC	850.70	M/3	L	5.91	3.92	3.00
Cantius	*abditus*	116753	20110099	UDC	851.40	M/3	L	5.46	3.24	2.75
Cantius	*abditus*	116850	20110193	UDC	851.60	M/1	L	4.32	3.51	2.72
Cantius	*abditus*	116563	20100109	UDC	851.80	M/2	R	3.99	3.73	2.65

Cantius	*abditus*	116883	20110224	UDC	851.90	M/2	R	4.92	4.52	2.97
Cantius	*abditus*	116576	20100122	UDC	852.30	M/1	R	4.53	3.54	2.78
Cantius	*abditus*	116904	20110241	UDC	862.40	M/1	R	4.78	4.24	3.01
Cantius	*abditus*	117556	20120062	UDC	876.10	M/2	R	4.43	4.08	2.81
Cantius	*abditus*	116599	20100143	UDC	899.50	M/2	R	5.30	4.79	3.07
Cantius	*abditus*	92051	19871099	UDC	909.50	M/1	R	4.76	3.70	2.87
Cantius	*abditus*	94782	19881539	UDC	909.50	M/3	L	5.31	3.13	2.69
Cantius	*abditus*	94764	19881521	UDC	909.50	M/2	L	3.93	4.17	2.73
Cantius	*abditus*	94779	19881536	UDC	909.50	M/1	R	4.89	4.00	2.97
Cantius	*abditus*	99624	19920594	UDC	909.50	M/3	L	5.94	3.36	2.86
Cantius	*abditus*	93760	19880522	WT	840.00	M/1	R	4.93	4.00	2.98
Cantius	*abditus*	93769	19880531	WT	840.00	M/1	L	4.81	3.92	2.94
Cantius	*abditus*	93771	19880533	WT	840.00	M/1	R	4.63	3.67	2.83
Cantius	*abditus*	93790	19880552	WT	840.00	M/1	R	4.73	4.03	2.95
Cantius	*abditus*	93803	19880565	WT	840.00	M/2	R	4.85	4.35	2.93
Cantius	*abditus*	117308	MP13005	WT	917.55	M/1	R	4.47	3.56	2.77
Diacodexis	*metsiacus*	116410	GHF10014	GH	830.00	P/4	L	5.26	2.82	2.70
Diacodexis	*metsiacus*	116977	MP11003	GH	842.00	M/1	L	4.00	3.32	2.59
Diacodexis	*metsiacus*	117173	MP12017	GH	909.20	M/1	R	3.92	3.04	2.48
Diacodexis	*metsiacus*	117042	MP11059	GH	911.20	M/3	R	5.16	3.05	2.54
Diacodexis	*metsiacus*	117183	MP12023	GH	911.70	M/1	R	3.92	2.97	2.46
Diacodexis	*metsiacus*	117324	MP13017	GH	912.30	M/2	L	4.10	3.55	2.51
Diacodexis	*metsiacus*	117157	MP12011	GH	912.80	M/1	R	3.92	3.01	2.47
Diacodexis	*metsiacus*	93316	19880080	GH	915.00	M/2	R	3.92	3.27	2.40
Diacodexis	*metsiacus*	117323	MP13016	GH	915.20	M/3	L	4.77	3.05	2.48
Diacodexis	*metsiacus*	116802	20110148	UDC	840.36	M/3	L	5.36	3.16	2.59
Diacodexis	*metsiacus*	116752	20110098	UDC	847.19	M/1	L	4.35	3.52	2.73
Diacodexis	*metsiacus*	116724	20110073	UDC	848.14	M/1	R	4.20	3.22	2.60
Diacodexis	*metsiacus*	116790	20110136	UDC	848.70	M/3	L	5.70	3.17	2.63
Diacodexis	*metsiacus*	116748	20110094	UDC	848.96	M/3	R	4.86	3.10	2.51
Diacodexis	*metsiacus*	116842	20110186	UDC	849.64	M/3	L	5.49	3.27	2.63
Diacodexis	*metsiacus*	116564	20100110	UDC	851.08	M/2	R	4.48	3.78	2.64
Diacodexis	*metsiacus*	116534	20100083	UDC	851.20	M/3	L	5.20	3.38	2.62
Diacodexis	*metsiacus*	116570	20100116	UDC	851.33	M/1	R	4.54	3.83	2.85
Diacodexis	*metsiacus*	116871	20110214	UDC	853.38	P/4	R	5.10	2.64	2.62
Diacodexis	*metsiacus*	116840	20110184	UDC	856.32	M/1	L	4.00	3.33	2.59

Diacodexis	*metsiacus*	116879	20110220	UDC	861.51	M/1	R	4.23	3.29	2.63
Diacodexis	*metsiacus*	116679	20110052	UDC	901.84	M/2	R	4.31	3.77	2.60
Diacodexis	*metsiacus*	116485	20100041	UDC	908.51	M/3	R	7.10	3.94	2.93
Diacodexis	*metsiacus*	99618	19920588	UDC	909.50	M/2	L	4.39	3.75	2.61
Diacodexis	*metsiacus*	94735	19881492	UDC	909.50	M/1	AVG	3.62	2.91	2.35
Diacodexis	*metsiacus*	99624	19920594	UDC	909.50	M/3	L	5.80	3.34	2.68
Diacodexis	*metsiacus*	93765	19880527	WT	840.00	M/2	R	4.37	3.73	2.60
Diacodexis	*metsiacus*	116984	MP11009	WT	840.85	M/3	L	5.51	3.25	2.63
Diacodexis	*metsiacus*	116990	MP11015	WT	858.15	M/2	L	4.63	3.90	2.69
Diacodexis	*metsiacus*	117078	MP11073	WT	864.85	M/3	L	5.58	3.21	2.63
Diacodexis	*metsiacus*	117026	MP11044	WT	866.00	M/1	L	4.21	3.49	2.69
Diacodexis	*metsiacus*	117437	MP13087	WT	898.65	M/1	L	4.03	3.11	2.53
Diacodexis	*metsiacus*	117107	MP11086	WT	909.20	M/2	R	3.77	3.39	2.39
Hyopsodus	*simplex*	117242	MP12056	GH	909.13	M/2	R	3.95	3.10	2.32
Hyopsodus	*simplex*	117101	MP11083	GH	909.60	M/2	R	3.93	3.29	2.36
Hyopsodus	*simplex*	117360	MP13044	GH	910.00	M/2	R	3.84	3.06	2.29
Hyopsodus	*simplex*	117357	MP13042	GH	910.70	M/2	R	3.51	3.31	2.28
Hyopsodus	*simplex*	117179	MP12020	GH	911.70	M/1	L	3.52	2.76	2.27
Hyopsodus	*simplex*	113247	20050302	GH	915.00	P/4	R	3.44	2.28	2.22
Hyopsodus	*simplex*	113249	20050304	GH	915.00	M/1	R	3.53	3.04	2.37
Hyopsodus	*simplex*	117420	MP13072	GH	915.20	M/1	L	2.94	2.46	1.85
Hyopsodus	*simplex*	116794	20110140	UDC	835.40	M/1	L	3.30	2.84	2.24
Hyopsodus	*simplex*	116796	20110142	UDC	836.10	M/1	L	3.39	3.01	2.32
Hyopsodus	*simplex*	116561	20100107	UDC	848.20	M/1	L	3.42	2.75	2.24
Hyopsodus	*simplex*	116841	20110185	UDC	849.20	M/3	R	3.61	2.14	2.16
Hyopsodus	*simplex*	116853	20110196	UDC	850.40	M/1	R	3.42	2.79	2.26
Hyopsodus	*simplex*	116837	20110181	UDC	851.20	M/1	R	3.47	2.76	2.26
Hyopsodus	*simplex*	116872	20110215	UDC	852.00	M/2	L	3.79	3.02	2.27
Hyopsodus	*simplex*	116762	20110108	UDC	852.70	M/1	R	3.45	2.87	2.29
Hyopsodus	*simplex*	116861	20110204	UDC	852.70	M/2	R	3.66	3.02	2.24
Hyopsodus	*simplex*	116863	20110206	UDC	852.80	P//4	L	3.09	2.30	2.19
Hyopsodus	*simplex*	116864	20110207	UDC	853.00	P/4	R	2.91	2.24	2.16
Hyopsodus	*simplex*	116897	20110235	UDC	853.00	M/1	R	3.17	2.58	2.10
Hyopsodus	*simplex*	116578	20100124	UDC	853.70	M/3	AVG	4.28	2.61	2.35
Hyopsodus	*simplex*	116884	20110225	UDC	856.70	M/1	L	3.29	2.71	2.19
Hyopsodus	*simplex*	116834	20110178	UDC	860.80	M/1	L	3.33	2.75	2.21

Hyopsodus	*simplex*	117555	20120061	UDC	877.20	M/2	R	3.33	2.62	2.06
Hyopsodus	*simplex*	116478	20100035	UDC	898.00	M/1	R	3.34	2.91	2.27
Hyopsodus	*simplex*	116601	20100145	UDC	899.50	M/2	R	3.85	3.28	2.35
Hyopsodus	*simplex*	116608	20100152	UDC	903.80	M/1	R	3.09	2.56	2.07
Hyopsodus	*simplex*	94736	19881493	UDC	909.50	M/1	R	3.53	2.73	2.27
Hyopsodus	*simplex*	94737	19881494	UDC	909.50	M/2	R	3.89	3.12	2.32
Hyopsodus	*simplex*	94775	19881532	UDC	909.50	M/1	L	2.93	2.47	1.98
Hyopsodus	*simplex*	99615	19920585	UDC	909.50	M/1	R	3.19	2.63	2.12
Hyopsodus	*simplex*	99616	19920586	UDC	909.50	M/1	R	3.19	2.80	2.19
Hyopsodus	*simplex*	116982	MP11008	WT	858.15	M/1	R	3.33	2.90	2.27
Hyopsodus	*simplex*	117093	MP11080	WT	863.85	M/3	L	3.67	2.19	2.18
Hyopsodus	*simplex*	117077	MP11073	WT	864.85	M/1	AVG	3.26	2.65	2.16
Hyopsodus	*simplex*	117439	MP13088	WT	897.05	M/1	R	3.08	2.42	2.01
Hyopsodus	*simplex*	117002	MP11024	WT	898.90	M/2	AVG	3.30	2.67	2.07
Hyopsodus	*simplex*	117305	MP13002	WT	914.85	M/1	L	3.17	2.44	2.05
Hyopsodus	*simplex*	117306	MP13003	WT	918.65	M/1	L	3.40	2.85	2.27

Appendix E. List of *Philantomba* specimens and associated tooth size data. Tooth area was calculated using length × width measurements of the tooth crown (in mm).

Museum	Specimen	Genus	species	Latitude	Longitude	Month	Year	Sex	Tooth Position	L/R	Ln (tooth area)
AMNH	88994	*Philantomba*	*monticola*	-11.740144	24.423274	Jan.	1939	F	m/1	R	3.42
AMNH	89207	*Philantomba*	*monticola*	-11.740144	24.423274	Jul.	1939	F	m/1	L	3.36
AMNH	89815	*Philantomba*	*monticola*	-11.740144	24.423274	Aug.	1939	M	m/1	L	3.5
AMNH	81305	*Philantomba*	*monticola*	-9.111667	33.528007	Jun.	1929	F	m/1	L	3.35
AMNH	55457	*Philantomba*	*monticola*	-7.041700	37.647400	Feb.	1922	F	m/1	R	3.52
AMNH	55458	*Philantomba*	*monticola*	-7.041700	37.647400	Sep.	1922	F	m/1	R	3.47
AMNH	55460	*Philantomba*	*monticola*	-7.041700	37.647400	Oct.	1922	M	m/1	R	3.43
AMNH	55495	*Philantomba*	*monticola*	-7.041700	37.647400	Sep.	1922	F	m/1	R	3.41
AMNH	55005	*Philantomba*	*monticola*	-5.897522	22.417226	Oct.	1924	F	m/1	L	3.37
AMNH	55060	*Philantomba*	*monticola*	-5.897522	22.417226	--	1924		m/1	L	3.32
AMNH	86719	*Philantomba*	*monticola*	-1.075607	17.160268	Sep.	1930		m/1	L	3.05
AMNH	86722	*Philantomba*	*monticola*	-1.075607	17.160268	Aug.	1930		m/1	L	3.14
AMNH	86725	*Philantomba*	*monticola*	-1.075607	17.160268	Aug.	1930		m/1	L	3
AMNH	86726	*Philantomba*	*monticola*	-1.075607	17.160268	Aug.	1930		m/1	R	3.02
AMNH	86727	*Philantomba*	*monticola*	-1.075607	17.160268	Aug.	1930		m/1	R	3.15
AMNH	119835	*Philantomba*	*maxwelli*	-0.700000	9.050000	--	--		m/1	L	3.29
AMNH	119836	*Philantomba*	*maxwelli*	-0.700000	9.050000	--	--		m/1	R	3.31
AMNH	34736	*Philantomba*	*monticola*	0.766667	35.516667	Jan.	1913	M	m/1	L	3.03
AMNH	52757	*Philantomba*	*monticola*	1.583333	27.216667	Dec.	1909	F	m/1	L	3.3
AMNH	52758	*Philantomba*	*monticola*	1.583333	27.216667	Dec.	1909	F	m/1	L	3.09
AMNH	52760	*Philantomba*	*monticola*	1.583333	27.216667	Dec.	1909	F	m/1	R	3.21
AMNH	52761	*Philantomba*	*monticola*	1.583333	27.216667	Dec.	1909	M	m/1	L	3.27
AMNH	52750	*Philantomba*	*monticola*	2.389307	27.302880	Mar.	1910	M	m/1	L	3.34
AMNH	52753	*Philantomba*	*monticola*	2.389307	27.302880	May	1910	M	m/1	R	3.23
AMNH	52754	*Philantomba*	*monticola*	2.389307	27.302880	May	1910	M	m/1	L	3.41
AMNH	52755	*Philantomba*	*monticola*	2.389307	27.302880	Aug.	1910	M	m/1	R	3.24
AMNH	269894	*Philantomba*	*monticola*	2.500000	16.166667	Nov.	1996	F	m/1	R	3.33
AMNH	269923	*Philantomba*	*monticola*	2.500000	16.166667	Dec.	1996	M	m/1	L	3.1
AMNH	269924	*Philantomba*	*monticola*	2.500000	16.166667	Dec.	1996	F	m/1	R	3.17

AMNH	52718	*Philantomba*	*monticola*	2.933333	26.833333	Sep.	1913	F	m/1	L	3.44
AMNH	52721	*Philantomba*	*monticola*	2.933333	26.833333	Sep.	1913	F	m/1	L	3.23
AMNH	52723	*Philantomba*	*monticola*	2.933333	26.833333	Sep.	1913	F	m/1	L	3.36
AMNH	52726	*Philantomba*	*monticola*	2.933333	26.833333	Oct.	1913	F	m/1	R	3.12
AMNH	52729	*Philantomba*	*monticola*	2.933333	26.833333	Oct.	1913	M	m/1	L	3.28
AMNH	52730	*Philantomba*	*monticola*	2.933333	26.833333	Oct.	1913	M	m/1	L	3.27
AMNH	52732	*Philantomba*	*monticola*	2.933333	26.833333	Oct.	1913	M	m/1	L	3.08
AMNH	52734	*Philantomba*	*monticola*	2.933333	26.833333	Oct.	1913	F	m/1	L	3.36
AMNH	52739	*Philantomba*	*monticola*	2.933333	26.833333	Oct.	1913	M	m/1	L	3.41
AMNH	52740	*Philantomba*	*monticola*	2.933333	26.833333	Oct.	1913	M	m/1	L	3.28
AMNH	52741	*Philantomba*	*monticola*	2.933333	26.833333	Oct.	1913	M	m/1	R	3.22
AMNH	52743	*Philantomba*	*monticola*	2.933333	26.833333	Oct.	1913	M	m/1	R	3.24
AMNH	52744	*Philantomba*	*monticola*	2.933333	26.833333	Oct.	1913	M	m/1	L	3.24
AMNH	89390	*Philantomba*	*monticola*	3.077633	10.410159	Sep.	1939		m/1	L	3.32
AMNH	89622	*Philantomba*	*monticola*	3.077633	10.410159	Sep.	1939		m/1	R	3.55
AMNH	89624	*Philantomba*	*monticola*	3.077633	10.410159	Sep.	1939		m/1	L	3.27
AMNH	52764	*Philantomba*	*monticola*	3.136012	26.896923	Jul.	1913	F	m/1	L	3.36
AMNH	52766	*Philantomba*	*monticola*	3.136012	26.896923	Aug.	1913	M	m/1	R	3.21
AMNH	52767	*Philantomba*	*monticola*	3.136012	26.896923	Aug.	1913	M	m/1	R	3.37
AMNH	52768	*Philantomba*	*monticola*	3.136012	26.896923	Aug.	1913	F	m/1	L	3.34
AMNH	52769	*Philantomba*	*monticola*	3.136012	26.896923	Aug.	1913	M	m/1	R	3.21
AMNH	52770	*Philantomba*	*monticola*	3.136012	26.896923	Aug.	1913	M	m/1	R	3.19
AMNH	52771	*Philantomba*	*monticola*	3.136012	26.896923	Aug.	1913	F	m/1	L	3.19
AMNH	52772	*Philantomba*	*monticola*	3.136012	26.896923	Aug	1913	M	m/1	L	3.25
AMNH	52773	*Philantomba*	*monticola*	3.136012	26.896923	Aug.	1913	F	m/1	L	3.14
AMNH	52747	*Philantomba*	*monticola*	3.321786	28.550190	Apr.	1913	M	m/1	L	3.45
AMNH	52748	*Philantomba*	*monticola*	3.321786	28.550190	Apr.	1913	F	m/1	L	3.22
AMNH	52749	*Philantomba*	*monticola*	3.321786	28.550190	Apr.	1913	M	m/1	R	2.87
AMNH	135019	*Philantomba*	*monticola*	3.416667	20.450000	--	--	F	m/1	L	3.24
AMNH	135035	*Philantomba*	*monticola*	3.416667	20.450000	Nov.	1949		m/1	L	3.21
AMNH	236496	*Philantomba*	*monticola*	3.642679	10.783083	Jan.	1974	M	m/1	L	3.36
AMNH	52762	*Philantomba*	*monticola*	3.679655	27.889747	Apr.	1913	M	m/1	R	3.33
AMNH	170420	*Philantomba*	*monticola*	4.750000	11.216667	--	--		m/1	L	3.13

AMNH	170421	*Philantomba*	*monticola*	4.750000	11.216667				m/1	L	3.18
AMNH	170422	*Philantomba*	*monticola*	4.750000	11.216667	Dec.	1934		m/1	L	3.17
AMNH	170424	*Philantomba*	*monticola*	4.750000	11.216667	Oct.	1936		m/1	L	3.35
AMNH	170425	*Philantomba*	*monticola*	4.750000	11.216667	--	--		m/1	L	3.18
AMNH	170426	*Philantomba*	*monticola*	4.750000	11.216667	Jul.	1936		m/1	L	2.85
AMNH	170427	*Philantomba*	*monticola*	4.750000	11.216667	Oct.	1936		m/1	L	3.35
AMNH	170430	*Philantomba*	*monticola*	4.750000	11.216667	Apr.	1936		m/1	L	3.29
AMNH	170433	*Philantomba*	*monticola*	4.750000	11.216667	May	1934		m/1	R	3.16
AMNH	170434	*Philantomba*	*monticola*	4.750000	11.216667	Dec.	1934		m/1	L	3.1
AMNH	170435	*Philantomba*	*monticola*	4.750000	11.216667	Dec.	1934		m/1	R	3.27
AMNH	170436	*Philantomba*	*monticola*	4.750000	11.216667	Apr.	1934		m/1	L	3.37
AMNH	170437	*Philantomba*	*monticola*	4.750000	11.216667	Dec.	1934		m/1	L	3.37
AMNH	89429	*Philantomba*	*maxwelli*	5.056767	-8.850789	Jul.	1940		m/1	L	3.66
AMNH	89430	*Philantomba*	*maxwelli*	5.056767	-8.850789	Jul.	1940		m/1	L	3.7
AMNH	89431	*Philantomba*	*maxwelli*	5.056767	-8.850789	Jul.	1940		m/1	L	3.81
AMNH	89432	*Philantomba*	*maxwelli*	5.056767	-8.850789	Aug.	1940		m/1	L	3.66
AMNH	241398	*Philantomba*	*monticola*	5.666358	9.424210	Dec.	1971	M	m/1	R	3.35
AMNH	89402	*Philantomba*	*maxwelli*	6.075223	-7.896006	Apr.	1940	M	m/1	R	3.68
AMNH	89404	*Philantomba*	*maxwelli*	6.075223	-7.896006	Mar.	1940	F	m/1	R	3.7
AMNH	89625	*Philantomba*	*maxwelli*	6.747380	-7.362460	Jul.	1939	M	m/1	R	3.56
AMNH	55396	*Philantomba*	*monticola*	7.083333	13.283333	Feb.	1927	M	m/1	L	3.28
AMNH	265836	*Philantomba*	*maxwelli*	8.191118	-9.723267	Mar.	1990		m/1	R	3.52
AMNH	265837	*Philantomba*	*maxwelli*	8.191118	-9.723267	Mar.	1990	M	m/1	R	3.78
AMNH	265838	*Philantomba*	*maxwelli*	8.191118	-9.723267	Mar.	1990	F	m/1	L	3.61
AMNH	265839	*Philantomba*	*maxwelli*	8.191118	-9.723267	Mar.	1990	F	m/1	L	3.78
AMNH	265840	*Philantomba*	*maxwelli*	8.191118	-9.723267	Mar.	1990	F	m/1	L	3.65
AMNH	89623	*Philantomba*	*monticola*	8.995199	11.746690	Oct.	1939	F	m/1	L	3.23
FMNH	177244	*Philantomba*	*monticola*	-15.445951	36.981182	Jun.	1905		M/1	R	3.35
FMNH	177241	*Philantomba*	*monticola*	-15.366667	37.033333	Aug.	2003?	M	M/1	L	3.38
FMNH	177242	*Philantomba*	*monticola*	-15.366667	37.033333	Aug.	2003?	F	M/1	R	3.45
FMNH	177243	*Philantomba*	*monticola*	-15.366667	37.033333	Jun.	1905		M/1	L	3.26
FMNH	81603	*Philantomba*	*monticola*	-9.256970	17.074614	Jun.	1954	M	M/1	R	3.31
FMNH	1288	*Philantomba*	*monticola*	-3.162356	10.908999		1894	M	M/1	L	3.22

FMNH	27543	*Philantomba*	*monticola*	-1.429674	28.074225	Mar.	1924	M	M/1	R	3.39
FMNH	27548	*Philantomba*	*monticola*	-1.429674	28.074225	Mar.	1924	F	M/1	R	3.26
FMNH	154182	*Philantomba*	*monticola*	-0.538067	29.858377	Nov.	1994	F	M/1	R	3.34
FMNH	34281	*Philantomba*	*monticola*	3.795348	10.136717	Jul.	1922	M	M/1	R	3.19
FMNH	34282	*Philantomba*	*monticola*	3.795348	10.136717	Sep.	1922	F	M/1	L	3.22
FMNH	34283	*Philantomba*	*monticola*	3.795348	10.136717	Aug.	1922	M	M/1	L	3.34
FMNH	34284	*Philantomba*	*monticola*	3.795348	10.136717	Sep.	1922	M	M/1	R	3.17
FMNH	34285	*Philantomba*	*monticola*	3.795348	10.136717	Jun.	1922	M	M/1	R	3.28
FMNH	34286	*Philantomba*	*monticola*	3.795348	10.136717	Aug.	1922	M	M/1	R	3.37
FMNH	1289	*Philantomba*	*monticola*	5.118882	18.427605		1892	F	M/1	L	3.16
FMNH	54450	*Philantomba*	*maxwellii*	5.929556	-0.972509			F	M/1	R	3.5
FMNH	54451	*Philantomba*	*maxwellii*	5.929556	-0.972509		1944-46	M	M/1	L	3.54
FMNH	62198	*Philantomba*	*maxwellii*	5.929556	-0.972509			F	M/1	L	3.67
FMNH	62199	*Philantomba*	*maxwellii*	5.929556	-0.972509			M	M/1	L	3.48
FMNH	62765	*Philantomba*	*maxwellii*	5.929556	-0.972509			F	M/1	R	3.5
FMNH	42693	*Philantomba*	*maxwellii*	6.923491	5.777390			F	M/1	R	3.82
NMNH	241578	*Philantomba*	*monticola*	-4.904019	35.779846	Nov.	1926	M	m/1	L	3.38
NMNH	220304	*Philantomba*	*monticola*	-1.900000	9.450000	Aug.	1918	F	m/1	R	3.1
NMNH	220305	*Philantomba*	*monticola*	-1.900000	9.450000	Aug.	1918	F	m/1	L	3.13
NMNH	220306	*Philantomba*	*monticola*	-1.900000	9.450000	Aug.	1918	M	m/1	R	3.35
NMNH	218475	*Philantomba*	*monticola*	-1.575187	9.259157	May	1917	M	m/1	R	3.36
NMNH	218833	*Philantomba*	*monticola*	-1.575187	9.259157	Nov.	1917	M	m/1	R	3.21
NMNH	220099	*Philantomba*	*monticola*	-1.575187	9.259157	Nov.	1917	F	m/1	R	3.36
NMNH	220100	*Philantomba*	*monticola*	-1.575187	9.259157	Nov.	1917	F	m/1	L	3.39
NMNH	220101	*Philantomba*	*monticola*	-1.575187	9.259157	Dec.	1917	M	m/1	R	3.2
NMNH	220103	*Philantomba*	*monticola*	-1.575187	9.259157	Dec.	1917	M	m/1	L	3.44
NMNH	220104	*Philantomba*	*monticola*	-1.575187	9.259157	Dec.	1917	F	m/1	R	3.25
NMNH	220105	*Philantomba*	*monticola*	-1.575187	9.259157	Dec.	1917	M	m/1	L	3.44
NMNH	220106	*Philantomba*	*monticola*	-1.575187	9.259157	Dec.	1917	F	m/1	L	3.31
NMNH	220107	*Philantomba*	*monticola*	-1.575187	9.259157	Dec.	1917	M	m/1	R	3.22
NMNH	220108	*Philantomba*	*monticola*	-1.575187	9.259157	Dec.	1917	M	m/1	R	3.24
NMNH	220109	*Philantomba*	*monticola*	-1.575187	9.259157	Dec.	1917	F	m/1	R	3.22

NMNH	220110	*Philantomba*	*monticola*	-1.575187	9.259157	Dec.	1917	M	m/1	L	3.45
NMNH	220111	*Philantomba*	*monticola*	-1.575187	9.259157	Dec.	1917	M	m/1	L	3.21
NMNH	220112	*Philantomba*	*monticola*	-1.575187	9.259157	Dec.	1917	F	m/1	L	3.23
NMNH	220113	*Philantomba*	*monticola*	-1.575187	9.259157	Dec.	1917	M	m/1	L	3.4
NMNH	220114	*Philantomba*	*monticola*	-1.575187	9.259157	Dec.	1917	F	m/1	L	3.36
NMNH	220115	*Philantomba*	*monticola*	-1.575187	9.259157	Dec.	1917	M	m/1	L	2.85
NMNH	220116	*Philantomba*	*monticola*	-1.575187	9.259157	Dec.	1917	M	m/1	L	3.35
NMNH	220117	*Philantomba*	*monticola*	-1.575187	9.259157	Dec.	1917	M	m/1	L	3.28
NMNH	220118	*Philantomba*	*monticola*	-1.575187	9.259157	Jan.	1918	M	m/1	L	3.41
NMNH	220119	*Philantomba*	*monticola*	-1.575187	9.259157	Jan.	1918	F	m/1	L	3.18
NMNH	220300	*Philantomba*	*monticola*	-1.575187	9.259157	May	1918	M	m/1	R	3.35
NMNH	220301	*Philantomba*	*monticola*	-1.575187	9.259157	Jun.	1918	F	m/1	L	3.27
NMNH	220302	*Philantomba*	*monticola*	-1.575187	9.259157	Jun.	1918	F	m/1	R	3.32
NMNH	220307	*Philantomba*	*monticola*	-1.575187	9.259157	Sep.	1918	M	m/1	R	3.21
NMNH	220384	*Philantomba*	*monticola*	-1.575187	9.259157	Sep.	1918	F	m/1	L	3.15
NMNH	220385	*Philantomba*	*monticola*	-1.574372	10.283203	Jan.	1919	F	m/1	L	3.24
NMNH	220303	*Philantomba*	*monticola*	-1.572610	10.873718	Aug.	1918	M	m/1	L	3.3
NMNH	182387	*Philantomba*	*monticola*	-0.091702	34.767957	Feb.	1912	F	m/1	L	3.19
NMNH	182394	*Philantomba*	*monticola*	-0.091702	34.767957	Feb.	1912	M	m/1	R	3.27
NMNH	220308	*Philantomba*	*monticola*	0.100000	9.683333	Oct.	1918	M	m/1	L	3.27
NMNH	220309	*Philantomba*	*monticola*	0.100000	9.683333	Oct.	1918	M	m/1	L	3.2
NMNH	220310	*Philantomba*	*monticola*	0.100000	9.683333	Oct.	1918	F	m/1	L	3.26
NMNH	220311	*Philantomba*	*monticola*	0.100000	9.683333	Oct.	1918	F	m/1	R	3.22
NMNH	220312	*Philantomba*	*monticola*	0.100000	9.683333	Oct.	1918	M	m/1	R	3.17
NMNH	220313	*Philantomba*	*monticola*	0.100000	9.683333	Oct.	1918	F	m/1	R	3.27
NMNH	220315	*Philantomba*	*monticola*	0.100000	9.683333	Nov.	1918	F	m/1	R	3.38
NMNH	220316	*Philantomba*	*monticola*	0.100000	9.683333	Nov.	1918	F	m/1	L	3.16
NMNH	220317	*Philantomba*	*monticola*	0.100000	9.683333	Dec.	1918	F	m/1	R	3.28
NMNH	220318	*Philantomba*	*monticola*	0.100000	9.683333	Dec.	1918	M	m/1	L	3.25
NMNH	220320	*Philantomba*	*monticola*	0.100000	9.683333	Dec.	1918	F	m/1	R	3.36
NMNH	220321	*Philantomba*	*monticola*	0.100000	9.683333	Dec.	1918	M	m/1	L	3.09
NMNH	220322	*Philantomba*	*monticola*	0.100000	9.683333	Jan.	1919	M	m/1	R	3.38
NMNH	220323	*Philantomba*	*monticola*	0.100000	9.683333	Dec.	1918	F	m/1	R	3.26

NMNH	220381	*Philantomba*	*monticola*	0.100000	9.683333	Jan.	1919	F	m/1	L	3.19
NMNH	220382	*Philantomba*	*monticola*	0.100000	9.683333	Dec.	1918	F	m/1	R	3.24
NMNH	220383	*Philantomba*	*monticola*	0.100000	9.683333	Dec.	1918	F	m/1	R	3.24
NMNH	220386	*Philantomba*	*monticola*	0.100000	9.683333	Jan.	1919	M	m/1	R	3.38
NMNH	164554	*Philantomba*	*monticola*	0.347596	32.582520	Sep.	1909	M	m/1	R	3.21
NMNH	537896	*Philantomba*	*monticola*	2.350000	21.510000	Jun.	1979	F	m/1	L	3.24
NMNH	537897	*Philantomba*	*monticola*	2.350000	21.510000	Jun.	1979	M	m/1	L	3.23
NMNH	377550	*Philantomba*	*maxwellii*	6.104604	5.893434	Jan.	1966	M	m/1	L	3.58
NMNH	482010	*Philantomba*	*maxwellii*	6.130000	-8.080000	Jul.	1971	F	m/1	L	3.55
NMNH	482011	*Philantomba*	*maxwellii*	6.130000	-8.080000	Jul.	1971	F	m/1	R	3.71
NMNH	482013	*Philantomba*	*maxwellii*	6.130000	-8.080000	Jul.	1971	M	m/1	R	3.76
NMNH	377551	*Philantomba*	*maxwellii*	6.205929	6.695894	Feb.	1966	F	m/1	R	3.56

Appendix F. List of *Philantomba monticola* specimens and associated climate data. Climate data were extracted via WorldClim. Temperature data is reported as (°C × 10), and seasonality data is reported as the standard deviation of monthly mean temperatures × 100.

Museum	Specimen	Genus	species	Latitude	Longitude	Mean T Coldest Month	Mean T Warmest Month	Mean Precipitation (mm)	Mean Annual Temperature	Seasonality
AMNH	88994	*Philantomba*	*monticola*	-11.740144	24.423274	162	224	1401	200	2032
AMNH	89207	*Philantomba*	*monticola*	-11.740144	24.423274	162	224	1401	200	2032
AMNH	89815	*Philantomba*	*monticola*	-11.740144	24.423274	162	224	1401	200	2032
AMNH	81305	*Philantomba*	*monticola*	-9.111667	33.528007	160	210	1728	188	1575
AMNH	55457	*Philantomba*	*monticola*	-7.041700	37.647400	147	198	1303	178	1785
AMNH	55458	*Philantomba*	*monticola*	-7.041700	37.647400	147	198	1303	178	1785
AMNH	55460	*Philantomba*	*monticola*	-7.041700	37.647400	147	198	1303	178	1785
AMNH	55495	*Philantomba*	*monticola*	-7.041700	37.647400	147	198	1303	178	1785
AMNH	55005	*Philantomba*	*monticola*	-5.897522	22.417226	242	256	1653	247	383
AMNH	55060	*Philantomba*	*monticola*	-5.897522	22.417226	242	256	1653	247	383
AMNH	86719	*Philantomba*	*monticola*	-1.075607	17.160268	250	263	1623	255	412
AMNH	86722	*Philantomba*	*monticola*	-1.075607	17.160268	250	263	1623	255	412
AMNH	86725	*Philantomba*	*monticola*	-1.075607	17.160268	250	263	1623	255	412
AMNH	86726	*Philantomba*	*monticola*	-1.075607	17.160268	250	263	1623	255	412
AMNH	86727	*Philantomba*	*monticola*	-1.075607	17.160268	250	263	1623	255	412
AMNH	34736	*Philantomba*	*monticola*	0.766667	35.516667	146	167	1228	157	674
AMNH	52757	*Philantomba*	*monticola*	1.583333	27.216667	239	258	1922	250	560
AMNH	52758	*Philantomba*	*monticola*	1.583333	27.216667	239	258	1922	250	560
AMNH	52760	*Philantomba*	*monticola*	1.583333	27.216667	239	258	1922	250	560
AMNH	52761	*Philantomba*	*monticola*	1.583333	27.216667	239	258	1922	250	560
AMNH	52750	*Philantomba*	*monticola*	2.389307	27.302880	231	248	2074	241	519
AMNH	52753	*Philantomba*	*monticola*	2.389307	27.302880	231	248	2074	241	519
AMNH	52754	*Philantomba*	*monticola*	2.389307	27.302880	231	248	2074	241	519
AMNH	52755	*Philantomba*	*monticola*	2.389307	27.302880	231	248	2074	241	519
AMNH	269894	*Philantomba*	*monticola*	2.500000	16.166667	240	257	1633	248	580
AMNH	269923	*Philantomba*	*monticola*	2.500000	16.166667	240	257	1633	248	580
AMNH	269924	*Philantomba*	*monticola*	2.500000	16.166667	240	257	1633	248	580
AMNH	52718	*Philantomba*	*monticola*	2.933333	26.833333	230	248	1954	241	575

AMNH	52721	*Philantomba*	*monticola*	2.933333	26.833333	230	248	1954	241	575
AMNH	52723	*Philantomba*	*monticola*	2.933333	26.833333	230	248	1954	241	575
AMNH	52726	*Philantomba*	*monticola*	2.933333	26.833333	230	248	1954	241	575
AMNH	52729	*Philantomba*	*monticola*	2.933333	26.833333	230	248	1954	241	575
AMNH	52730	*Philantomba*	*monticola*	2.933333	26.833333	230	248	1954	241	575
AMNH	52732	*Philantomba*	*monticola*	2.933333	26.833333	230	248	1954	241	575
AMNH	52734	*Philantomba*	*monticola*	2.933333	26.833333	230	248	1954	241	575
AMNH	52739	*Philantomba*	*monticola*	2.933333	26.833333	230	248	1954	241	575
AMNH	52740	*Philantomba*	*monticola*	2.933333	26.833333	230	248	1954	241	575
AMNH	52741	*Philantomba*	*monticola*	2.933333	26.833333	230	248	1954	241	575
AMNH	52743	*Philantomba*	*monticola*	2.933333	26.833333	230	248	1954	241	575
AMNH	52744	*Philantomba*	*monticola*	2.933333	26.833333	230	248	1954	241	575
AMNH	89390	*Philantomba*	*monticola*	3.077633	10.410159	244	270	2341	260	927
AMNH	89622	*Philantomba*	*monticola*	3.077633	10.410159	244	270	2341	260	927
AMNH	89624	*Philantomba*	*monticola*	3.077633	10.410159	244	270	2341	260	927
AMNH	52764	*Philantomba*	*monticola*	3.136012	26.896923	230	250	1921	242	610
AMNH	52766	*Philantomba*	*monticola*	3.136012	26.896923	230	250	1921	242	610
AMNH	52767	*Philantomba*	*monticola*	3.136012	26.896923	230	250	1921	242	610
AMNH	52768	*Philantomba*	*monticola*	3.136012	26.896923	230	250	1921	242	610
AMNH	52769	*Philantomba*	*monticola*	3.136012	26.896923	230	250	1921	242	610
AMNH	52770	*Philantomba*	*monticola*	3.136012	26.896923	230	250	1921	242	610
AMNH	52771	*Philantomba*	*monticola*	3.136012	26.896923	230	250	1921	242	610
AMNH	52772	*Philantomba*	*monticola*	3.136012	26.896923	230	250	1921	242	610
AMNH	52773	*Philantomba*	*monticola*	3.136012	26.896923	230	250	1921	242	610
AMNH	52747	*Philantomba*	*monticola*	3.321786	28.550190	236	260	1821	248	868
AMNH	52748	*Philantomba*	*monticola*	3.321786	28.550190	236	260	1821	248	868
AMNH	52749	*Philantomba*	*monticola*	3.321786	28.550190	236	260	1821	248	868
AMNH	135019	*Philantomba*	*monticola*	3.416667	20.450000	241	257	1694	248	556
AMNH	135035	*Philantomba*	*monticola*	3.416667	20.450000	241	257	1694	248	556
AMNH	236496	*Philantomba*	*monticola*	3.642679	10.783083	231	266	2091	252	1164
AMNH	52762	*Philantomba*	*monticola*	3.679655	27.889747	233	258	1728	246	748
AMNH	170420	*Philantomba*	*monticola*	4.750000	11.216667	237	264	1548	251	911
AMNH	170421	*Philantomba*	*monticola*	4.750000	11.216667	237	264	1548	251	911

AMNH	170422	*Philantomba*	*monticola*	4.750000	11.216667	237	264	1548	251	911
AMNH	170424	*Philantomba*	*monticola*	4.750000	11.216667	237	264	1548	251	911
AMNH	170425	*Philantomba*	*monticola*	4.750000	11.216667	237	264	1548	251	911
AMNH	170426	*Philantomba*	*monticola*	4.750000	11.216667	237	264	1548	251	911
AMNH	170427	*Philantomba*	*monticola*	4.750000	11.216667	237	264	1548	251	911
AMNH	170430	*Philantomba*	*monticola*	4.750000	11.216667	237	264	1548	251	911
AMNH	170433	*Philantomba*	*monticola*	4.750000	11.216667	237	264	1548	251	911
AMNH	170434	*Philantomba*	*monticola*	4.750000	11.216667	237	264	1548	251	911
AMNH	170435	*Philantomba*	*monticola*	4.750000	11.216667	237	264	1548	251	911
AMNH	170436	*Philantomba*	*monticola*	4.750000	11.216667	237	264	1548	251	911
AMNH	170437	*Philantomba*	*monticola*	4.750000	11.216667	237	264	1548	251	911
AMNH	89429	*Philantomba*	*maxwelli*	5.056767	-8.850789	244	260	3846	252	533
AMNH	89430	*Philantomba*	*maxwelli*	5.056767	-8.850789	244	260	3846	252	533
AMNH	89431	*Philantomba*	*maxwelli*	5.056767	-8.850789	244	260	3846	252	533
AMNH	89432	*Philantomba*	*maxwelli*	5.056767	-8.850789	244	260	3846	252	533
AMNH	241398	*Philantomba*	*monticola*	5.666358	9.424210	252	277	2770	264	803
AMNH	89402	*Philantomba*	*maxwelli*	6.075223	-7.896006	247	281	1920	264	986
AMNH	89404	*Philantomba*	*maxwelli*	6.075223	-7.896006	247	281	1920	264	986
AMNH	89625	*Philantomba*	*maxwelli*	6.747380	-7.362460	239	270	1513	256	1023
AMNH	55396	*Philantomba*	*monticola*	7.083333	13.283333	214	242	1550	225	926
AMNH	265836	*Philantomba*	*maxwelli*	8.191118	-9.723267	231	253	2686	243	661
AMNH	265837	*Philantomba*	*maxwelli*	8.191118	-9.723267	231	253	2686	243	661
AMNH	265838	*Philantomba*	*maxwelli*	8.191118	-9.723267	231	253	2686	243	661
AMNH	265839	*Philantomba*	*maxwelli*	8.191118	-9.723267	231	253	2686	243	661
AMNH	265840	*Philantomba*	*maxwelli*	8.191118	-9.723267	231	253	2686	243	661
AMNH	89623	*Philantomba*	*monticola*	8.995199	11.746690	237	291	1081	257	1714
FMNH	177244	*Philantomba*	*monticola*	-15.445951	36.981182	181	250	1832	222	2491
FMNH	177241	*Philantomba*	*monticola*	-15.366667	37.033333	124	175	1752	156	1854
FMNH	177242	*Philantomba*	*monticola*	-15.366667	37.033333	124	175	1752	156	1854
FMNH	177243	*Philantomba*	*monticola*	-15.366667	37.033333	124	175	1752	156	1854
FMNH	81603	*Philantomba*	*monticola*	-9.256970	17.074614	204	215	1458	209	316
FMNH	1288	*Philantomba*	*monticola*	-3.162356	10.908999	216	256	1652	239	1346
FMNH	27543	*Philantomba*	*monticola*	-1.429674	28.074225	229	240	1559	236	301

FMNH	27548	*Philantomba*	*monticola*	-1.429674	28.074225	229	240	1559	236	301
FMNH	154182	*Philantomba*	*monticola*	-0.538067	29.858377	217	224	1047	221	247
FMNH	34281	*Philantomba*	*monticola*	3.795348	10.136717	246	279	2598	267	1145
FMNH	34282	*Philantomba*	*monticola*	3.795348	10.136717	246	279	2598	267	1145
FMNH	34283	*Philantomba*	*monticola*	3.795348	10.136717	246	279	2598	267	1145
FMNH	34284	*Philantomba*	*monticola*	3.795348	10.136717	246	279	2598	267	1145
FMNH	34285	*Philantomba*	*monticola*	3.795348	10.136717	246	279	2598	267	1145
FMNH	34286	*Philantomba*	*monticola*	3.795348	10.136717	246	279	2598	267	1145
FMNH	1289	*Philantomba*	*monticola*	5.118882	18.427605	237	265	1496	250	903
FMNH	54450	*Philantomba*	*maxwellii*	5.929556	-0.972509	246	275	1572	264	892
FMNH	54451	*Philantomba*	*maxwellii*	5.929556	-0.972509	246	275	1572	264	892
FMNH	62198	*Philantomba*	*maxwellii*	5.929556	-0.972509	246	275	1572	264	892
FMNH	62199	*Philantomba*	*maxwellii*	5.929556	-0.972509	246	275	1572	264	892
FMNH	62765	*Philantomba*	*maxwellii*	5.929556	-0.972509	246	275	1572	264	892
FMNH	42693	*Philantomba*	*maxwellii*	6.923491	5.777390	242	279	1543	261	1174
NMNH	220304	*Philantomba*	*monticola*	-1.900000	9.450000	231	272	1979	256	1316
NMNH	220305	*Philantomba*	*monticola*	-1.900000	9.450000	231	272	1979	256	1316
NMNH	220306	*Philantomba*	*monticola*	-1.900000	9.450000	231	272	1979	256	1316
NMNH	218475	*Philantomba*	*monticola*	-1.575187	9.259157	231	271	2005	257	1304
NMNH	218833	*Philantomba*	*monticola*	-1.575187	9.259157	231	271	2005	257	1304
NMNH	220099	*Philantomba*	*monticola*	-1.575187	9.259157	231	271	2005	257	1304
NMNH	220100	*Philantomba*	*monticola*	-1.575187	9.259157	231	271	2005	257	1304
NMNH	220101	*Philantomba*	*monticola*	-1.575187	9.259157	231	271	2005	257	1304
NMNH	220103	*Philantomba*	*monticola*	-1.575187	9.259157	231	271	2005	257	1304
NMNH	220104	*Philantomba*	*monticola*	-1.575187	9.259157	231	271	2005	257	1304
NMNH	220105	*Philantomba*	*monticola*	-1.575187	9.259157	231	271	2005	257	1304
NMNH	220106	*Philantomba*	*monticola*	-1.575187	9.259157	231	271	2005	257	1304
NMNH	220107	*Philantomba*	*monticola*	-1.575187	9.259157	231	271	2005	257	1304
NMNH	220108	*Philantomba*	*monticola*	-1.575187	9.259157	231	271	2005	257	1304
NMNH	220109	*Philantomba*	*monticola*	-1.575187	9.259157	231	271	2005	257	1304
NMNH	220110	*Philantomba*	*monticola*	-1.575187	9.259157	231	271	2005	257	1304
NMNH	220111	*Philantomba*	*monticola*	-1.575187	9.259157	231	271	2005	257	1304
NMNH	220112	*Philantomba*	*monticola*	-1.575187	9.259157	231	271	2005	257	1304

NMNH	220113	*Philantomba*	*monticola*	-1.575187	9.259157	231	271	2005	257	1304
NMNH	220114	*Philantomba*	*monticola*	-1.575187	9.259157	231	271	2005	257	1304
NMNH	220115	*Philantomba*	*monticola*	-1.575187	9.259157	231	271	2005	257	1304
NMNH	220116	*Philantomba*	*monticola*	-1.575187	9.259157	231	271	2005	257	1304
NMNH	220117	*Philantomba*	*monticola*	-1.575187	9.259157	231	271	2005	257	1304
NMNH	220118	*Philantomba*	*monticola*	-1.575187	9.259157	231	271	2005	257	1304
NMNH	220119	*Philantomba*	*monticola*	-1.575187	9.259157	231	271	2005	257	1304
NMNH	220300	*Philantomba*	*monticola*	-1.575187	9.259157	231	271	2005	257	1304
NMNH	220301	*Philantomba*	*monticola*	-1.575187	9.259157	231	271	2005	257	1304
NMNH	220302	*Philantomba*	*monticola*	-1.575187	9.259157	231	271	2005	257	1304
NMNH	220307	*Philantomba*	*monticola*	-1.575187	9.259157	231	271	2005	257	1304
NMNH	220384	*Philantomba*	*monticola*	-1.575187	9.259157	231	271	2005	257	1304
NMNH	220385	*Philantomba*	*monticola*	-1.574372	10.283203	230	270	2026	256	1270
NMNH	220303	*Philantomba*	*monticola*	-1.572610	10.873718	236	279	2021	264	1343
NMNH	220308	*Philantomba*	*monticola*	0.100000	9.683333	247	272	2559	264	888
NMNH	220309	*Philantomba*	*monticola*	0.100000	9.683333	247	272	2559	264	888
NMNH	220310	*Philantomba*	*monticola*	0.100000	9.683333	247	272	2559	264	888
NMNH	220311	*Philantomba*	*monticola*	0.100000	9.683333	247	272	2559	264	888
NMNH	220312	*Philantomba*	*monticola*	0.100000	9.683333	247	272	2559	264	888
NMNH	220313	*Philantomba*	*monticola*	0.100000	9.683333	247	272	2559	264	888
NMNH	220315	*Philantomba*	*monticola*	0.100000	9.683333	247	272	2559	264	888
NMNH	220316	*Philantomba*	*monticola*	0.100000	9.683333	247	272	2559	264	888
NMNH	220317	*Philantomba*	*monticola*	0.100000	9.683333	247	272	2559	264	888
NMNH	220318	*Philantomba*	*monticola*	0.100000	9.683333	247	272	2559	264	888
NMNH	220320	*Philantomba*	*monticola*	0.100000	9.683333	247	272	2559	264	888
NMNH	220321	*Philantomba*	*monticola*	0.100000	9.683333	247	272	2559	264	888
NMNH	220322	*Philantomba*	*monticola*	0.100000	9.683333	247	272	2559	264	888
NMNH	220323	*Philantomba*	*monticola*	0.100000	9.683333	247	272	2559	264	888
NMNH	220381	*Philantomba*	*monticola*	0.100000	9.683333	247	272	2559	264	888
NMNH	220382	*Philantomba*	*monticola*	0.100000	9.683333	247	272	2559	264	888
NMNH	220383	*Philantomba*	*monticola*	0.100000	9.683333	247	272	2559	264	888
NMNH	220386	*Philantomba*	*monticola*	0.100000	9.683333	247	272	2559	264	888
NMNH	164554	*Philantomba*	*monticola*	0.347596	32.582520	211	226	1738	221	419

NMNH	537896	*Philantomba*	*monticola*	2.350000	21.510000	242	257	1701	249	552
NMNH	537897	*Philantomba*	*monticola*	2.350000	21.510000	242	257	1701	249	552
NMNH	377550	*Philantomba*	*maxwellii*	6.104604	5.893434	246	276	2132	262	1013
NMNH	482010	*Philantomba*	*maxwellii*	6.130000	-8.080000	248	281	1962	265	970
NMNH	482011	*Philantomba*	*maxwellii*	6.130000	-8.080000	248	281	1962	265	970
NMNH	482013	*Philantomba*	*maxwellii*	6.130000	-8.080000	248	281	1962	265	970
NMNH	377551	*Philantomba*	*maxwellii*	6.205929	6.695894	255	289	1749	272	1112

Appendix G. List of *Madoqua* specimens and associated tooth size data. Tooth area was calculated using length × width measurements of the tooth crown (in mm).

Museum	Specimen	Genus	species	Latitude	Longitude	Month	Year	Sex	Tooth Position	L/R	Ln (tooth area)
NMNH	182176	*Madoqua*	*guentheri*	-2.022878	36.119957	Sep.	1911	M	m/1	R	3.24
NMNH	182175	*Madoqua*	*guentheri*	-2.022878	36.119957	Sep.	1911	F	m/1	L	3.13
NMNH	182154	*Madoqua*	*guentheri*	-0.152138	37.308408	Sep.	1911	M	m/1	R	3.18
NMNH	182145	*Madoqua*	*guentheri*	-0.152138	37.308408	Sep.	1911	F	m/1	L	3.24
NMNH	182144	*Madoqua*	*guentheri*	-0.152138	37.308408	Sep.	1911	F	m/1	L	3.31
NMNH	182153	*Madoqua*	*guentheri*	-0.152138	37.308408	Sep.	1911	M	m/1	L	3.32
NMNH	182050	*Madoqua*	*guentheri*	0.564230	37.402954	Jul.	1911	M	m/1	L	3.3
NMNH	182070	*Madoqua*	*guentheri*	1.404553	37.738037	Jul.	1911	F	m/1	R	3.27
NMNH	182064	*Madoqua*	*guentheri*	1.404553	37.738037	Jul.	1911	F	m/1	R	3.03
NMNH	182098	*Madoqua*	*guentheri*	1.404553	37.738037	Jul.	1911	M	m/1	L	3.12
NMNH	182097	*Madoqua*	*guentheri*	1.404553	37.738037	Jul.	1911	F	m/1	L	3.11
NMNH	182071	*Madoqua*	*guentheri*	1.797938	37.856140	Jul.	1911	F	m/1	L	3.27
NMNH	173007	*Madoqua*	*guentheri*	2.531608	35.751694	Oct.	1910	F	m/1	L	3.27
NMNH	173006	*Madoqua*	*guentheri*	2.531608	35.751694	Oct.	1910	M	m/1	R	3.43
NMNH	173008	*Madoqua*	*guentheri*	2.531608	35.751694	Oct.	1910	M	m/1	R	3.18
FMNH	32924	*Madoqua*	*guentheri*	3.966667	38.433333	Jun.	1929	M	M/1	L	3.09
FMNH	32922	*Madoqua*	*guentheri*	3.966667	38.433333	Jun.	1929	F	M/1	L	3.1
FMNH	32925	*Madoqua*	*guentheri*	3.966667	38.433333	Jun.	1929	F	M/1	L	3.24
FMNH	32921	*Madoqua*	*guentheri*	3.966667	38.433333	Jun.	1929	M	M/1	R	3.33
FMNH	32923	*Madoqua*	*guentheri*	3.966667	38.433333	Jun.	1929	F	M/1	R	3.11
NMNH	299862	*Madoqua*	*guentheri*	4.410240	32.574038	Dec.	1949	M	m/1	L	3.17
NMNH	299866	*Madoqua*	*guentheri*	4.410240	32.574038	Feb.	1950	F	m/1	R	3.3
NMNH	299865	*Madoqua*	*guentheri*	4.410240	32.574038	Feb.	1950	M	m/1	L	3.14
NMNH	299864	*Madoqua*	*guentheri*	4.410240	32.574038	Feb.	1950	M	m/1	R	3.28
NMNH	299863	*Madoqua*	*guentheri*	4.410240	32.574038	Feb.	1950	F	m/1	L	3.23
FMNH	66882	*Madoqua*	*guentheri*	4.413333	32.567778	Nov.	1949	M	M/1	L	3.17
FMNH	66879	*Madoqua*	*guentheri*	4.413333	32.567778	Dec.	1949	F	M/1	R	3.23
FMNH	66878	*Madoqua*	*guentheri*	4.413333	32.567778	Dec.	1949	M	M/1	L	3.12
FMNH	66993	*Madoqua*	*guentheri*	4.413333	32.567778	Feb.	1950	M	M/1	R	3.24
FMNH	66988	*Madoqua*	*guentheri*	4.413333	32.567778	Feb.	1950	M	M/1	R	3.21
FMNH	85424	*Madoqua*	*guentheri*	4.650930	33.722191	Mar.	1948	F	M/1	L	3.23

NMNH	318119	*Madoqua*	*guentheri*	4.857999	31.563721	Apr.	1948	M	m/1	L	3.13
FMNH	26995	*Madoqua*	*guentheri*	7.746377	40.706936	Dec.	1926	F	M/1	R	3.2
FMNH	1342	*Madoqua*	*guentheri*	8.224194	43.565500	Aug.	1896	M	M/1	L	3.12
NMNH	112993	*Madoqua*	*guentheri*	9.600875	41.850142	Oct.	1899	M	m/1	L	3.15
FMNH	8776	*Madoqua*	*kirkii*	-11.202692	17.873887			M	M/1	R	3.33
FMNH	8777	*Madoqua*	*kirkii*	-11.202692	17.873887	Jan.	1901	F	M/1	L	3.31
NMNH	251819	*Madoqua*	*kirkii*	-6.162959	35.751607	Jul.	1926	M	m/1	L	3.28
NMNH	251817	*Madoqua*	*kirkii*	-6.162959	35.751607	Jun.	1926	F	m/1	R	3.46
NMNH	251825	*Madoqua*	*kirkii*	-6.162959	35.751607	Jul.	1926	F	m/1	L	3.3
NMNH	251824	*Madoqua*	*kirkii*	-6.162959	35.751607	Jul.	1926	F	m/1	L	3.28
NMNH	251823	*Madoqua*	*kirkii*	-6.162959	35.751607	Aug.	1926	M	m/1	R	3.29
NMNH	251822	*Madoqua*	*kirkii*	-6.162959	35.751607	Jul.	1926	M	m/1	R	3.28
FMNH	27272	*Madoqua*	*kirkii*	-4.166667	38.166667	Jul.	1926	M	M/1	L	3.18
FMNH	27273	*Madoqua*	*kirkii*	-4.166667	38.166667	Jul.	1926	F	M/1	L	3.18
NMNH	182268	*Madoqua*	*kirkii*	-3.800000	39.383333	Dec.	1911	M	m/1	R	3.25
NMNH	182269	*Madoqua*	*kirkii*	-3.800000	39.383333	Dec.	1911	F	m/1	L	3.23
FMNH	156114	*Madoqua*	*kirkii*	-3.769114	36.018677	Jul.	1995	M	M/1	R	3.09
NMNH	182255	*Madoqua*	*kirkii*	-3.495721	38.594114	Nov.	1911	M	m/1	R	3.37
FMNH	86000	*Madoqua*	*kirkii*	-3.483300	36.433300	Aug.	1956	M	M/1	R	3.08
FMNH	86001	*Madoqua*	*kirkii*	-3.483300	36.433300	Aug.	1956	M	M/1	R	3.4
NMNH	18968	*Madoqua*	*kirkii*	-3.399786	37.673249	--	1888	M	m/1	R	3.21
NMNH		*Madoqua*	*kirkii*	-3.399786	37.673249	--	1888	M	m/1	L	3.27
NMNH		*Madoqua*	*kirkii*	-3.399786	37.673249	--	1888	F	m/1	L	3.24
NMNH		*Madoqua*	*kirkii*	-3.399786	37.673249	--	1888	F	m/1	R	3.27
FMNH	1088	*Madoqua*	*kirkii*	-3.067425	37.355627			M	M/1	R	3.31
FMNH	1089	*Madoqua*	*kirkii*	-3.067425	37.355627			F	M/1	R	3.19
NMNH	181823	*Madoqua*	*kirkii*	-2.691731	38.166215	Apr.	1911	M	m/1	R	3.23
NMNH	201009	*Madoqua*	*kirkii*	-2.153994	34.685651	Apr.	1914	F	m/1	L	3.22
NMNH	201008	*Madoqua*	*kirkii*	-2.153994	34.685651	Apr.	1914	M	m/1	L	3.41
NMNH	181965	*Madoqua*	*kirkii*	-1.433594	35.064304	Apr.	1911	F	m/1	L	3.35
NMNH	181992	*Madoqua*	*kirkii*	-1.415473	35.562401	Apr.	1911	M	m/1	L	3.4
NMNH	181952	*Madoqua*	*kirkii*	-1.415473	35.562401	Apr.	1911	M	m/1	R	3.31
NMNH	162859	*Madoqua*	*kirkii*	-1.400000	36.638056	Aug.	1909	F	m/1	L	3.26
NMNH	182401	*Madoqua*	*kirkii*	-1.400000	36.638056	Jan.	1911	M	m/1	L	3.42
NMNH	165506	*Madoqua*	*kirkii*	-1.298004	35.802630	Jun.	1909	F	m/1	L	3.28
NMNH	161985	*Madoqua*	*kirkii*	-0.983333	37.983333	Apr.	1909	F	m/1	L	3.41

FMNH	17835	*Madoqua*	*kirkii*	-0.953966	36.593195	Jan.	1906	F	M/1	R	3.28
NMNH	163039	*Madoqua*	*kirkii*	-0.775384	36.371476	Jul.	1909	M	m/1	L	3.51
NMNH	163038	*Madoqua*	*kirkii*	-0.775384	36.371476	Jul.	1909	M	m/1	L	3.38
NMNH	163040	*Madoqua*	*kirkii*	-0.775384	36.371476	Jul.	1909	F	m/1	R	3.29
NMNH	163037	*Madoqua*	*kirkii*	-0.690673	35.111061	Jul.	1909	M	m/1	L	3.38
NMNH	163036	*Madoqua*	*kirkii*	-0.690673	35.111061	Jun.	1909	F	m/1	L	3.27
NMNH	163041	*Madoqua*	*kirkii*	-0.690673	35.111061	Jun.	1909	M	m/1	L	3.36
NMNH	163045	*Madoqua*	*kirkii*	-0.690673	35.111061	Jun.	1909	F	m/1	L	3.34
NMNH	163044	*Madoqua*	*kirkii*	-0.690673	35.111061	Jun.	1909	M	m/1	L	3.34
NMNH	163043	*Madoqua*	*kirkii*	-0.690673	35.111061	Jun.	1909	F	m/1	L	3.27
NMNH	164673	*Madoqua*	*kirkii*	-0.690673	35.111061	Aug.	1909	M	m/1	L	3.27
FMNH	20674	*Madoqua*	*kirkii*	-0.690673	35.111061	Jun.	1913	M	M/1	L	3.25
FMNH	20673	*Madoqua*	*kirkii*	-0.690673	35.111061	Jun.	1913	F	M/1	L	3.19
FMNH	17786	*Madoqua*	*kirkii*	-0.450000	36.250000	Feb.	1906	M	M/1	L	3.27
FMNH	17832	*Madoqua*	*kirkii*	-0.450000	36.250000	Feb.	1906	F	M/1	R	3.39
FMNH	17784	*Madoqua*	*kirkii*	-0.450000	36.250000	Feb.	1906	M	M/1	R	3.44
FMNH	17785	*Madoqua*	*kirkii*	-0.450000	36.250000	Feb.	1906	M	M/1	L	3.4
FMNH	17834	*Madoqua*	*kirkii*	-0.450000	36.250000	Feb.	1906	F	M/1	R	3.49
FMNH	17833	*Madoqua*	*kirkii*	-0.450000	36.250000	Feb.	1906	F	M/1	L	3.36
NMNH	164528	*Madoqua*	*kirkii*	-0.171844	36.886597	Jun.	1909	F	m/1	L	3.51
NMNH	199093	*Madoqua*	*kirkii*	-0.171844	36.886597	--	1913	M	m/1	L	3.26
NMNH	182159	*Madoqua*	*kirkii*	0.156944	37.349167	Sep.	1911	M	m/1	L	3.19
NMNH	182160	*Madoqua*	*kirkii*	0.156944	37.349167	Sep.	1911	M	m/1	L	3.17
NMNH	164531	*Madoqua*	*kirkii*	0.564230	37.402954	Jun.	1909	F	m/1	L	3.28
NMNH	164529	*Madoqua*	*kirkii*	0.564230	37.402954	Jun.	1909	M	m/1	L	3.32
NMNH	182035	*Madoqua*	*kirkii*	1.151930	39.182739	Jul.	1911	F	m/1	L	3.12
NMNH	182057	*Madoqua*	*kirkii*	1.404553	37.738037	Jul.	1911	M	m/1	L	3.26
NMNH	182089	*Madoqua*	*kirkii*	1.404553	37.738037	Jul.	1911	F	m/1	R	3.1
NMNH	182088	*Madoqua*	*kirkii*	1.404553	37.738037	Jul.	1911	F	m/1	R	3.35
NMNH	182055	*Madoqua*	*kirkii*	1.797938	37.856140	Jul.	1911	M	m/1	L	3.16
NMNH	182061	*Madoqua*	*kirkii*	1.797938	37.856140	Jul.	1911	M	m/1	R	3.19
NMNH	182060	*Madoqua*	*kirkii*	1.797938	37.856140	Jul.	1911	F	m/1	L	3.32
NMNH	182059	*Madoqua*	*kirkii*	1.797938	37.856140	Jul.	1911	M	m/1	R	2.99
NMNH	182058	*Madoqua*	*kirkii*	1.797938	37.856140	Jul.	1911	M	m/1	R	3.07
NMNH	182108	*Madoqua*	*kirkii*	1.797938	37.856140	Aug.	1911	M	m/1	R	3.11
FMNH	32920	*Madoqua*	*kirkii*	3.966667	38.433333	Jun.	1929	F	M/1	L	3.18

FMNH	26994	*Madoqua*	*kirkii*	7.516667	40.483333	Dec.	1926	F	M/1	R	3.18
FMNH	26991	*Madoqua*	*kirkii*	7.516667	40.483333	Dec.	1926	F	M/1	R	3.17
FMNH	27195	*Madoqua*	*kirkii*	7.516667	40.483333	Dec.	1926	F	M/1	R	3.16
FMNH	27001	*Madoqua*	*kirkii*	7.746377	40.706936	Dec.	1926	M	M/1	R	3.17
FMNH	168100	*Madoqua*	*kirkii*	7.802800	35.756400	Sep.	2000	F	M/1	L	3.17
FMNH	26993	*Madoqua*	*saltiana*	6.940901	36.986257	Dec.	1926	F	M/1	R	2.97
FMNH	26996	*Madoqua*	*saltiana*	7.746377	40.706936	Dec.	1926	F	M/1	L	2.93
FMNH	26999	*Madoqua*	*saltiana*	7.746377	40.706936	Dec.	1926	M	M/1	R	2.6
FMNH	1320	*Madoqua*	*saltiana*	8.224194	43.565500	Aug.	1896	F	M/1	R	3
FMNH	1321	*Madoqua*	*saltiana*	8.224194	43.565500	Aug.	1896	M	M/1	L	2.7
FMNH	27002	*Madoqua*	*saltiana*	8.991737	40.163188	Jan.	1927	F	M/1	L	3.12
FMNH	1310	*Madoqua*	*saltiana*	9.166667	44.800000	Jun.	1896	F	M/1	L	2.68
FMNH	1322	*Madoqua*	*saltiana*	9.542374	44.096031	Sep.	1896	F	M/1	R	2.88
FMNH	1313	*Madoqua*	*saltiana*	9.542374	44.096031	Jul.	1896	F	M/1	L	2.9
FMNH	1318	*Madoqua*	*saltiana*	9.542374	44.096031	Aug.	1896	F	M/1	R	2.84
FMNH	15643	*Madoqua*	*saltiana*	9.542374	44.096031	May	1896	M	M/1	L	2.67
FMNH	1316	*Madoqua*	*saltiana*	9.583429	44.033887	Jul.	1896	M	M/1	L	2.79
FMNH	27004	*Madoqua*	*saltiana*	9.683333	37.066667	Dec.	1926	F	M/1	L	2.75
FMNH	27000	*Madoqua*	*saltiana*	9.683333	37.066667	Dec.	1926	M	M/1	R	2.95
FMNH	15649	*Madoqua*	*saltiana*	10.007000	44.776000	May	1896	M	M/1	L	3.08
FMNH	15648	*Madoqua*	*saltiana*	10.007000	44.776000	May	1896	M	M/1	R	3.03
FMNH	15646	*Madoqua*	*saltiana*	10.214992	44.818311	May	1896	M	M/1	L	2.89
FMNH	15647	*Madoqua*	*saltiana*	10.214992	44.818311	May	1896	M	M/1	L	2.85
NMNH	300298	*Madoqua*	*saltiana*	11.416262	42. 078180	Jul.	1950	M	m/1	R	2.97
NMNH	377056	*Madoqua*	*sp.*	-3.330056	39.878483	Jan.	1966	?	m/1	L	3.25

Appendix H. Correlation matrix describing strength of linear relationships between response variables. Strength of correlation is highlighted in color: deepest reds for strongest negative correlations, deepest blues for strongest positive correlations.

	Latitude	Longitude	Ln(area)	Coldest Month Mean T	Warmest Month Mean T	Annual Precipitation	Annual Temperature	Seasonality
Latitude	1.0000	-0.4876	0.1768	0.7075	0.5410	0.2273	0.5944	-0.5734
Longitude	-0.4876	1.0000	-0.4341	-0.5646	-0.6851	-0.4932	-0.6473	0.0023
Ln(area)	0.1768	-0.4341	1.0000	-0.0507	0.0134	0.2622	-0.0238	0.0988
Coldest Month Mean T	0.7075	-0.5646	-0.0507	1.0000	0.8889	0.3785	0.9545	-0.5567
Warmest Month Mean T	0.5410	-0.6851	0.0134	0.8889	1.0000	0.3443	0.9790	-0.1194
Annual Precipitation	0.2273	-0.4932	0.2622	0.3785	0.3443	1.0000	0.3983	-0.1612
Annual Temperature	0.5944	-0.6473	-0.0238	0.9545	0.9790	0.3983	1.0000	-0.2951
Seasonality	-0.5734	0.0023	0.0988	-0.5567	-0.1194	-0.1612	-0.2951	1.0000